PRINCIPLES OF EXCITATORY AND INHIBITORY FUNCTIONAL CONNECTIVITY IN CEREBELLAR CORTEX IN VIVO

Charlotte Arlt

University College London

Thesis submitted for the degree of
Doctor of Philosophy in Neuroscience

2017

Declaration

I, Charlotte Arlt, confirm that the work presented in this thesis is my own. Where information has been derived from other sources, I confirm that this has been indicated.

London, January 2017

Abstract

Determining the functional impact of single interneurons on neuronal output, and how interneurons are recruited by physiological patterns of excitation, are crucial to our understanding of inhibition. In the cerebellar cortex, molecular layer interneurons and their targets, Purkinje cells, receive excitatory inputs from granule cells and climbing fibres, the latter signalling to interneurons via glutamate spillover. How these feed-forward pathways are engaged by physiological patterns of activity *in vivo* is insufficiently understood. Using dual patch-clamp recordings from interneurons and Purkinje cells in mice *in vivo*, I have probed the spatiotemporal interactions between these circuit elements. I demonstrate that single spikes in single interneurons can potently inhibit the spiking of Purkinje cells. Granule cell input activates both interneurons and the Purkinje cells they inhibit, generating local feed-forward inhibition. Climbing fibre input activates interneurons via glutamate spillover, but only rarely activates interneurons that inhibit spiking of the same Purkinje cell receiving the climbing fibre input. Rather, by activating inhibition among interneurons, climbing fibre glutamate spillover results in delayed inhibition of interneurons controlling Purkinje cell spike output, forming a disinhibitory motif. Functional climbing fibre-interneuron inhibition, inhibition among interneurons, and interneuron-Purkinje cell inhibition are vertically organised in the molecular layer, providing an anatomical substrate for this microcircuit motif. During sensory processing, these motifs account for pathway-specific recruitment of interneurons, generating fast and delayed excitatory interneuron responses via the granule cell and climbing fibre pathway, respectively. Sensory stimulation recruits granule cell input into INs and PCs near-simultaneously, resulting in rapid feed-forward inhibition. Together, these findings quantify the functional impact of single interneurons on their targets *in vivo*, and reveal how granule cell and climbing fibre inputs differentially recruit inhibitory microcircuits to diversify cerebellar computations.

Acknowledgements

I would like to thank Michael Häusser for giving me the freedom to develop independently as a scientist, and for creating a diverse working environment with excellent colleagues.
I am moreover grateful to Christian Wilms for taking me under his wing early on, for creating an atmosphere in which there truly are no stupid questions, and for providing conceptual and technical help on various levels along the way, also after his departure from the lab.
I would also like to thank Arnd Roth and Beverley Clark, for their scientific and personal support.
My thanks also belong to many brilliant lab members, postdocs, and students that I was lucky enough to get to know and learn from, and that have made this experience fun, beery and ripe of new friendships: Matt Hoddinott, Soyon Chun, Bilal Haider, Christoph Schmidt-Hieber, Adam Packer, Ingrid van Welie, Mehmet Fisek, Dimitar Kostadinov, Nick Robinson, Christina Buetfering, Eran Eldar, Jeffrey Seely, Alex Mathy, James Cottam, Sarah Rieubland, Jonathan Cornford, Yuya Kanemoto, Gabija Toleikyte, Matej Macak, Lea Götz, Noah Pettit, Lloyd Russell, Henry Dalgleish, Oli Gauld and Joanna Lau.

Thank you to my family: to my dad for his unconditional enthusiasm about my work, to my siblings for listening to my complaints, and to my mother and uncle, who keep supporting me even in their absence.

Finally, thank you to my best friend, for everything.

Table of contents

DECLARATION **2**

ABSTRACT **3**

ACKNOWLEDGEMENTS **4**

TABLE OF CONTENTS **5**

TABLE OF FIGURES **9**

ABBREVIATIONS **11**

1 INTRODUCTION **12**

1.1 THE NEURON DOCTRINE AND RECEPTIVE FIELDS 12

1.2 MODELS OF NEURAL NETWORKS 15

1.3 INHIBITION AND ITS ROLE IN MICROCIRCUITS 17

1.3.1 Ionic mechanisms of excitation and inhibition *17*

1.3.2 Diversity of inhibitory cell types *19*

1.3.3 Postsynaptic effects of inhibition depend on target location *19*

1.3.4 Inhibitory microcircuit motifs and function *21*

1.4 STUDYING CIRCUIT ARCHITECTURE AND ACTIVITY 25

1.5 THE CEREBELLAR CORTEX 29

1.5.1 Gross anatomical organisation and distal connectivity *29*

1.5.2 Anatomy and physiology of the cerebellar cortex *30*

1.5.3 Plasticity in the cerebellar cortex *34*

1.5.4 Theories of cerebellar function *35*

1.5.5 Experimental models of cerebellar function *39*

1.5.6 Molecular layer inhibition and cerebellar function *41*

1.6 AIMS OF THIS THESIS 43

2 MATERIALS & METHODS **44**

2.1 ANIMALS 44

2.2 SURGERY FOR ELECTROPHYSIOLOGICAL RECORDINGS 44

2.3 TWO-PHOTON TARGETED ELECTROPHYSIOLOGICAL RECORDINGS 45

2.4 SENSORY STIMULATION 46

2.5 VIRAL INJECTIONS 46

2.6 TAMOXIFEN ADMINISTRATION 47

2.7 LIGHT-ACTIVATED OPSIN STIMULATION 47

2.8 HISTOCHEMISTRY 47

2.9 CONFOCAL MICROSCOPY 48
2.10 DATA ANALYSIS 48
2.10.1 - Electrophysiology: Spontaneous and electrically induced activity - *48*
2.10.2 - Electrophysiology: Sensory-evoked activity - *49*
2.10.3 - Metrics for quantifying spiking response amplitudes: The baseline-normalised binned rate versus the net spike change - *50*
2.10.4 - Two-photon stacks of pipette positions - *53*
2.10.5 - Statistics - *54*
3 FUNCTIONAL INTERNEURON-PURKINJE CELL CONNECTIVITY 55
IN VIVO **55**
3.1 INTRODUCTION 55
3.2 RESULTS 57
3.2.1 Functional IN-PC inhibition in vivo *57*
3.2.2 Spatial organisation of interneuron-Purkinje cell inhibition *64*
3.3 DISCUSSION 69
3.3.1 Functional IN-PC inhibition *69*
3.3.2 Spatial profile of functional IN-PC inhibition *70*
3.3.3 Functional implications *72*
4 FUNCTIONAL CLIMBING FIBRE-INTERNEURON CONNECTIVITY 74
4.1 INTRODUCTION 74
4.2 RESULTS 76
4.2.1 Functional CF-IN connectivity in vivo *76*
4.2.2 Spatial organisation of climbing fibre – interneuron effects *82*
4.3 DISCUSSION 84
4.3.1 Spatiotemporal patterns of functional CF-IN connectivity in vivo *84*
4.3.2 The source of delayed interneuron inhibition after CF input *86*
4.3.2 Functional implications *88*
5 INHIBITION AND SYNCHRONY WITHIN THE MOLECULAR LAYER INTERNEURON NETWORK *IN VIVO* **90**
5.1 INTRODUCTION 90
5.2 RESULTS 91
5.2.1 Variety of interactions between interneurons *91*
5.2.2 Synchrony between interneurons *95*
5.2.3 Inhibition between interneurons *97*
5.3 DISCUSSION 100

5.3.1 The relationship between IN connectivity and cross-correlograms of IN spike trains ... *100*
5.3.2 Functional implications ... *103*

6 DIFFERENTIAL RECRUITMENT OF FEED-FORWARD INHIBITORY NETWORKS BY GRANULE CELL AND CLIMBING FIBRE INPUT ... **105**
6.1 INTRODUCTION ... 105
6.2 RESULTS ... 106
6.2.1 Interneuron-Purkinje cell inhibition: The recruitment by granule cell input ... *106*
6.2.2 Interneuron-Purkinje cell inhibition: The recruitment by climbing fibre input ... *109*
6.2.3 The effect of INs on PC spiking after CF input ... *112*
6.3 DISCUSSION ... 118
6.3.1 Granule cell input recruits PC feed-forward inhibition via INs ... *118*
6.3.2 A circuit motif of climbing fibre-PC disinhibition via INs ... *120*
6.3.3 Effects of optogenetic IN inhibition ... *121*
6.3.4 Functional implications ... *123*

7 FUNCTIONAL INTERNEURON-PURKINJE CELL CONNECTIVITY DURING SENSORY PROCESSING ... **125**
7.1 Introduction ... *125*
7.2 RESULTS ... 127
7.2.1 Sensory responses of Purkinje cell simple spikes, complex spikes, and interneurons ... *127*
7.2.2 Interneuron-Purkinje cell inhibition during sensory processing ... *131*
7.2.3 Pathway-specific recruitment of INs during sensory processing ... *135*
7.3 DISCUSSION ... 138
7.3.1 Rapid granule cell responses in INs and PCs ... *139*
7.3.2 Feed-forward inhibition during sensory processing ... *141*
7.3.3 IN recruitment and sensory-evoked climbing fibre input ... *142*
7.3.4 Functional implications ... *143*

8 GENERAL DISCUSSION ... **146**
8.1 PRECISE TEMPORAL RELATIONSHIPS ... 148
8.2 VERTICAL ROUTES OF FUNCTIONAL CONNECTIVITY ... 149
8.3 CLIMBING FIBRE GLUTAMATE VOLUME TRANSMISSION IN THE CEREBELLAR CORTEX ... 150
8.4 EFFECTS OF ANAESTHESIA ... 152
8.5 DIFFERENTIAL SOMATO-DENDRITIC INHIBITION OF PCS ... 154

8.6 OUTLOOK 155

9 REFERENCES 156

Table of figures

Fig 1.1 A drawing of cerebellar cortex by Ramón y Cajal 13
Fig 1.2 Inhibitory circuit motifs 21
Fig 1.3 The circuitry of the cerebellar cortex 31
Fig 1.4 The cerebellar perceptron by Albus 36
Fig 1.5 The cerebellar cortex as an adaptive filter 37
Fig 2.1 Quantifying spiking responses as normalised rates or spike changes 51
Fig 2.2 Relationship between PC baseline rate, spike change and normalised spike rate for IN-PC inhibition 52
Fig 2.3 Relationship between IN baseline rate and sensory-evoked spike change 53
Fig 3.1 Dual recordings from IN-PC pairs in vivo 58
Fig 3.2 The effect of single IN spikes on PC activity in vivo 61
Fig 3.3 The effects of spontaneous and induced IN spikes on PC activity are similar 62
Fig 3.4 Spike induction in a single IN does not recruit a coupled IN 63
Fig 3.5 Spatial sampling of IN-PC pairs 64
Fig 3.6 IN-PC inhibition depends on vertical and transverse distance 66
Fig 3.7 Inducing single spikes in INs with low vertical positions inhibits PCs 67
Fig 3.8 Relationship between IN-PC vertical distance and PC inhibition 68
Fig 4.1 INs respond to CF input with rate increases, delayed decreases, or both 78
Fig 4.2 Amplitude and timecourse of IN responses to CF input 81
Fig 4.3 Climbing fibre–IN inhibition depends on vertical distance 83
Fig 5.1 Dual IN recordings in vivo 92
Fig 5.2 Spatial sampling of IN pairs 93
Fig 5.3 Correlated and anti-correlated activity in IN pairs 93
Fig 5.4 Variability of functional connectivity between IN pairs 94
Fig 5.5 Synchrony of IN firing indicative of gap junction coupling 96
Fig 5.6 IN synchrony without inhibitory interactions 97
Fig 5.7 Inhibition within the IN network is vertically organised 99
Fig 5.8 Inhibition can co-occur with precise synchrony 100
Fig 6.1 IN-PC pairs with common granule cell input are connected 108
Fig 6.2 Climbing fibre input inhibits INs with impact on PC spiking 110
Fig 6.3 Opposing recruitment of IN feed-forward circuitry by granule cell and climbing fibre inputs 111

Fig 6.4 Timecourse of IN and PC responses to climbing fibre input 113
Fig 6.5 Optogenetic inhibition of INs disinhibits PCs 115
Fig 6.6 Effects of IN inactivation on PC post complex spike activity 116
Fig 6.7 ArchT expression in INs co-occurs with PC degeneration 118
Fig 7.1 Sensory stimulation induces rapid and delayed responses in INs and PCs 128
Fig 7.2 Rapid PC responses precede rapid IN responses by 1 ms 129
Fig 7.3 Rapid IN responses depend on vertical IN position 131
Fig 7.4 Relationship between spontaneous and sensory-evoked IN-PC cross-correlograms 133
Fig 7.5 The effect of IN spikes on PC sensory responses 135
Fig 7.6 The recruitment of INs during sensory processing is pathway-specific 137
Fig 8.1. Principles of microcircuit connectivity in the cerebellar molecular layer. 147

Abbreviations

ACSF	Artificial cerebrospinal fluid
AMPA	α -amino-3-hydroxy-5-methyl-isoxazolepropionic acid
ANOVA	Analysis of variance
CC	Cerebellar cortex
CF	Climbing fibre
CreER	Cre-estrogen receptor fusion gene
DCN	Deep cerebellar nuclei
FBI	Feedback inhibition
FFI	Feed-forward inhibition
GABA	γ -Aminobutyric acid
GC	Granule cell
IN	Molecular layer interneuron
IO	Inferior olive
LTD	Long-term depression
LTP	Long-term potentiation
nNOS	Neuronal nitric oxide synthase
NMDA	N-Methyl-D-aspartic acid
PBS	Phosphate-buffered saline
PC	Purkinje cell
PF	Parallel fibre
PSTH	Peri-stimulus time histogram
PV	Parvalbumin
SD	Standard deviation
SEM	Standard error of the mean
SOM	Somatostatin
VIP	Vasoactive intestinal polypeptide
VOR	Vestibulo-ocular reflex
Vs	Versus

1 Introduction

'I had always considered my thoughts as something abstract, but they weren't; they were as material as the heart beating in my chest. The same was true of the mind, the soul, the personality; all of it was fixed in the cells and originated as a result of various ways in which these cells reacted with one another. All of our systems, too – communism, capitalism, religion, science – they also originated in electrochemical currents flowing through this three-pound lump of flesh encased in the skull.

All of which was saying nothing. It was like examining a stone in the foundation wall to find the answer to the secret of St. Peter's Basilica.'

Karl Ove Knausgaard

1.1 The neuron doctrine and receptive fields

In the early 19th century, Jean Pierre Flourens carried out ablation studies in the central nervous system of live animals and concluded that the brain was where movement, sensation and cognition were generated (Flourens, 1824). Since then, researchers have been seeking to understand the function of the brain in various ways, driven by the tools available at the time. While Sigmund Freud found the state of nervous system research not advanced enough to explain psychodynamic concepts and therefore abandoned the field (Northoff, 2012), others delved deep into the fine architecture of the brain using histological techniques. With a silver nitrate staining method developed by and named after Camillo Golgi, it became possible to visualize individual neurons in nervous tissue due to the sparsity of the resulting labelling. Golgi himself proposed that neurons form a syncytium, a single continuous network.

Ramón y Cajal, by many considered the founder of modern neuroscience (Sotelo, 2003), adopted and improved the Golgi method to visualize individual neurons. With enormous attention to detail and artistic excellence, he created beautiful drawings of individual neurons as well as of several neurons stained together in the same

preparation (Ramón y Cajal, 1888) (Fig 1.1). Based on careful observation, he reached a conclusion contrasting Golgi's: remarking only contiguity, but not continuity between cell processes, Cajal postulated that nervous tissue does not consist of a continuous network, but that individual neurons are the structural and functional building blocks. This concept became known as the neuron doctrine, and has had a fundamental impact on the development of modern neuroscience (Sotelo, 2003; Yuste, 2015).

Cajal's legacy even goes beyond the notion of individual neurons: he also identified different classes of neurons based on large differences in morphology (Fig 1.1.). He furthermore realized that these various neuron types were arranged in stereotypical manners in different parts of the brain. While it was known that the gross anatomy of the brain seemed to exhibit different areas such as the neocortex and the cerebellum, Cajal highlighted early on that nervous tissue is made up of stereotyped microcircuits, a notion at the heart of systems neuroscience.

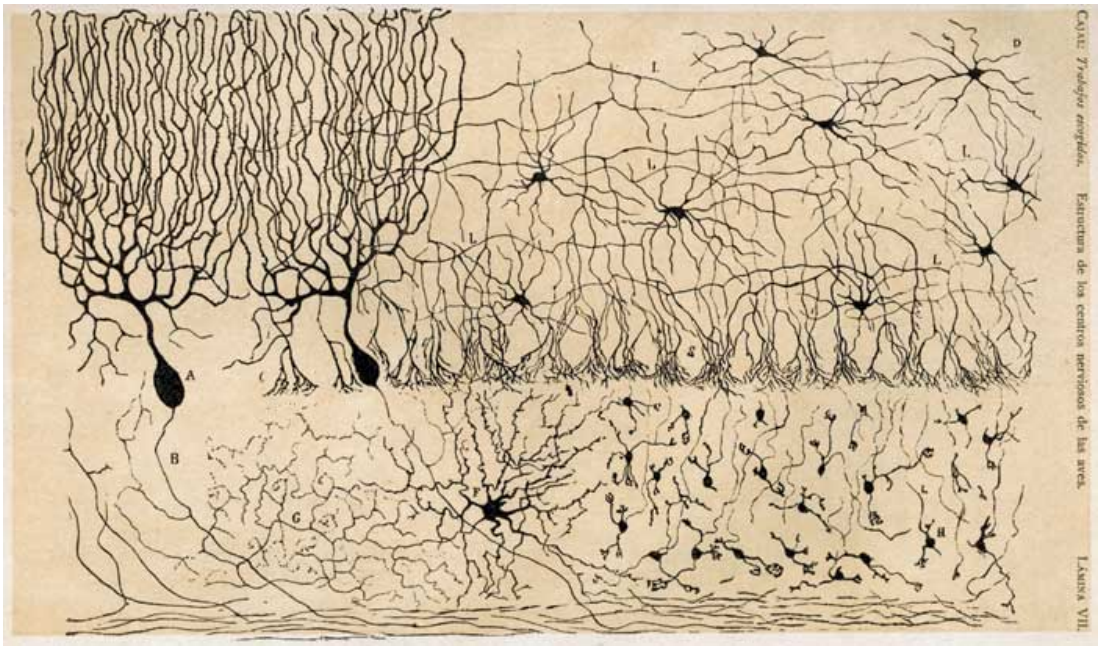

Fig 1.1 A drawing of cerebellar cortex by Ramón y Cajal

This drawing of the cerebellar cortex of a chick depicts five different neuron types: (A) Purkinje cell, (D) stellate cell, (F) Golgi cell, (H) granule cell, (S) axons of basket cells. Reproduced from Sotelo 2003, Cajal 1888.

The neuron doctrine was later irrefutably confirmed by the identification of synapses in electron microscopic images (Palay, 1956; Porter et al., 1945): Palay concluded that in all electron microscopic studies to date, 'there is a discontinuity between the cytoplasm's of the pre- and postsynaptic elements, each of which is surrounded by its own cell membrane' (Palay, 1956). He further noted the presence of presynaptic vesicles, and suggested them to contain chemical transmitters of neural activity, a claim that was later experimentally verified.

The relevance of the neuron doctrine in the following decades of neuroscience research is mirrored in functional studies describing the activity of individual neurons. With the advent of microelectrode techniques, it became possible to record the electrical activity of single neurons in the intact animal. Single neurons could thus not only be studied anatomically, but also functionally, by identifying stimuli that a given neuron responded to with changes of activity levels. In this way, the function of single neurons was defined by their 'receptive field', i.e. the landscape of e.g. visual input that would drive firing rate changes in a given neuron. This approach allowed for the generation of maps of sensory-driven activity in the retina as well as in neocortical areas (Hubel and Wiesel, 1962, 1959). In their seminal studies on visual responses of single neurons in the cat, Hubel and Wiesel described that neurons in visual cortex, in contrast to retinal ganglion cells, were not easily driven by large visual stimuli, but instead by bars presented at a specific orientation or moving in a certain direction. They furthermore described 'complex cells' that were only driven by more complicated stimuli, suggesting that convergence of simple cells with different receptive fields could give rise to the firing patterns of complex cells.

This concept of hierarchical processing, with neurons building more and more abstract and invariant representations of sensory input along the hierarchy of sensory pathways, ultimately culminated in the description of highly invariant object recognition cells in the medial temporal lobe of monkeys and humans. Single neurons were found to consistently respond to specific categories of objects such as faces across a wide range of metric image features, indicating abstract representations (Kreiman et al., 2000). Even more sensational, researchers later described neurons that only responded to presentations of specific famous people, coining the 'Jennifer Aniston cell' and the 'Halle Berry cell' (Quian Quiroga et al., 2005). The level of invariance in these neurons seemed especially high, as they did

not only respond to images of the respective people, but also to letter strings of their names.

How is one 'Halle Berry' neuron generated, and what is the exact role of these single neurons in perception and recognition? How many 'Halle Berry cells' are there, and how does their activity as a population enable recognition? As useful as microelectrode recordings have been and continue to be for the description of feature selectivity in individual neurons, they cannot create complete representations of inputs into the central nervous system, especially given high trial-to-trial variability of individual neurons to identical sensory stimuli (Shadlen and Newsome, 1998). Instead, what has been learned from a parallel approach of building artificial neural networks and investigating their computing capabilities, in order to understand nervous system function?

1.2 Models of neural networks

Equally inspired by the neuron doctrine as physiologists studying receptive fields, theorists started using the computing capacity of individual neurons to build neural network models. Considering neurons to be binary units, i.e. either spiking or non-spiking, and to have a threshold for spike generation that individual inputs could summate to reach, individual neurons could perform basic logical Boolean operations, such as AND or OR. Out of these building blocks, McCulloch and Pitts assembled strings and loops of neurons to build simple mechanistic models of the brain, and demonstrated that they could perform any logical operations that a Turing machine could (McCulloch and Pitts, 1943). Importantly, they identified redundancy and generality: Any logical operation could be performed by some network, and different networks could perform the same logical operation. The resulting dilemma was captured accurately in a letter from von Neumann to Wiener, Pitt's supervisor at the time:

"Indeed these authors have demonstrated in absolute and hopeless generality that anything and everything …can be done by (…) a neural mechanism – and that even one, definite mechanism can be 'universal'. Inverting the argument: Nothing that we may know or learn about the functioning of the organism can give, without 'microscopic', cytological work any clues regarding the further details of the neural mechanism." (Gefter, 2015).

Thus, while McCulloch's and Pitt's work was visionary for the development of computing machines and artificial intelligence, it highlighted that in order to understand nervous system function, information on the architecture of neural networks was indispensable.

More complex models of neural network function inspired by network architecture emerged in the following decades. One classical example is the perceptron, pioneered by Rosenblatt in the fifties (Rosenblatt, 1958). Based on the notion that the gross structure of the nervous system was known, but the precise connectivity was not, Rosenblatt formulated a model in terms of probability theory and not on symbolic logic like his predecessors. This model thereby took into account that neural connectivity may not be identical between different individuals, but emerging from the same basic structure based on experience and learning. The structure of a perceptron is feed-forward, consisting of several areas with mostly unidirectional flow of information, and randomly connected units. It had the capacity to learn to associate specific stimuli with specific responses, and could also correctly associate new stimuli with higher-than chance probability. Crucially, the model's learning capacity could be probed as a function of anatomical and physiological variables such as absolute number of units, convergence ratios, and activity thresholds, paving the way for linking learning curves with measurable variables of biological systems. While Rosenblatt visualized the principle of a perceptron using the visual system in his original publication, its general applicability became obvious when Albus suggested that the cerebellar cortex might function as a perceptron. He mapped the different stages of feed-forward processing precisely onto the different elements of the cerebellar circuit, generating testable predictions for connectivity and the implementation of learning rules (Albus, 1971).

Another class of neural network models that emerged is characterized by recurrent architecture, i.e. by feedback instead of predominantly feed-forward connections. These networks can spontaneously form stable activity patterns called 'attractors', and have been proposed as mechanistic explanations of e.g. pattern completion capabilities and sequential neuronal activity during spatial navigation (Rajan et al., 2016; Schmidt-Hieber and Häusser, 2013; Yuste, 2015). Again, these models suggest specific connectivity patterns (and learning rules) to underlie the

computation, and the exact mapping of computational unit to neuronal circuit unit is not known.

The principle that emerges from the consideration of neural network models echoes the implications of receptive field studies: Knowing the activity of single neurons is not sufficient, and more detailed knowledge about the concerted activity of neuronal microcircuits is necessary to obtain a coherent picture of how the central nervous system functions.

1.3 Inhibition and its role in microcircuits

In the analysis of neural circuit structure, it soon emerged that nervous system function relies on the interplay of two opposing building blocks: excitation and inhibition. Based on his extensive studies on the spinal flexion-reflex of the leg, Sir Charles Sherrington concluded as early as 1932 that inhibition seemed as ubiquitous as excitation, and that understanding the interaction of the two was essential to elucidate nervous system function (Sherrington, 1932). Eccles later not only contributed to the identification of chloride being the main ionic mediator of inhibition at the synapse (Eccles, 1943), but also was among the first to demonstrate the implementation of inhibition on the microcircuit scale by identifying hippocampal basket cells as inhibitory neurons mediating feedback inhibition (Andersen et al., 1963). Since then, what function has emerged for inhibition in the central nervous system? After describing the basic mechanisms of excitation and inhibition below, I will subsequently illustrate different aspects of inhibitory neurons, which will again highlight the importance of information on neural circuit activity on the microcircuit level.

1.3.1 Ionic mechanisms of excitation and inhibition

Excitation and inhibition are mediated by different ionic and molecular mechanisms. Synaptic excitation and inhibition involve the release of specific neurotransmitters that are subsequently bound by postsynaptic (and extrasynaptic) ionotropic and/or metabotropic receptors. Ionotropic receptors are ligand-gated transmembrane ion channels forming an ion channel pore, temporarily increasing the membrane's

conductance to specific ions, whereas metabotropic receptors do not form an ion pore themselves, but interact with ion channels in the membrane through intracellular second messenger cascades. The resulting increase of membrane conductance to specific ions leads to a change in relative ionic concentration inside the neuron and thus to a change in membrane potential (Kandel et al., 2000) .

Excitation is predominantly implemented by neurons releasing glutamate, the most abundant neurotransmitter in the vertebrate nervous system. Postsynaptically, it is commonly bound by AMPA receptors (AMPARs). These are ionototropic glutamate receptors forming a tetramer from four types of subunits. Upon binding of glutamate, AMPARs increase their permeability to cations, i.e. sodium, potassium and calcium, with a reversal potential of 0 mV, meaning that at membrane potentials below 0 mV, activation of AMPARs will result in net inward flow of cations, leading to an excitatory postsynaptic potential (EPSP) (Kandel et al., 2000). The receptor's subunit composition greatly affects its permeability to calcium, which is modifiable through synaptic activity (Liu and Cull-Candy, 2000). AMPARs mediate rapid excitatory neurotransmission the brain, with the exact kinetics being determined by the receptor's subunit composition.

Another crucial class of ionotropic glutamate receptors are NMDA receptors (NMDARs), which are also permeable to cations. However, NMDAR cation channels are blocked by intracellular Mg^{2+} at resting membrane potentials. The Mg^{2+} block is voltage-dependent, i.e. it is released at depolarised membrane potentials, such that NMDARs only contribute to postsynaptic excitation when the neuron is already depolarised, e.g. by previous AMPAR activation. NMDARs exhibit much slower kinetics than AMPARs and mediate large and long-lasting Ca^{2+} influxes, thus playing an important role in synaptic plasticity.

Inhibition in the central nervous system is primarily mediated by neurons releasing the neurotransmitter GABA. GABA then commonly acts upon $GABA_A$ receptors ($GABA_A$Rs), which are ionotropic receptors permeable to chloride and bicarbonate anions with a reversal potential of around - 70mV, thus resulting in inward anion flow and an inhibitory postsynaptic potential (IPSP) at common membrane potentials above -70 mV (Isaacson and Scanziani, 2011). In developing neurons, however, responses to GABA are often excitatory, as the intracellular chloride concentration in

developing neurons is higher due to the developmentally delayed expression of the K^+-Cl^--transporter KCC2 (Ben-Ari, 2002). $GABA_A$Rs are pentamers made up of different subunit combinations and, like AMPARs, exhibit fast kinetics, with the exact characteristics depending on the specific subunit composition. $GABA_A$Rs can also be activated by ambient GABA in a tonic manner, resulting in a tonic inhibitory conductance that affects synaptic integration (Farrant and Nusser, 2005). Unlike $GABA_A$Rs, $GABA_B$ receptors are metabotropic, exerting inhibition through a G-protein linked activation of potassium channels, with a reversal potential of around -100 mV.

1.3.2 Diversity of inhibitory cell types

Inhibitory neurons are often referred to as interneurons because their axonal projections tend to stay local within a given microcircuit. They exhibit great variety in terms of various features, especially in the neocortex, and to this day no consensus has been reached as to their classification into different categories (Markram et al., 2004; Tremblay et al., 2016). Historically, morphological and electrophysiological characteristics were the criterion by which interneurons were distinguished. This approach has more recently been complemented with analyses of the molecular makeup of interneurons. In some cases, molecular markers seem to unite morphologically distinct classes of interneurons, whereas in others, groupings of various characteristics are incongruent with each other (Tremblay et al., 2016). Ongoing efforts of RNA-sequencing large numbers of interneurons and searching for clusters in their high-dimensional genetic profiles is another promising approach of categorization (Zeisel et al., 2015).

1.3.3 Postsynaptic effects of inhibition depend on target location

One important characteristic differing between interneuron classes is the location of the interneurons' axonal projections onto their postsynaptic targets. Interneurons often synapse onto principal cells, i.e. the projection cells that transmit local computations to other brain areas. Some interneuron classes, such as the neocortical SOM cells (identified by the expression of the peptide hormone somatostatin) target the dendrites of principal cells, whereas neocortical PV cells

(identified by the expression of the calcium-binding protein parvalbumin) target the somatic region. Given that action potentials are generated depending on the local voltage at the axon initial segment (Clark et al., 2009), and postsynaptic potentials decay exponentially with distance from the synaptic input site following the laws of cable theory (Rall, 1967), an inhibitory synapse located in the perisomatic region can have a strong inhibitory effect on postsynaptic spike output (Miles et al., 1996). Inhibitory synapses located in the dendrite, in contrast, cause postsynaptic inhibitory potentials that are strongly attenuated at the postsynaptic spike initiation site, thus being bound to have minimal effects on spiking. Moreover, the neuronal membrane acts as a low-pass filter, so that postsynaptic potentials originating at great electrotonic distances from the soma exhibit slower kinetics (Rall, 1967).

The specific targeting of dendritic instead of somatic postsynaptic regions by some interneuron classes suggests that inhibition may have functional relevance beyond decreasing postsynaptic spiking directly. The basis for such functional relevance lies in the fact that dendrites themselves can be considered computational units, owed to their morphology and excitability. In many cases, dendrites do not simply act as passive cables to relay current to the soma, but can amplify currents and even generate local dendritic spikes by being endowed with voltage-gated ion channels and/or NMDA receptors (NMDARs) (London and Häusser, 2005).
Dendritic spikes can be evoked by synaptic inputs and can trigger axonal action potentials, thus directly influence the output of a neuron (Golding and Spruston, 1998). They can be facilitated by the simultaneous occurrence of synaptic inputs and axonal spikes back-propagating into the dendritic tree, then resulting in axonal burst firing (Larkum et al., 1999). In principal cells of visual cortex, dendritic spikes are implied in the feature selectivity of sensory responses (Smith et al., 2013), and in hippocampus, their presence precedes the formation of place-specific axonal firing (Sheffield and Dombeck, 2015). Finally, as dendritic spikes are often accompanied by a transient increase in intracellular calcium concentration, they are crucial for plasticity (Holthoff et al., 2006).

Importantly, dendritic inhibitory inputs can strongly influence these dendritic electrical processes (Miles et al., 1996). In addition to their hyperpolarising effects, distal inhibitory inputs can create local shunting effects: increasing the local conductance, they decrease the neuron's input resistance, thereby lowering the

amplitude of the neuron's voltage response to nearby excitatory inputs active at similar times (Liu, 2004). Accordingly, dendritic inhibitory inputs have been shown to block the generation of dendritic calcium spikes measured electrically (Kim et al., 1995; Larkum et al., 1999), and optically (Callaway et al., 1995). Modelling the effect of dendritic inhibition on regenerative dendritic events revealed that especially distal inhibitory synapses, in opposition to proximal synapses 'on-path' between a dendritic segment and the soma, are potent attenuators of dendritic non-linearities, due to higher local input resistances towards the sealed ends of dendrites (Gidon and Segev, 2012).

Thus, dendritic inhibition appears to control local integration of excitatory inputs and plasticity, while somatic inhibition can potently affect the spike output of its target cell.

1.3.4 Inhibitory microcircuit motifs and function

Given a profound understanding of somatic and dendritic inhibition in isolation, it is further necessary to review how inhibition is actually implemented in local microcircuits, as this information is directly linked to possible functions of inhibition on the network level. Certain circuit motifs have been repeatedly identified across different brain regions, suggesting that they represent generalizable operations of inhibition in the central nervous system (Tremblay et al., 2016).

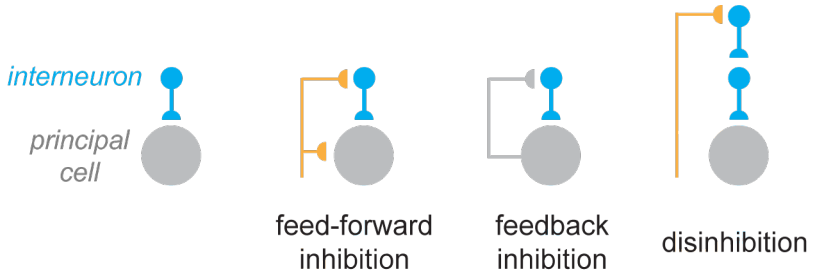

Fig 1.2 Inhibitory circuit motifs

Local interneurons (blue) inhibiting principal cells (grey) are embedded in different microcircuit motifs. In feed-forward inhibition (FFI), both the interneuron and the principal cell are excited by common afferents. In feedback inhibition (FBI), the interneuron is excited by the target it inhibits. In disinhibition, excitatory afferents excite interneurons that inhibit the interneurons delivering inhibition to the principal cell.

One such motif is **feed-forward inhibition** (FFI, Fig 1.2). It refers to a circuit organisation in which excitatory afferent inputs do not only contact a given principal cell, but also local interneurons that in turn inhibit the principal cell synaptically. Due to this arrangement, whenever the excitatory afferent is active, excitatory input into the principal cell is quickly followed by inhibition with one synaptic delay. Thus the occurrences of excitation and inhibition in this circuit are tightly linked. FFI seems ubiquitous in the central nervous system, especially in afferent sensory pathways such as thalamo-cortical projections to L4 of neocortex (Gabernet et al., 2005), as well as in the cerebellar cortex, both at the transformation of mossy fibre to granule cell activity at the input stage (Kanichay and Silver, 2008) and at the transformation of granule cell to Purkinje cell activity at the output stage (Andersen et al., 1964; Mittmann et al., 2005). It is also prevalent in the hippocampal formation, in transmission from CA3 to CA1. Interestingly, in many cases where FFI was described, the interneurons mediating FFI are PV-positive interneurons synapsing onto the somatic regions of their postsynaptic targets. Not only the location of their axonal projections, but also their intrinsic electrophysiological features are crucial: PV neurons are fast spiking, i.e. they respond to depolarising current steps with spikes of high frequency and small width (Hu et al., 2014).

The functions ascribed to PV interneurons across neural circuits are tightly linked to their position in FFI circuits: The FFI design imposes a certain proportionality between excitation and inhibition, possibly maintaining the delicate 'balance' of excitation and inhibition that seems crucial for nervous system function (Isaacson and Scanziani, 2011). FFI has been described as modulating the gain and increasing the dynamic range of principal cell responses to excitatory input: with the progressive recruitment of more interneurons by greater afferent excitation, more excitatory input is necessary to bring the principal cell to spike threshold, allowing cortical structures to respond to both small and large stimuli without saturation (Pouille et al., 2009). This function of FFI relies on the fact that interneurons are more rapidly recruited by afferent input than their principal cell targets.

Finally, the optimization for speed is reflected in FFI enforcing temporal precision in principal cell spiking. By delivering rapid somatic inhibition within milliseconds of excitation, FFI narrows the time window in which excitatory inputs can summate to drive spiking in the principal cell. Therefore, FFI can enforce coincidence detection in neural circuits, allowing principal neurons to respond to synchronous excitatory inputs only (Mittmann et al., 2005; Pouille and Scanziani, 2001). Finally, the

precision of interneuron spiking itself again can be controlled by FFI onto interneurons, relying on inhibitory synaptic connectivity between interneurons (Mittmann et al., 2005) and adding another layer of temporal precision in spiking.

Another microcircuit motif involving inhibitory interneurons is **feedback inhibition** (FBI, Fig 1.2). In this arrangement, the sources of excitatory drive to interneurons are not afferents with distant origins projecting into the local network, but excitatory input from within the network, namely from the population of principal cells that the interneurons inhibit. FBI thus implements inhibition that is proportional to the activity of the local network itself. FBI is a common circuit motif encountered e.g. in neocortex, the hippocampal formation, and the cerebellar cortex (Cesana et al., 2013; Pouille and Scanziani, 2004; Tremblay et al., 2016).

Both PV and SOM interneurons mediate FBI, but do so differently owing to differences in short-term dynamics to high-frequency synaptic inputs: PV interneuron responses are strong at the beginning of a high-frequency stimulus train, but depress quickly afterwards, whereas SOM interneuron responses are initially weak and facilitate over the course of the activation. Given that PVs and SOMs target the somatic and dendritic region of principal cells, respectively, inhibition is 'rerouted' from the soma to the dendrites during high-frequency firing of principal cells, with initial somatic inhibition and delayed dendritic inhibition (Pouille and Scanziani, 2004). FB inhibition via PV neurons is suited to act as a coincidence detector, as PV neurons, due to their fast time constants, will only respond to multiple synchronous excitatory inputs. In contrast, FB inhibition via SOM neurons can report integration of inputs over longer time scales, thereby feeding back the overall rate of spikes in the network.

FB inhibition has also been implicated in the generation of neural network oscillations such as cortical gamma-oscillations, which are proposed to allow the combination of information processed in different cortical areas by 'binding' ensembles of neurons oscillating in phase (Isaacson and Scanziani, 2011).

As inhibitory connectivity to principal cells is often dense (Packer and Yuste, 2011), and excitatory interconnectivity is sparse, activity from a small population of principal cells can cause inhibition of other principal cells that were not previously active. This form of FBI is sometimes termed lateral inhibition, and is suggested to mediate the competition between different cell assemblies: groups of principal cells that are the

most active in a given time window could inhibit other less active principal cells via FB interneurons in a 'winner-takes-all' scenario (Tremblay et al., 2016).

A final circuit motif whose relevance has emerged recently is **disinhibition** (Fig 1.2), where not principal cells, but the interneurons providing inhibition to principal cells are inhibited, thereby resulting in principal cell disinhibition. Disinhibition differs from FFI and FBI especially in the selective inhibition of a group of interneurons. This inhibition of interneuron activity relies on the phenomena that groups of interneurons with different effects on principal cell activity often inhibit each other (Pfeffer et al., 2013), and that afferent excitation into a local circuit can preferentially activate one group over the other. Disinhibitory motifs have been described across a range of neural circuits including neocortex, the amygdala, and hippocampus.

In neocortex, one disinhibitory motif is mediated by the selective activation of VIP (vasoactive intestinal polypeptide) neurons, a subclass of 5HT3a neurons, i.e. neurons expressing this specific ionotropic serotonin receptor. VIP neurons are a major target of cortico-cortico projections, e.g. VIP neurons in somatosensory cortex get excitatory drive from motor cortex. VIP neurons in turn preferentially inhibit SOM interneurons. Accordingly, during whisking activity, VIP neurons in somatosensory cortex are depolarized, whereas SOM neurons are hyperpolarized (Gentet et al., 2012; Lee et al., 2013). The inhibition of SOM neurons leads to disinhibition of principal cell dendrites and is associated with principal cell burst firing (Gentet et al., 2012; Royer et al., 2012). Thus, VIP-mediated disinhibition has been suggested to underlie sensorimotor integration, and top-down computations in general. In addition to horizontal inputs from other cortical regions, VIP neurons across neocortex are also excited by subcortical neuromodulatory systems: during locomotion, VIP neurons are activated by nicotinic inputs from the basal forebrain, leading to increased responsiveness of principal neurons to sensory stimuli (Fu et al., 2014).

Finally, disinhibition seems to play a crucial role in associative learning. In fear conditioning studies, the pairing of a neutral (e.g. auditory) with an aversive (e.g. foot shock) stimulus leads to the initially neutral stimulus evoking fear-related behaviour. Foot shock stimuli have been shown to activate interneurons in the superficial layer, i.e. L1, of neocortex, that in turn mediate inhibition of both PV and SOM cells, resulting in strong disinhibition of principal cells. This disinhibition leads to larger responses of principal cells in auditory cortex to the concomitantly

presented auditory stimulus, thereby possibly gating plasticity induction and memory formation (Letzkus et al., 2015, 2011).

While the identification of these inhibitory circuit motifs represents a major advance in our understanding of how interneurons contribute to circuit computations, it is important to stress that often, a given class of interneurons can be part of several microcircuit motifs, and that the function of a given interneuron class will depend on the context in which the circuit is activated. More precisely, contextual information includes the network state, e.g. neuromodulatory influences, as well as anatomical and physiological details of the local circuit, e.g. connection probabilities, synaptic strengths between microcircuit elements, and their short-term dynamics. Importantly, connectivity diagrams of neural circuits are constantly expanded and refined (Cesana et al., 2013; Jiang et al., 2015), and a lot of crucial information about functional connectivity between different circuit elements is still lacking.

1.4 Studying circuit architecture and activity

How can neural circuit architecture be studied, especially the interaction between excitatory and inhibitory microcircuit elements, both anatomically and functionally? There is a range of available tools differing in their ability to reveal detailed connectivity or functional interactions, their applicability to *in vivo* settings, and their throughput.

On one end of the spectrum, electron microscopy allows for the detailed reconstruction of dense neural connectivity in fixed brain tissue, with sub-micrometer resolution revealing the structure of synaptic connections unambiguously. This approach allows the creation of a complete map of all connections in a piece of brain, termed connectome. While serial electron microscopy enables the automation of cutting the tissue into thin slices, the bottleneck in applying electron microscopic techniques to large datasets is image processing. The reconstruction of the entire connectome of the worm *C. elegans*, consisting of around 300 neurons and 7000 synapses, took over a decade of work, relying on manual image segmentation (White et al., 1986). New machine learning algorithms are promising means of semi-

automated or even fully automated segmentation, but still need to be improved to reach human expert levels (Jain et al., 2010).

Electron microscopy thus allows for a highly quantitative analysis of connectivity between different cell types in a given block of tissue, including connection probabilities as well as numbers and positions of synaptic contacts. In isolation, however, it cannot inform on the statistics of input into the system, and can thus only make predictions based on locally generated activity patterns. Moreover, neuronal transmission does not only occur synaptically, but also extrasynaptically via volume transmission: Transmitters released at a given presynapse have been shown to not only activate receptors in the postsynapse, but also extrasynaptic receptors on the same postsynaptic neuron, and even receptors on other neurons in the vicinity (Oláh et al., 2009; Szapiro and Barbour, 2007). This form of transmission also termed 'spillover' transmission cannot be captured by the wiring diagram alone, but requires functional measurements of neural activity.

Such functional measurements of connectivity, on the other hand, are available with electrophysiological methods. *In vitro* whole-cell recordings using the patch-clamp method have been used extensively not just for morphological and electrophysiological analysis of individual neurons, but also to study the functional connectivity between neurons, both chemical and electrical. In this manner, pairwise connectivity and also higher-order connectivity maps have been generated, including measures of synaptic strength (Jiang et al., 2015; Pfeffer et al., 2013; Rieubland et al., 2014). Instead of testing connectivity by evoking presynaptic action potentials via a whole-cell recording, action potentials can also be evoked in cell-attached configuration, allowing for pipette reuse and higher throughput (Barbour and Isope, 2000; Isope and Barbour, 2002).

Paired *in vitro* recordings have also been combined with optical stimulation methods: Using focal one-photon glutamate uncaging, neurons situated within around 50-100 μm of the stimulation centre can be induced to spike, enabling rapid screening of layer-specific inputs into pairs of excitatory neurons. This method revealed that excitatory cortical neurons form subnetworks in which synaptically connected pairs are more likely to receive common input (Yoshimura et al., 2005). Two-photon uncaging, offering single-cell precision of presynaptic stimulation, in combination with fluorescent labelling of PV neurons and multiple patch-clamp recordings from excitatory cells, further enabled the finding that PV interneurons

exhibit dense, unspecific connectivity to local excitatory neurons (Packer and Yuste, 2011).

Another optical stimulation method that has advanced microcircuit dissection also *in vivo* is optogenetics, which refers to the manipulation of neural activity via the expression of depolarising and/or hyperpolarising opsins in neurons. Neuronal opsin expression can be achieved via electroporation, via viral vectors or via genetic modification of the organism, with the Cre-Lox system enabling transfection of molecularly defined cell types. This technique has been used to manipulate the activity of many neurons of a given interneuron class simultaneously *in vivo*, shedding light on their contribution to sensory tuning in neocortex (Adesnik et al., 2012; Olsen et al., 2012). Again, the two-photon effect can be employed to increase spatial specificity and achieve single-neuron resolution of stimulation in deeper tissue layers (Packer et al., 2012). However, the reliability of spike induction and the precise number of spikes induced by optogenetic stimulation varies between neurons depending on opsin expression levels, depth in the tissue and stimulation parameters, so that precise manipulation with single-spike resolution requires calibration via electrophysiological recordings (Pala and Petersen, 2015).

The two-photon effect has not only been used for precise stimulation, but also for monitoring the activity of visually identified neurons via fluorescent activity indicators. Calcium imaging has been used extensively to study population activity during sensory processing and behaviour (Dombeck et al., 2010; Ohki et al., 2005; Stosiek et al., 2003). The spatial unambiguity of two-photon calcium imaging, however, comes at the price of temporal precision: the timecourse of intracellular calcium signals associated with somatic spikes, as well as the kinetics of calcium indicators hamper the temporal resolution of calcium-aging. This issue is especially apparent in interneurons with high spontaneous firing rates, where calcium indicators can only report changes of firing rate over time as opposed to single spikes (Franconville et al., 2011).

A promising strategy to relate microcircuit activity during sensory processing to connectivity is to combine various complementary *in vivo* and *in vitro* methods. For example, *in vivo* two-photon calcium imaging of neuronal populations during sensory stimulation was combined with subsequent *in vitro* electrophysiological connectivity

assays of the same neurons. In these very challenging experiments, sensory tuning of excitatory neurons in primary visual cortex was found to relate to their interconnectivity: neurons with the same orientation preference exhibited increased probabilities of being connected to each other (Ko et al., 2011), and also showed much stronger synaptic connections (Cossell et al., 2015), suggesting that recurrent excitation is a dominant factor determining sensory tuning in layer 2/3 of visual cortex.

Finally, functional interactions of neurons within microcircuits *in vivo* are not only studied by presynaptic manipulation, but have also been inferred from monitoring the spontaneous spiking activity of different neurons simultaneously with tetrode recordings and subsequently cross-correlating the timing of their action potentials. With this approach, putative monosynaptic excitatory and inhibitory connections have been reported in various brain regions including neocortex, entorhinal cortex, and cerebellar cortex (Barthó et al., 2004; Blot et al., 2016; Buetfering et al., 2014). However, with extracellular multi-unit recording techniques such as tetrode recordings, the spatial location of a given neuron can only be estimated so that exact spatiotemporal interactions between neurons remain unknown.

One way to maintain the temporal resolution of electrophysiology and still unambiguously identify the neurons giving rise to the activity measured consists of patch-clamp recordings of several neurons simultaneously *in vivo*. This method has been used to investigate correlations of subthreshold activity of different neurons, excitatory synaptic transmission in neocortex (Jouhanneau et al., 2015; Poulet and Petersen, 2008) and synchronous spiking mediated by gap junction coupling in the cerebellar cortex (van Welie et al., 2016). It allows both the monitoring as well as the manipulation of neural activity with high temporal resolution, making it especially suitable for microcircuits with high spontaneous firing rates such as the molecular layer of the cerebellar cortex.

1.5 The cerebellar cortex

Since the drawings of Ramón y Cajal, the cerebellum has fascinated scientists with its crystalline structure, inspiring early theories of cerebellar function that still guide research today.

1.5.1 Gross anatomical organisation and distal connectivity

The cerebellum is divided into the cerebellar cortex (CC) containing the beautiful Purkinje cells (PCs) as principal projection cells, and the deep cerebellar nuclei (DCN). Communication between these areas is predominantly mediated by the inhibitory effect of Purkinje cells on DCN neurons via GABAergic synapses. Cerebellar output is exclusively carried by DCN neurons and has various targets including projections to neocortex via the thalamus and to the spinal cord via the brainstem.

The CC and the DCN receive excitatory inputs from two different sources. One source is the inferior olive (IO), whose axons entering the cerebellum are called climbing fibres (CFs). The IO receives inputs from many different sources such as ascending spinal inputs and descending neocortical inputs. The other source of excitation to the cerebellum is mossy fibres, again originating from many sources such as the pontine nuclei, vestibular nuclei, reticular formation and spinal cord.

The cerebellum is part of several anatomical loops highlighting its integrative, sensorimotor nature. With the IO, it forms the olivocerebellar loop: Each olivary subnucleus contralaterally projects to a single or several longitudinal zones of PCs in the CC, and also sends collaterals to a specific region of the DCN. Zonally organised PCs inhibit these DCN neurons which in turn inhibit the IO subnucleus from which they receive collaterals, resulting in a reciprocal topographic organisation (Chaumont et al., 2013; De Zeeuw et al., 1998). The IO and the cerebellum are furthermore part of the mesodiencephalic loop, which is formed of excitatory DCN projections to the mesodiencephalic junction that in turn excites the IO, again in a seemingly topographical manner (De Zeeuw et al., 1998). Finally, a functional loop between neocortex and the CC has been demonstrated, involving motor and sensory neocortical projections to the pontine nuclei that send converging inputs to PCs via the mossy fibre pathway. Again, PC activity is fed back into motor cortex, closing the loop (Proville et al., 2014).

Interestingly, the number of neurons in the neocortex and the cerebellum are correlated across many mammalian species (Herculano-Houzel, 2010), furthermore suggesting that the cerebellum functions in concert with other integrative brain areas.

1.5.2 Anatomy and physiology of the cerebellar cortex

Much focus in describing cerebellar anatomy has been on the cerebellar cortex (CC, Fig 1.3), due to its lattice-like repetitive architecture. The CC is divided into the granular layer, the molecular layer and the Purkinje cell layer, with the former being the input and the latter the output stage of the CC. Purkinje cells form the centrepiece of cerebellar cortex structure with their characteristic elaborate, parasagittally oriented dendritic trees spanning the vertical extent of the molecular layer, with minimal extension in the transverse plane. Being spontaneously active even in the absence of excitatory inputs (Häusser and Clark, 1997), Purkinje cells deliver tonic inhibition to their predominant targets in the deep cerebellar nuclei. In addition, PCs provide some feedback collaterals to other PCs as well as to interneurons (Witter et al., 2016).

Excitatory pathways

Climbing fibres from the inferior olive directly synapse onto PC proximal dendrites, forming the most powerful synaptic connection in the entire nervous system. Each PC receives input from a single CF via glutamatergic synapses, with a single CF innervating roughly 10 PCs (Llinás, 2013). Every CF spike results in a high-frequency burst of somatic PC spikes called the ‘complex spike’ lasting several milliseconds (Eccles et al., 1966). Being electrically coupled, IO neurons can fire synchronously, resulting in PC complex spike synchrony in sagittally oriented microbands defined by their CF input (Ozden et al., 2009). Mossy fibres, the other excitatory input into the CC, form synapses onto granule cells (GC), small and compact neurons in the granular layer that represent the most numerous neuron type in the brain. With on average four main dendrites and a single mossy fibre input per dendrite, each GC receives input from around four mossy fibres.

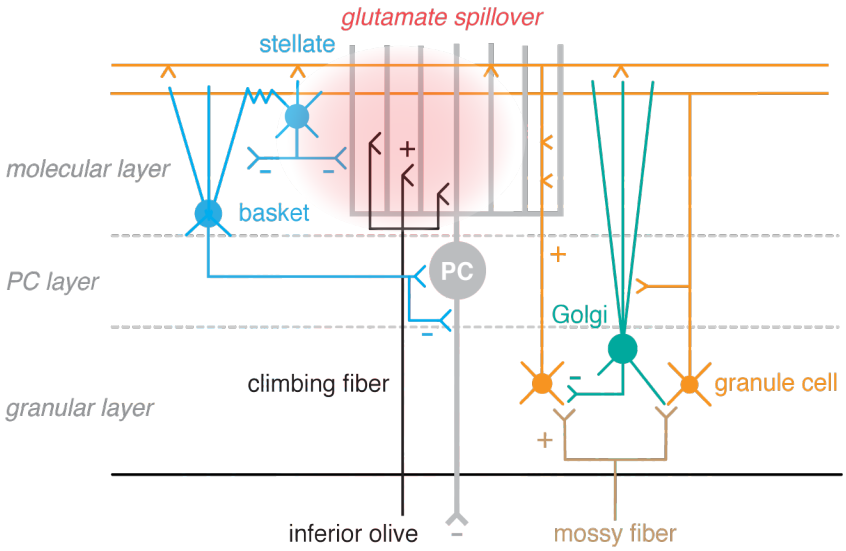

Fig 1.3 The circuitry of the cerebellar cortex

'<' denotes synaptic connections, + signs denote excitatory, - signs denote inhibitory connections. PC: Purkinje cell, the output cell. Excitatory afferents are mossy fibres and climbing fibres. Inhibitory interneurons are Golgi cells and molecular layer interneurons. The latter are traditionally divided into stellate and basket cells and are electrically coupled via gap junctions on their dendrites. Climbing fibre activity results in synaptic activation of the PC dendrite and in glutamate spillover activating neighbouring structures.

Glutamatergic contacts between mossy fibres and GCs are located in so-called glomeruli where a single mossy fibre synapses onto dendrites of around 15 different granule cells. As each mossy fibre gives input to around 40 glomeruli, the divergence ratio from mossy fibres to granule cells is estimated to be 600 (Eccles et al., 1967). Within a glomerulus, glutamate released from a given mossy fibre terminal does not only activate AMPA receptors on the directly opposing postsynaptic site of a single GC dendrite, but can diffuse to AMPA receptors on neighbouring GCs, resulting in spillover currents (DiGregorio et al., 2002).

The next excitatory circuit node, the granule cell-PC synapse, is not only a site of divergence, but also of great convergence. GC axons travel towards the top of the molecular layer and then bifurcate into parallel fibres running perpendicularly to PC dendrites for several millimetres. Granule cells can thus synapse onto directly overlying PCs via ascending axons, and onto several hundreds of PCs across large transverse distances via parallel fibres. Each PC gets synaptic input from as many as 175,000 parallel fibres (Napper and Harvey, 1988), but many of these inputs

appear silent, generating no detectable postsynaptic response (Isope and Barbour, 2002). Several reports suggest that the ascending axon synapses might have larger excitatory effects on PCs, as the functional granule cell-PC connection rate drops off with transverse distance (Isope and Barbour, 2002), and the unitary connection strength was found to be larger for ascending axon than for parallel fibre synapses (Sims and Hartell, 2005). However, the relative contribution of ascending axon synapses and parallel fibre synapses to PC spiking remains controversial and might rather be specific to cerebellar modules (Valera et al., 2016).

Interneurons

Various classes of inhibitory interneurons complement the architecture of the cerebellar cortex, each embedded in different microcircuits. At the input stage of the cerebellar cortex, Golgi cells provide potent inhibition to granule cells via predominantly GABAergic transmission. Golgi cell axons partake in the glomerulus, and Golgi cell-granule cell inhibition does not only occur in a phasic, but also in a tonic manner, meaning that even in the absence of phasic presynaptic vesicle release, GCs have a GABA-mediated conductance stemming from the activation of $GABA_A$ receptors (Chadderton et al., 2004; Farrant and Nusser, 2005; Kaneda et al., 1995). Golgi cells get excitatory input from mossy fibres, but also from granule cell ascending axons and parallel fibres, so that they can generate both feed-forward and feedback inhibition onto GCs (Cesana et al., 2013; Kanichay and Silver, 2008). Due to their microcircuit connectivity, Golgi cells have been implicated in controlling the precision and the gain of GC sensory-evoked responses. Furthermore, Golgi cell inhibition can precede mossy fibre excitation in GCs during sensory processing, suggesting parallel lines of mossy fibre input into GABAergically connected Golgi cell-GC pairs and implying a role for Golgi cells in ensuring the reproducibility of GC responses (Duguid et al., 2015). Finally, Golgi cells are electrically coupled to each other via gap junctions, enabling them to spike with precise synchrony and generating oscillations implicated in motor control (Dugué et al., 2009; van Welie et al., 2016).

Another major class of inhibitory interneurons is made up of molecular layer interneurons (INs). INs are found throughout the molecular layer, and are oriented similarly to PCs, with parasagittal dendrites and axons occupying the space between adjacent PC dendritic trees. They inhibit PCs via GABAergic synapses

(Andersen et al., 1964; Häusser and Clark, 1997; Midtgaard, 1992a; Vincent and Marty, 1996), with each PC receiving synaptic input from circa 7 to 10 INs (Häusser and Clark, 1997; Kim et al., 2014) and each IN contacting several PCs. Various features of INs vary across the vertical extent of the molecular layer, resulting in classical IN categorization into 'stellate cells' at the top and 'basket cells' at the bottom of the molecular layer (Palay and Chan-Palay, 1974): stellate cells have smaller somata and target PC dendritic segments, whereas basket cells have larger somata, more extensive dendritic trees, and target the PC soma and axon initial segment with basket-like axonal arborisations. Due to their axonal target locations, basket cells are positioned to have large inhibitory effects on PC spike output. Stellate cells targeting PC dendrites, on the other hand, are suggested to rather regulate PC dendritic excitability. Granule cells excite INs predominantly via synaptic AMPA receptors (Clark and Cull-Candy, 2002), resulting in feed-forward inhibition (Andersen et al., 1964; Mittmann et al., 2005) and lateral inhibition (Cohen and Yarom, 1998) onto PCs. Furthermore, INs are excited by climbing fibre input to PCs, solely via the spillover of glutamate onto IN AMPA and NMDA receptors (Szapiro and Barbour, 2007). Like Golgi cells, INs are also electrically coupled to each other, but also inhibit each other via GABAergic transmission, with each IN being coupled to 1 to 9 and inhibited by at least 2 INs (Alcami and Marty, 2013; Häusser and Clark, 1997; Kondo and Marty, 1998; Mann-Metzer and Yarom, 1999; Rieubland et al., 2014). INs have been implicated in PC spike timing precision, gain control, sensory feature selectivity, and plasticity.

Other less numerous interneuron classes in the cerebellar cortex have not been characterized in as much detail, including the Lugaro cells. These neurons situated in the granular layer are excited by serotonin, inhibited by PC recurrent collaterals, and seem to provide inhibition to several neuronal classes in the CC, including molecular layer interneurons, Golgi cells, and PCs (Dieudonné and Dumoulin, 2000). Another interneuron type is the unipolar brush cell, predominantly found in cerebellar regions involved in vestibular processing. It stands out by being the only excitatory interneuron in the CC, suggested to amplify and coordinate vestibular mossy fibre inputs by means of feed-forward excitation onto granule and Golgi cells (Schilling et al., 2008). Unipolar brush cells appear to form two subclasses based on differential expression of the molecular marker calretinin and the metabotropic glutamate receptor mGluR1α (Mugnaini et al., 2011), but defining unipolar brush

cells unambiguously in terms of their molecular makeup remains challenging as no specific molecular marker exists (Schilling et al., 2008). The most enigmatic interneuron class is the candelabrum cell found in between PC somata, for which no inputs and targets have been defined unambiguously (Schilling et al., 2008).

1.5.3 Plasticity in the cerebellar cortex

The cerebellum is believed to be a critical site of associative learning, and numerous forms of plasticity, i.e. activity-dependent changes in neuronal transmission, have been identified that could underlie various aspects of learning. The form of plasticity that for a long time was thought to be the key to cerebellar function is parallel fibre (pf)-PC long-term depression (LTD), guided by climbing fibre (CF) input. In this form of plasticity, PC responses to pf inputs decrease after repeated pairing of pf and CF input (Ito and Kano, 1982). Repeated pf activation alone, conversely, has been shown to lead to pf-PC LTP (long-term potentiation) (Lev-Ram et al., 2002). Whether LTP or LTD is induced depends on the postsynaptic calcium concentration, with large CF-associated calcium levels in PCs favouring LTD, resulting in an anti-Hebbian learning rule for PC plasticity (Coesmans et al., 2004; Piochon et al., 2012). This anti-Hebbian plasticity rule contrasts the classical Hebbian postulate, now often known as 'cells that fire together, wire together'. At many other synapses throughout the CNS, spike-timing dependent plasticity appears to implement this rule, as postsynaptic spikes serve as instructive signals to potentiate previously active synaptic input, leading to LTP (Piochon et al., 2012). IN PCs, however, the instructive CF signal weakens previously active parallel fibre inputs into the PC, thus representing an inversion of classical Hebbian learning.

Plasticity of synapses onto INs, on the other hand, appears to follow a learning rule that is opposite to the one at pf-PC synapses and thus in line with classical, Hebbian learning: Stimulation of pfs alone results in pf-IN LTD (Liu and Cull-Candy, 2000), whereas stimulation of pfs in conjunction with somatic IN depolarisation favours LTP (Rancillac and Crépel, 2004).

Synaptic plasticity has also been demonstrated at various elements of the granular layer: mossy fibre-granule cell synapses can undergo both LTP and LTD, and pf-Golgi cell synapses can show LTD (Gao et al., 2012). Moreover, many cell types in

the cerebellar network can display intrinsic plasticity, i.e. modification of a neuron's electrical properties through changes in ion channel expression. Ultimately, cerebellar function and learning are suggested to rely on synergistic, distributed plasticity across the cerebellar cortex, rather than on one single mechanism for different types of motor learning (Gao et al., 2012).

1.5.4 Theories of cerebellar function

The Marr-Albus theory and the adaptive filter model

Since the first experimental lesion studies by Flourens revealing large motor deficits after cerebellar insult (Flourens, 1824), cerebellar function has predominantly been considered in the context of motor execution and motor learning. Early theories of cerebellar function thus aimed at creating a framework that allows the cerebellar network to learn specific movements. In 1969, Marr published his 'theory of cerebellar cortex', at the heart of which is the special relationship between a Purkinje cell, its thousands of pf inputs, and its single CF input. He suggested that CF input, representing a 'cerebral instruction for an elemental movement', would potentiate concurrently active parallel fibre inputs that signal the context of a given movement to the PC. Thereby, after learning, the context itself, i.e. the given set of active parallel fibres, would suffice to generate the movement (Marr, 1969). He further postulated that no other synapse in the circuit should be modifiable. The mossy fibre-GC divergence was said to be a 'pattern separator', amplifying differences between similar input patterns. With regards to molecular layer interneurons, Marr's theory required them to have a powerful influence over PC output, but their main function should be setting an appropriate threshold for PC activity.

Equally inspired by the compelling anatomy of massive divergence and subsequent convergence of inputs in the cerebellar cortex, Albus published his independently generated 'theory of cerebellar function' in 1971. He suggested that the cerebellar cortex functions as a perceptron, a pattern classification device under the control of CF input (Fig 1.4). Similar to Marr's work in many ways, Albus' ideas differed in several aspects: conjunctive pf and CF input was proposed to lead to LTD and not LTP of pf-inputs into PCs (Albus, 1971), which was experimentally proved to be

correct (Ito and Kano, 1982) and in accordance with many pf-PC synapses being silent (Isope and Barbour, 2002).

Moreover, Albus did not consider molecular layer interneurons to be mere threshold setting devices, but to have a crucial role in the pattern separation capabilities of the perceptron by also being modifiable by CF input. A pattern-recognition device based only on excitatory weight adjustments has low capacity and learns slowly, so Albus fathomed that if pf-IN synapses were modifiable by CF input, recognition capacity would be increased thousandfold. In setting up the required learning rules for INs, he classified INs according to whether they receive the same parallel fibre input as their PC target, in essence based on their participation in feed-forward inhibition. He then argued that only such INs that share pf input with their targets should exhibit an opposite learning rule to PCs: conjunctive pf and CF input should then lead to LTP instead of LTD. This setup would act in synergy with pf-PC plasticity. Ultimately, PCs were postulated to pause their spiking in response to learned parallel fibre input patterns.

In both theories, the CF input provides a teaching signal to parallel fibre inputs, implementing a supervised learning algorithm.

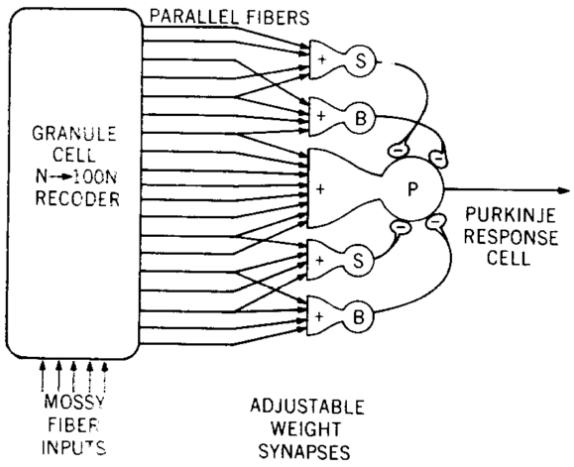

Fig 1.4 The cerebellar perceptron by Albus

The cerebellar cortex as a perceptron. P: Purkinje cell, S: stellate cell, B: basket cell. Mossy fibre input is recoded in the granular layer and conveyed to PCs and interneurons via parallel fibre synapses whose weights are adjustable. Reproduced from (Albus, 1971).

Decades later, the Marr-Albus theory was reformulated in terms of linear system analysis as an adaptive linear filter to allow for the processing of time-analogue signals such as neuronal firing rates (Fujita, 1982). In an adaptive filter, an input signal is transduced through a bank of fixed filters into a set of signals that are then combined through adjustable weights to form an output signal. Applying this to the cerebellar cortex, the mossy fibre input signals are transduced into parallel fibre component signals that are recombined at the PC, with weights according to individual pf-PC synapses (Fig 1.5). The filter is an adaptive one as the components' weights are bidirectionally adjustable, again under the control of the CF, according to the covariance learning rule: positive pf-CF correlations lead to weight decreases (LTD), whereas negative pf-CF correlations cause weight increases (LTP), a notion in accordance with experimental data (Coesmans et al., 2004). If the teaching signal represents performance error, this learning rule theoretically minimizes the mean square performance error (Dean et al., 2010).

However, in simple adaptive filter models, the weights can switch between positive or negative values, whereas pf-PC synapses are excitatory and could thus theoretically signal minimal weights of 0, but not negative values. Again, the inclusion of molecular layer interneurons with opposite learning rules into the model provides a solution, as pf-IN-PC pathways could represent negative adjustable weights (Dean et al., 2010). Therefore, like in the original Albus model, adaptive filter models require pf-IN synapses to be plastic under the control of CF input.

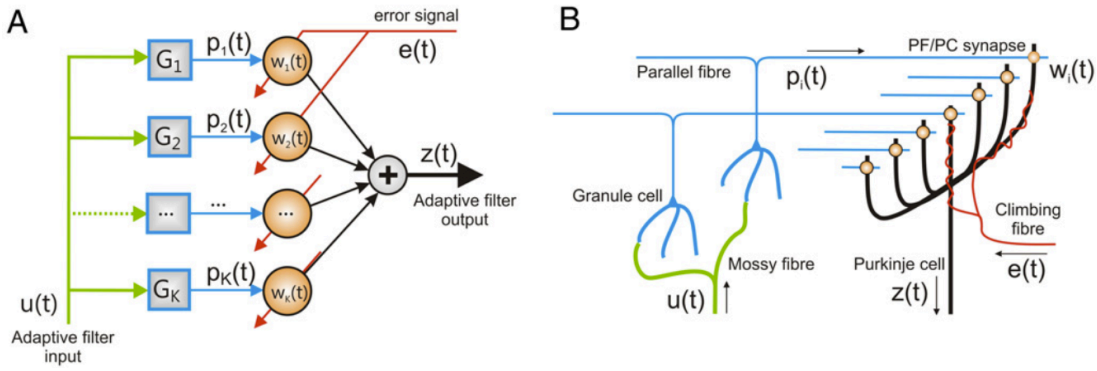

Fig 1.5 The cerebellar cortex as an adaptive filter

(A) Systems diagram of a general adaptive filter. Input signals (u) are transformed by a set of filters (G_1 – G_k) into signals (p_1 – p_k) that are recombined according to specific weights (w_1 – w_k) to form the output signal (z). Weights are adjusted by an error signal (e) following the

covariance learning rule. (B) Mapping of the adaptive filter components onto circuit elements of the cerebellar cortex. Reproduced from (Porrill et al., 2013).

Internal models

Cerebellar function is often considered to be the formation of internal models, categorized into inverse and forward models. Internal models have adaptive filters as their learning elements, and impose specific requirements on the external connectivity of the cerebellum (Porrill et al., 2013). In inverse models, the cerebellum acquires an inverse dynamics model of the controlled object, i.e. of the muscles targeted by its output. Such an inverse model appears necessary because commands instructing a desired trajectory for a body part must be converted into a form that is appropriate for the characteristics of the motor plant, introducing specific distortions. In these models, mossy fibre input carries information about the desired motion, and the error signal carried by the climbing fibres is a motor error, i.e. the difference between the desired and the actual motor commands to the motor plant. The latter requirement poses a challenge for the feasibility of inverse models, because such a thing as 'motor error' requires a transformation from sensory coordinates in the first instance, e.g. from visual, proprioceptive or cutaneous information mediating that a given movement was erroneous (Wolpert et al., 1998).

In another form of internal model termed forward model, the function of the cerebellum is to predict sensory consequences of movement by learning the association between motor commands and resulting sensation. This concept is in line with the notion that the intact cerebellum makes it impossible to tickle oneself by performing 'noise cancellation' (Porrill et al., 2013). In forward models, the mossy fibres carry a motor efference copy, and the climbing fibres carry the learning signal being error in model output. The model output must therefore target a structure that compares the model's predictions from the actual sensory consequences of movement, and feeds the difference back into the model via the CFs. The biological plausibility of internal models remains controversial, and assessing their possible implementation highlights the need to understand how the cerebellum is integrated into distributed brain circuits.

1.5.5 Experimental models of cerebellar function

The relevance of different plasticity forms and theories for cerebellar function has been assessed in various cerebellar-dependent learning paradigms, one being vestibulo-ocular reflex (VOR) adaption. In the VOR, vestibular signals from head rotation are converted into compensatory eye movements to stabilize the image on the retina. Adaption of this reflex by changing the gain of visual displacement accompanying vestibular stimulation depends on the cerebellar flocculus (Boyden et al., 2004). The error signal in VOR adaptation is of visual nature, i.e. the retinal slip. Another widely used paradigm is eyeblink conditioning, a form of classical conditioning. Through the repeated presentation of a neutral stimulus, e.g. a tone, followed by an airpuff to the eye, subjects learn to perform a well-timed eyeblink after tone onset in anticipation of the puff. Learning appropriately timed eyeblinks relies on the intact cerebellum (Yeo and Hesslow, 1998). In this paradigm, the error signal is the aversive airpuff.

In eyeblink conditioning, the expression of conditioned eyeblink responses correlates with pauses in Purkinje cell firing (Ohmae and Medina, 2015; ten Brinke et al., 2015). This is in agreement with Albus' original suggestion of learned PC pauses mediating movement, which has also been verified experimentally (Heiney et al., 2014). The pause of PC spiking mediating conditioned eyeblink responses may furthermore be mediated by inhibition from molecular layer interneurons (ten Brinke et al., 2015) and by intrinsic plasticity of the PC itself, via the metabotropic glutamate receptor mGluR7 (Johansson et al., 2015, 2014).

Many experimental studies, including VOR adaptation and eyeblink conditioning, support the notion of classical cerebellar theories that CF input transmits error signals: CF-evoked Purkinje cell complex spikes correlate with performance errors (Kimpo et al., 2014; Medina and Lisberger, 2008; ten Brinke et al., 2015). Moreover, the occurrence of CF input on a given trial correlates with improved performance as well as with stronger Purkinje cell suppression on the following trial, giving strong support to the idea that CF-mediated plasticity at the level of PCs indeed underlies motor learning (Medina and Lisberger, 2008). Finally, sensory-evoked CF input can be replaced by optogenetic CF activation to induce motor learning (Kimpo et al., 2014). In addition to conveying error signals, CF input may also be a motor signal mediating conditioned responses, i.e. the conditioned eyeblink, as complex spiking

was found to be related to the expression of conditioned responses (ten Brinke et al., 2015). However, in another study, no trial-to-trial relationship was found between complex spikes and conditioned eyeblinks. Rather, CF input could be elicited by novel stimuli, and by the conditioned stimulus at the end of conditioning, leading the authors to liken CF activity to dopaminergic teaching signals mediating both prediction errors and saliency (Ohmae and Medina, 2015). Furthermore, the ability of CF input to guide motor learning seems context-dependent: In contrast to VOR increase learning, VOR decrease learning is not achieved by optogenetic CF stimulation, despite CFs signalling motor errors in both types of learning (Kimpo et al., 2014).

Several studies have taken the approach to inhibit molecular pathways of plasticity, or to prevent the expression of specific postsynaptic receptors in molecularly defined cell types of mutant mice. Exposing these mice to cerebellar learning paradigms revealed that postsynaptic LTP in PCs seems crucial for motor coordination and motor learning, while genetic manipulations targeting LTD in PCs gave conflicting results (Gao et al., 2012).The relevance of synaptic PC LTD for cerebellar learning was further questioned by a study demonstrating that PC pauses to conditioned stimuli relied on the metabotropic mGluR7 receptor, bringing attention to mechanisms of intrinsic plasticity (Johansson et al., 2015).

Where does this heterogeneity of experimental results regarding mechanisms of cerebellar learning stem from? Despite its lattice-like repetitive structure, the cerebellar cortex shows regional heterogeneity, both molecularly and functionally, suggesting that different cerebellar regions may differentially implement various types of learning. Aldolase C / zebrin II is a common marker in PCs, revealing that the cerebellar cortex is organised into longitudinal zones (Brochu et al., 1990). Zebrin bands appear defined by their climbing fibre input, as PC complex spike synchrony drops off strongly at zebrin band borders (Tsutsumi et al., 2015). Furthermore, intrinsic PC activity differs between zebrin bands: in zebrin-negative regions, baseline PC simple spike and complex spike activity is higher than in zebrin-positive bands, suggesting that different bands operate at different target frequencies (Zhou et al., 2014). Zebrin-negative bands with high Purkinje cell activity may be more prone to pf-PC LTD, whereas in zebrin-positive bands with lower Purkinje cell activity, LTP may be favoured. As different motor learning paradigms

indeed depend on different areas of the cerebellar cortex (VOR learning depends on the flocculus, which is predominantly zebrin-negative, whereas eyeblink conditioning seems to depend on lobule HVI (Mostofi et al., 2010), a predominantly zebrin-positive region), it is conceivable that the intrinsic properties of different zones guide the predominant form of pf-PC plasticity observed, which in turn may be optimised for the type of behaviour that is controlled by a given zone.

1.5.6 Molecular layer inhibition and cerebellar function

As molecular layer interneurons (INs) provide inhibition to PCs, INs are in a position to cause PC spike suppression, leading to deep cerebellar nuclei disinhibition and ultimately movement (Heiney et al., 2014). INs exhibit considerable levels of spontaneous activity *in vivo*, providing tonic inhibition to their targets (Armstrong and Rawson, 1979; Eccles et al., 1966). *In vitro* results demonstrate that even single spikes in single INs can strongly inhibit spiking in postsynaptic PCs (Häusser and Clark, 1997), but the functional impact of single INs on PC spike output *in vivo*, with physiological levels of synaptic background input, remains unknown.

IN interconnectivity, consisting of gap junctions as well as of GABAergic synapses, is organised parasagittally (Rieubland et al., 2014), implying that IN function is local to parasagitally organised microzones defined by CF input. Gap junction coupling has been shown to increase the spatial convergence of IN-PC inhibition in the parasagittal plane (Kim et al., 2014). Furthermore, gap junctions may mediate synchrony *in vitro* (Mann-Metzer and Yarom, 1999), while inhibitory connections may serve to decorrelate the activity of the IN network, stabilizing it as a whole. The IN microcircuit activity patterns that result from the interplay of electrical coupling, synaptic inhibition and physiological excitatory inputs *in vivo* remain largely uncharacterized.

INs have been repeatedly implicated in controlling the exact timing of cerebellar output signals (Jörntell et al., 2010). Their electrophysiological characteristics of high input resistance and rapid responses to excitatory and inhibitory inputs seem optimized for transmission on fast time scales (Carter and Regehr, 2002), also evident in rapid, precisely-timed sensory-evoked responses (Chu et al., 2012). Their microcircuit position supposedly mediating feed-forward inhibition may enforce

coincidence detection of excitatory inputs to Purkinje cells (Mittmann et al., 2005). However, to what degree INs really do mediate feed-forward inhibition *in vivo*, that is whether they are activated by the same set of granule cell inputs as their PC targets, remains controversial (Dean et al., 2010).

One important prediction of adaptive filter models is that inhibition from INs to PCs can be adapted by a climbing fibre teaching signal. Thus, long before the pure spillover connection from CFs to INs was experimentally demonstrated (Szapiro and Barbour, 2007), INs were postulated to receive CF input. Direct evidence for IN activity modulation by physiological CF input *in vivo*, however, remains scarce, mostly limited to IN responses to electrical stimulation of the inferior olive (Jörntell and Ekerot, 2003). Intriguingly, pairing electrical inferior olive stimulation with parallel fibre activation resulted in the enlargement of receptive fields of INs, suggesting that pf-IN LTP had been induced (Jörntell and Ekerot, 2002). The same manipulation resulted in a decrease of PC receptive field size. These opposite effects on IN and PC responses to pf input are in accordance with the adaptive filter model postulating opposite learning rules for INs and PCs.

The importance of IN-PC inhibition for cerebellar function has further been demonstrated by studies on VOR adaptation in mice lacking $GABA_A$ receptors in PCs. These mice exhibited a marked down-regulation of pf-PC synaptic strength, compensating for the loss of inhibitory PC input, which resulted in behavioural deficits specifically in the consolidation of VOR adaptation learning (Clopath et al., 2014; Wulff et al., 2009). Thus, a chronic loss of IN-PC inhibition leads to substantial compensatory effects during development, highlighting the relevance of inhibition balancing excitation for proper cerebellar function, but also suggesting that acute, reversible manipulations of inhibition may be necessary to uncover its role in the intact circuit during ongoing processing.

1.6 Aims of this thesis

With this thesis, I intended to increase our understanding of molecular layer inhibition in the cerebellar cortex *in vivo*. I specifically wanted to elucidate the spatiotemporal functional interactions between molecular layer interneurons, their targets, and excitatory afferents into the cerebellar circuit. My method of choice to address this subject was to perform paired targeted electrophysiological recordings from molecular layer interneurons and Purkinje cells in mice *in vivo*.

My specific aims were thus to characterize:

1. The effect of spontaneous and electrically induced interneuron spikes on Purkinje cell spiking.
2. The effect of spontaneous climbing fibre input on interneuron activity.
3. The interactions between pairs of interneurons.
4. The principles governing the recruitment of interneurons and Purkinje cells by excitatory input.
5. How identified microcircuit motifs give rise to sensory responses in INs and PCs.

2 Materials & Methods

2.1 Animals

Animal procedures were performed under license from the UK Home Office in accordance with the Animal (Scientific Procedures) Act 1986. To target both INs and PCs for simultaneous electrophysiological recordings *in vivo*, heterozygous mice expressing EGFP in Parvalbumin-positive neurons (Meyer et al., 2002) crossed with C57Bl6 mice were used. EGFP-positive offspring was identified using blue excitation/green emission goggles to visualize EGFP in the musculature. To express hyperpolarising opsins specifically in INs, heterozygous mice of an nNOS-CreER line (https://www.jax.org/strain/014541) were used. nNOS-CreER positive mice were identified by genotyping using ear biopsies.

2.2 Surgery for electrophysiological recordings

Adult (p30-70) male and female mice were anaesthetized with Isoflurane (2% during surgery, 0.5-1% during recordings) and injected intraperitoneally with chlorprothixene (1 mg/kg) and dexamethasone (1 mg/kg). Body temperature was monitored using a rectal probe and maintained at 37.2 ± 0.2 °C using a feedback-controlled heating blanket. The animal's head was shaved with a razor blade, an area of scalp was removed, the neck muscles were partly detached and pushed back, and an acrylic headplate (11 mm inner diameter) (Judkewitz et al., 2009) was glued to the skull using dental cement above vermis lobule 5 (medial) or Crus II (on the right side of the animal). Using a dental drill, a craniotomy (1 mm^2 diameter) was made inside the headplate. Soaking the skull in HEPES buffered artificial cerebral spinal fluid (ACSF: 150 mM NaCl, 2.5 mM KCl, 10 mM HEPES, 2 mM $CaCl_2$ and 1 mM $MgCl_2$, pH 7.3) for several minutes allowed for removal of the bone cap without damage to the dura mater underneath. In most experiments with cell-attached recordings, the dura mater was left intact to minimize brain movement. In cases of strong brain movement, the brain was covered using 1.5% Agar in ACSF.

2.3 Two-photon targeted electrophysiological recordings

To perform simultaneous electrophysiological recordings from two visually identified neurons in cerebellar cortex *in vivo* (Margrie et al., 2003), the spatial resolution and tissue penetration provided by two-photon microscopy (Denk et al., 1990) was necessary. The principle of this imaging technique relies on two photons of lower energy infrared light exciting a fluorophore simultaneously, a process requiring a high flux of excitation photons enabled by the use of an ultrashort pulsed (femtosecond) laser. This results in excitation of fluorophores only in the focal volume, thus yielding a point-spread function with low axial spread. A custom-built two-photon microscope (MOM, Sutter) with a Ti:Sapphire laser (Mai Tai HP, Spectra-Physics) and a 16X, 0.8 numerical aperture water-immersion objective (Nikon) was used. The laser intensity at the sample was adjusted with a combination of a polarization-dependent beam splitter and a half-wave plate that was rotated using a stepper motor. Emitted fluorescence was spectrally separated with a dichroic mirror (565 DCXR, Chroma Technology), which, installed at an angle of 45°, transmits red light (580 – 880 nm) and reflects green light (below 530 nm). Red and green fluorescence were detected with two photomultiplier tubes (H-7422-P-40-MOD, Hamamatsu). Images were acquired using ScanImage (Pologruto et al., 2003) in conjunction with MATLAB (Mathworks). An excitation wavelength of 865 nm was used to visualize EGFP-positive neurons and the pipette solution containing 40 μM Alexa Fluor 594 (Thermo Fisher) in ACSF for loose-patch recordings. Patch pipettes were pulled using a vertical puller (Narishige) from thick walled borosilicate glass and had a resistance of 5 or 7 MΩ (when filled with the pipette solution) for PC and IN recordings, respectively. The two pipettes for simultaneous recordings from two neurons were oriented at 0° and 135° in the x-y plane (horizontal) and both at 43° in the z-plane (vertical). The angle of the diagonal axis of the motorized stage moving the microscope objective matched the vertical angle of 43°. Recordings were made using a Multiclamp 700B amplifier (Molecular Devices). Data were acquired at 20 kHz in voltage-clamp and filtered at 6-10 kHz using an ITC-18 board (Instrutech) in conjunction with Axograph software (Axograph Scientific). To record spontaneous spiking activity, loose-patch recordings were performed, with seal resistances varying from ~40 MΩ to several hundred MΩ. Spontaneous spiking activity was recorded for 5-20 minutes. To induce single spikes in INs recorded in loose-patch mode, a 200 mV voltage pulse of 0.2 ms duration was passed via the

recording pipette at 1 Hz. In case of a successfully induced spike, the repolarization of the IN spike could be clearly identified after the stimulus artifact offset. After each recording, a z-stack of the two pipette positions was recorded at 256x256 pixel resolution, with a 3 μm z-distance between each frame.

2.4 Sensory stimulation

To record sensory-evoked spiking activity in cerebellar cortex, recordings were performed in Crus II (3.5 mm lateral and 1 mm posterior of lambda, right side of animal). A 60 ms, 60 PSI airpuff was delivered to the ipsilateral whisker pad and/or perioral region of the mouse through a small plastic tube using a Picospritzer II (Parker) at a rate of either 1 or 0.5 Hz. The exact position of the airpuff was varied until short-latency spiking responses were obvious in either the IN or the PC.

2.5 Viral injections

nNOS-CreER positive male and female mice (p22 – p35) were injected with the following Cre-inducible light-driven hyperpolarising opsin construct purchased from UNC Vector Core: rAAV1/FLEX-ArchT-GFP, containing the proton pump Archaerhodopsin, at a titre of $5x10^{12}$ viral genomes/ml, respectively. For virus injections, mice were anaesthetised with Isoflurane (2%) and intraperitoneally injected with buprenorphine diluted in saline (0.05 mg/kg, Vetergesic) and dexamethasone (1 mg/kg). Lacrilube (Allergan) was applied to the eyes for moisture. Mice were shaved and positioned in a stereotactic apparatus on a heating blanket. A small L-shaped skin flap was cut and a small craniotomy was made 3 mm lateral from lambda, right anterior of the interparietal bone suture. ~1 μl virus solution was tip-filled into a glass capillary tube (Blaubrand, Intramark) held in a stereotax (Narishige). At an orientation of 40 degrees and aligned to the anterior-posterior axis, the pipette was lowered 2.3 mm into the brain, retracted 0.3 mm, and ~1 μl virus solution was injected across 0.5 mm depth over 10 minutes. The pipette was left in position for another 5 mins before retraction to avoid backflow. The skin was glued with Vetbond, and mice were placed in a recovery chamber heated to 34°C for several hours.

2.6 Tamoxifen administration

To induce Cre-ERT2 fusion gene activity and thereby expression of the virally delivered floxed opsin in INs, 1.5 mg tamoxifen (0.1 ml of 15 mg/ml in corn oil) was administered to mice intraperitoneally for 3 consecutive days, starting one week after initial viral injection. To dissolve tamoxifen in corn oil, tamoxifen (Sigma) was originally dissolved in 100% ethanol, corn oil was added and ethanol was removed using a vacuum centrifuge. The resulting tamoxifen-corn oil mix was stored at -20°C and heated in a sonicator water bath on the day of injection.

2.7 Light-activated opsin stimulation

Neurons expressing ArchT-GFP were stimulated with amber light produced by an LED (595 nm peak output). The LED was connected to a light collimator and coupled into the widefield camera light path of the microscope by mounting it onto an epi-illuminator cube module containing a dichroic mirror (605 nm long-pass) to reflect yellow light. The LED light was thereby focused through the objective onto the brain. LED activity timing was controlled via an LED driver unit (all components from Thorlabs Ltd) that received TTL pulses generated in the electrophysiology acquisition software Axograph.

2.8 Histochemistry

At the end of two-photon targeted recording experiments, nNOS-CreER mice were decapitated and the brains were removed and stored in 4% paraformaldehyde for 24 h, following storage in 1x phosphate-buffered saline (PBS) for at least 24 h. 80 μm thick parasagittal slices of cerebellum were cut on a vibratome and washed in 0.4% Triton X-100 for 30 mins, then in 1xPBS for 10 mins before incubation in Neurotrace 530/615 red fluorescent Nissl stain (ThermoFisher Scientific, 1:200 in PBS) for 30 mins. Slices were washed in PBS again for 30 mins before they were mounted on slides.

2.9 Confocal microscopy

Confocal images were acquired using a Perkin Elmer UltraVIEW system in conjunction with Volocity software. Subsequently, confocal images containing information from the red and green channel were coloured and merged using FIJI (http://fiji.sc/).

2.10 Data analysis

2.10.1 - Electrophysiology: Spontaneous and electrically induced activity -

Analysis was performed offline using custom-written software in MATLAB (Mathworks). Spike onset times were detected semi-automatically based on a manual threshold. To distinguish simple and complex spikes, the variance of the raw voltage trace in a 3 ms window after the initial spike was plotted and the resulting two populations were separated with a manual threshold. Cross-correlograms between two spike trains were calculated by using spike times of one trace as the triggers and calculating the average firing rate of the target spike train 100 ms before and after the trigger, binned in 5 or 10 ms. For IN-PC simple spike cross-correlograms, IN spikes following a complex spike within 25 ms were excluded as trigger spikes, to avoid complex spike-simple spike interactions masking IN-PC inhibition. For electrically induced IN spikes, trials with successful and unsuccessful IN spike induction were sorted manually, and cross-correlograms of PC simple spikes triggered on successfully induced IN spikes (from -100 to +100 ms from induced IN spike) were calculated.

Cross-correlograms were tested for significance based on bootstrapping, by generating shuffled cross-correlograms as follows: for spontaneous activity, trigger spike times were shuffled by reordering 5 second periods of the recording randomly, and 500 shuffled cross-correlograms were calculated based on the shuffled trigger times. To test significance of PC responses to electrically induced IN spikes, 200 ms periods were randomly sampled from the PC recording, and 1000 shuffled cross-correlograms were generated based on these artificial random trigger times. To avoid artifacts from non-stationarities, the original and shuffled cross-correlograms

were normalised to their respective mean baseline rate (for PCs: -100- -80 ms from IN spike, for INs: -100-0 ms from complex spike), and the standard deviations of the shuffled cross-correlograms were normalised to the original's baseline rate, before a standard score (z-score) was calculated for each bin.

Z-scores of > 3 or < -3 were considered significant. To detect IN-PC inhibition, the 0-10 ms bin was tested. For CF-IN excitation, effects were considered significant if either of the 0-10 or 10-20 ms bin exceeded the positive threshold. For CF-IN inhibition, effects were considered significant if either of the 10-20 or 20-30 ms bin exceeded the negative threshold.

To analyse IN response timecourses upon CF input, the IN net spike change was used (Mittmann and Häusser, 2007), i.e. the average number of added or omitted IN spikes over time after CF input, using a baseline period of 100 ms pre complex spike.

To quantify these IN spike changes, a logistic model of the following form was fitted:

$$f(x) = \frac{a}{1 + e^{b(-x+c)}}$$

where a, b an c yield spike change amplitude, steepness, and midpoint (50% rise time), respectively. A non-linear regression model was used for fitting with initial values specified as $a0 = 0.1,\ b0 = 0.1,\ c0 = 0\ ms$.

2.10.2 - Electrophysiology: Sensory-evoked activity -

To analyse sensory response latencies across all recordings, a distribution of the latency of the first spike after stimulus onset was calculated for each recording. To directly compare the timing of fast responses in INs and PCs, only pairs with a distinct peak in the response latency distribution of both the IN and the PC were included, that is the maximum of the response latency distribution had to be greater than 4 standard deviations of the mean value of the response latency distribution.

To analyse the shape of sensory-evoked spiking responses, the net spike change was calculated using a baseline period of 200 ms (Mittmann and Häusser, 2007). When sorting sensory-evoked trials, all complex spikes within 100 ms of stimulus onset were considered sensory-evoked. To isolate rapid, granule cell-mediated IN responses, all IN spikes occurring within 20 ms of stimulus onset were used. To

measure the amplitude of delayed IN responses to sensory stimulation, a 50-120 ms time window post stimulus onset was used.

The amplitude of sensory responses in terms of net spike change was defined as the maximum of the mean spike change in a given time window. To obtain the net delayed IN spike change amplitude, the maximum value of the mean spike change in the fast response window (0-20 ms) was subtracted from the maximum value of the mean spike change in the delayed response window (50 – 120 ms).

When calculating sensory-evoked cross-correlograms, time windows of -200 to +100 ms from the sensory-evoked trigger spikes were used, and rates of the target spikes were normalised to the mean rate across this 300 ms time window.

2.10.3 - Metrics for quantifying spiking response amplitudes: The baseline-normalised binned rate versus the net spike change -

The rationale for using different response amplitude metrics for the analysis of IN-PC inhibition and IN sensory responses is explained in the following section.

In a given neuron, spiking response amplitudes to e.g. a spike in a presynaptic inhibitory neuron, or to a sensory stimulus, can be quantified using different metrics, each presenting different advantages and disadvantages in different contexts. The two metrics employed in this thesis are the 'baseline-normalised binned rate' and the 'net spike change'. The former metric expresses the change of firing rate in a given time window relative to the baseline firing rate, i.e. if the baseline-normalised binned rate is 0.9, the neuron fires at 90% of its baseline level. The net spike change, on the other hand, expresses an absolute measure, namely how many spikes are added or omitted in response to a given stimulus (Mittmann and Häusser, 2007). It is obtained as follows: the cumulative sum of all spike times triggered on the stimulus is calculated in a window of -100 to +100 ms from the time of the stimulus, and divided by the number of trials. A linear fit is fitted to the baseline (-100-0 ms from stimulus), extrapolated over the post-stimulus spike part of the trial (0-100 ms) and subtracted from the cumulative sum to yield the net spike change.

The two metrics are illustrated in Figure 2.1.

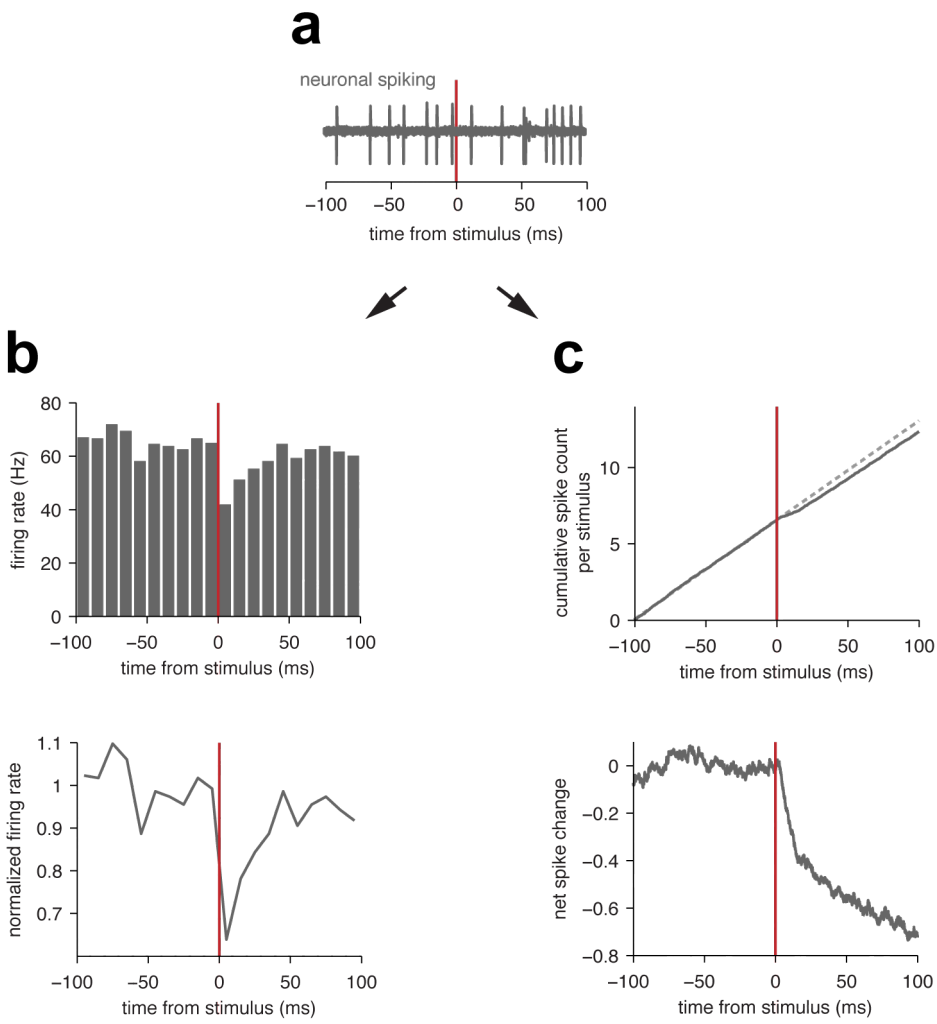

Fig 2.1 Quantifying spiking responses as normalised rates or spike changes

(a) Spikes of a given neuron are aligned to the timing of a stimulus, e.g. a spike in a neighbouring neuron or a sensory stimulus, indicated by the red line. Two different metrics are employed to quantify the neuron's response. (b) Histogram of the neuron's average firing rate surrounding the stimulus (bin size = 10 ms). Below: Like above, but normalised to the neuron's baseline firing rate, i.e. 65.55 Hz. (c) Spikes from all stimulus trials are summed cumulatively, and the number is divided by the number of trials (n = 246 trials) (grey solid trace). A linear fit is fit to the baseline (-100 – 0 ms from stimulus timing) and extrapolated over the entire trial duration (grey dotted trace). Subtracting the fit from the cumulative spike count yields the net spike change, shown below.

Importantly, when these two metrics were applied to measure the amplitude of PC inhibition after spontaneous IN spikes in my dataset, the amount of IN-PC inhibition expressed with the spike change metric was sensitive to PC baseline firing rates: The higher the PC baseline firing rate, the larger the average amount of dropped PC

spikes in response to an IN spike (Figure 2.2a). The amplitude of the baseline-normalised PC spike rate after an IN spike, however, did not depend on PC baseline firing rate (Fig 2.2b), and the two different metrics of inhibition were not correlated in amplitude (Fig 2.2c).

As PC baseline firing rates varied across cells (see chapter 3 of this thesis) and could also change throughout a single recording session within one cell, the baseline-normalised binned spike rate was employed to quantify the amount of IN-PC inhibition throughout this thesis.

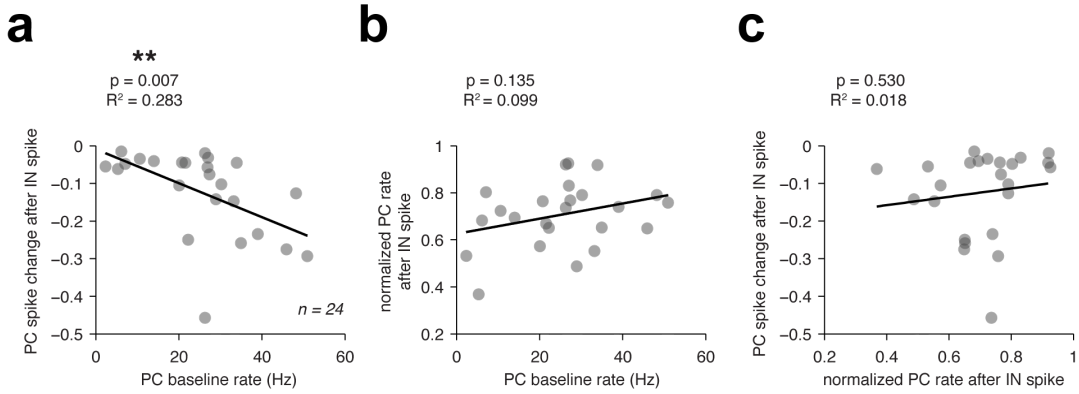

Fig 2.2 Relationship between PC baseline rate, spike change and normalised spike rate for IN-PC inhibition

(a) For IN-PC pairs with significant PC inhibition after the IN spike (n = 24 out of 56 pairs), the PC baseline rate correlates significantly with the net PC spike change after the IN spike. The linear regression line is shown in black. (b) The baseline-normalised PC rate after the IN spike does not correlate with the PC baseline rate. (c) The measures of baseline-normalised PC rate and the PC spike change do not correlate in amplitude. The same dataset was used for plots (a-c).

When quantifying excitatory IN responses to sensory input, however, the binned histograms were less suitable: with very temporally precise, single time-locked sensory-evoked spikes as present in INs (see chapter 7 of this thesis), spike counts per bin in histograms give very large numbers, but they don't represent the instantaneous firing rate, nor do they directly reflect the neuron's likelihood of responding to a sensory stimulus in a given trial. The net spike change, an integrated spike rate measure, offered the advantage of directly reflecting the neuron's likelihood of responding with a spike over time, i.e. a net spike change value of 0.5 within 20 ms of the stimulus signifies that in 50% of the trials, the

neuron responded with one rapidly evoked spike. Moreover, as no binning of spikes was required, the spike change metric enabled easy visualization of the time periods during which spiking changes over time. This property of the net spike change was furthermore useful when quantifying timecourses of spiking responses, and was therefore employed to compare the timecourses of excitatory and inhibitory spiking responses of INs to climbing fibre input in chapter 4.

Crucially, the amplitude of the IN spike change in response to a sensory stimulus did not depend on the IN baseline firing rate in my dataset (Figure 2.3). Therefore, sensory-evoked excitatory IN spike responses were expressed in terms of the IN spike change in chapter 7 of this thesis.

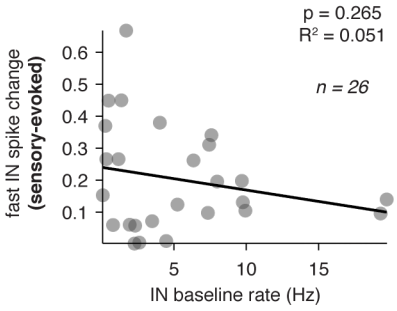

Fig 2.3 Relationship between IN baseline rate and sensory-evoked spike change

(a) There is no linear correlation between IN baseline firing rate and the amplitude of rapid (0-20 ms from stimulus onset) sensory-evoked IN responses measured as IN spike changes. The linear regression line is shown in black.

2.10.4 - Two-photon stacks of pipette positions -

2-photon images were analysed using FIJI (http://fiji.sc/) and MATLAB. In FIJI, the two channels containing measurements of green and red fluorescence were assigned green and red lookup tables, respectively, the channels were overlaid, and the angle of the parasagittal plane in the images was measured by drawing a line along the orientation of PC dendrites in the field of view. Images were then rotated by the measured angle to align PC dendrites vertically (at 90 degrees). The identity of the neurons recorded from was clear from the pipette tip positions touching the neurons' somata, and measurements of the positions of the somata centres, the PC layer and the dura mater were made in FIJI by placing cursors in the respective

positions and planes. Data were then exported to MATLAB to calculate Euclidean intersomatic distances in the transverse, sagittal and vertical planes.

2.10.5 - Statistics -

For paired data, the Wilcoxon signed-rank test was used to assess significance. For unpaired data, the Wilcoxon rank-sum test also referred to as the Mann-Whitney U test was used. When comparing mean values across more than 2 groups, the Kruskal-Wallis test was used. $P < 0.05$ was considered significant. For analysis of higher-order connectivity, that is to test the co-occurrence of different functional connectivity motifs in a given IN-PC pair for independence, Fisher's exact test was calculated using the QuickCalc tool on www.graphpad.com. The associated p-values are two-tailed p-values calculated using the method of summing small p-values. Data is reported as mean ± standard error of the mean, unless it is noted that the standard deviation is shown.

3 Functional interneuron-Purkinje cell connectivity *in vivo*

3.1 Introduction

Across neural circuits, the activity of principal neurons is regulated by local inhibitory neurons, so-called interneurons, and understanding the exact role of inhibition remains a central goal in systems neuroscience. The possible functions that have been ascribed to these interneurons vary widely from regulating principal cell spike timing to controlling principal cell feature selectivity, gain, plasticity, and rhythmicity (Tremblay et al., 2016). As neural circuits contain interneurons with vastly different characteristics, defining different types of interneurons based on morphological, electrophysiological and molecular properties as well as on their connectivity with other cell types, is an active area of research producing an increasing number of interneuron classes with different suggested functions, especially in the neocortex (Jiang et al., 2015).

One factor determining the effect of any given interneuron on principal cell firing, and thus its possible function in the network, is the exact location of its postsynaptic targets: Interneurons forming inhibitory synapses onto the postsynaptic soma or axon initial segment, such as neocortical basket cells and chandelier cells, are positioned to have strong effects on the timing of action potentials in the postsynaptic cell by producing inhibition close to the site of action potential initiation (Miles et al., 1996). Interneurons targeting dendritic regions on the other hand, such as neocortical Martinotti cells, could create localized distal inhibition to counteract excitation and/or prevent dendritic non-linearities from reaching threshold, thereby controlling local integration of excitatory inputs and plasticity.

In the cerebellar cortex, the main interneuron class delivering inhibition to Purkinje cells (PCs), the only output neuron of the circuit, are molecular layer interneurons (INs). While these neurons are as of yet assumed to be a molecularly uniform cell class, they have traditionally been divided into so-called stellate and basket cells based on their position in the molecular layer, their morphology and PC target

location: Stellate cells higher up in the molecular layer target Purkinje cell dendrites, whereas basket cells close to the PC layer form axonal projection patterns like 'baskets' around PC somata and the PC axon initial segment (Palay and Chan-Palay, 1974). Basket cells can thus have strong effects on PC output, whereas the effect of stellate cells on PC spiking has been suggested to be very weak. However, it still remains ambiguous to what degree INs can really be categorized into two distinct classes, as several studies suggest that they rather form one class with continuously varying parameters (Rieubland et al., 2014; Sultan and Bower, 1998). Moreover, INs also form inhibitory as well as electrical connections among each other within a parasagittal plane (Rieubland et al., 2014), possibly leading to inhibition and synchronization within the IN network (see Chapter 5 of this thesis) as well as to an increased convergence of INs onto PCs (Kim et al., 2014).

While evidence exists from *in vitro* studies that single INs can indeed delay PC spiking considerably (Blot and Barbour, 2014; Häusser and Clark, 1997), such data in *in vivo* conditions are lacking. Differences in the levels of activity (Bernander et al., 1991; Destexhe and Paré, 1999; Rapp et al., 1992; Waters and Helmchen, 2006), extracellular calcium levels (Borst, 2010) and neuromodulatory states *in vivo* make it challenging to extrapolate from slice studies to the *in vivo* situation. Moreover, the slicing procedure itself may also truncate or modify axonal and dendritic morphology (Barth et al., 2016; Kirov et al., 1999), thereby changing connectivity patterns and the efficacy of monosynaptic connections. That single interneurons can have an impact on the local network *in vivo* has been suggested by experiments in which activating single neocortical interneurons with trains of spikes could produce a behavioural report in rodents (Doron et al., 2014). However, how these interneurons exert their behavioural effects via network activity remains unknown, and the impact of single interneuron spikes has not been measured.

Thus, in order to elucidate the role of INs in information processing in the cerebellar cortex, probing the effect of single INs onto PC firing *in vivo*, as well as their recruitment by excitatory inputs, is essential. In the experiments described in this chapter, I used simultaneous two-photon targeted patch-clamp recordings from INs and PCs in anaesthetised mice to measure the functional interaction between identified INs and PCs. I quantified the impact of both spontaneous as well as electrically induced single IN spikes on PC simple spiking. In many IN-PC pairs,

spontaneous IN spikes correlated with PC inhibition on a fast time-scale of milliseconds. INs with inhibitory effects were positioned lower in the molecular layer and in the same sagittal plane as the PC. Moreover, inducing single IN spikes electrically caused PC inhibition of similar magnitude as spontaneous IN spikes, indicating that single IN spikes can inhibit PCs powerfully and that dual IN-PC recordings of spontaneous activity are an appropriate method to assess functional IN-PC interactions *in vivo*.

3.2 Results

3.2.1 Functional IN-PC inhibition *in vivo*

To assess the effect of IN activity on PC firing *in vivo*, I performed dual patch-clamp recordings from INs and PCs in vermis and Crus II of Isoflurane-anaesthetised PV^{+}-GFP mice under two-photon guidance (Fig 3.1a,b). As recordings in the whole-cell configuration are known to affect the physiological variance of inhibitory input amplitudes into PCs (Vincent and Marty, 1996), I recorded spontaneous spiking activity in cell-attached mode, taking advantage of INs and PCs being spontaneously active at relatively high rates (Häusser and Clark, 1997) to measure functional IN-PC interactions. PCs fire two kinds of spikes with different waveforms: regular spikes termed simple spikes and so-called complex spikes, a PC's unique multiphasic electrophysiological response to its powerful climbing fibre input (Davie et al., 2008; Eccles et al., 1966). IN spikes occurring within 25 ms of a complex spike were excluded when assessing the effect of IN spikes on PC simple spike firing. In line with previous reports (Chu et al., 2012; Kitamura and Häusser, 2011), INs and PCs exhibited spontaneous activity at high rates (IN spikes: 8.02 ± 7.73, PC simple spikes: 26.43 ± 15.52 Hz, n = 56), and PC complex spikes occurred at a rate of 1.18 ± 0.55 Hz, on average (Fig 3.1c, n = 56).

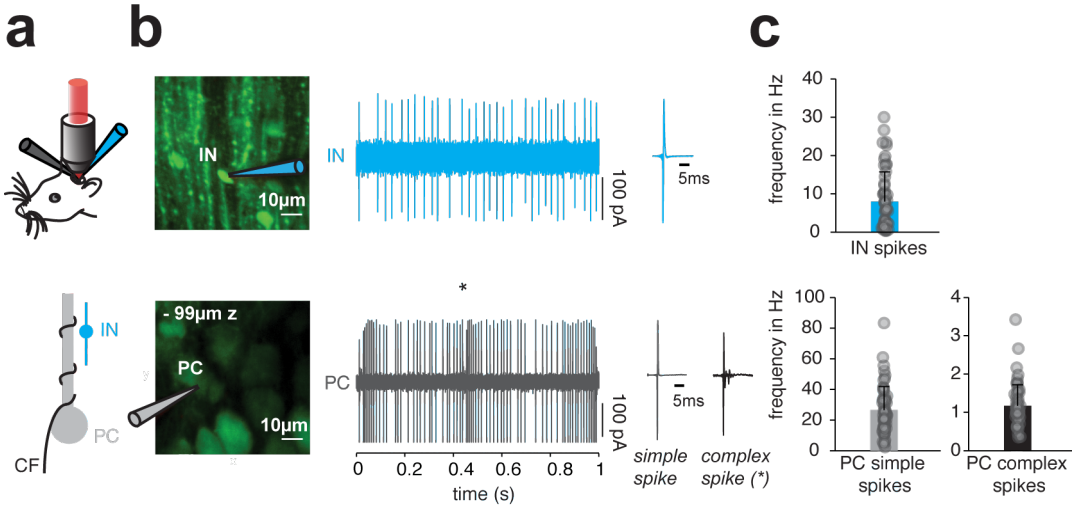

Fig 3.1 Dual recordings from IN-PC pairs in vivo

(a) Top: Schematic of experimental configuration allowing 2-photon targeted recordings from pairs of neurons in vivo. Bottom: Schematic of targeted neurons. (b): Left: 2-photon average intensity projections of targeted IN (top) and PC (bottom), the PC being positioned 99 µm below the IN. Both INs and PCs express GFP. The pipettes contained Alexa Fluor 594. Middle: Raw electrophysiological recordings and average spike waveforms of the corresponding IN and PC. (c) Average firing frequencies of IN spikes, PC simple spikes and complex spikes (n = 56). Error bars denote SD.

Cross-correlograms between spontaneous IN and PC simple spikes could reveal inhibitory correlations between single INs and PCs, as the example recording in Fig 3.2 illustrates: When PC spiking was aligned to the onset of IN spikes, an average reduction to 70% of the PC baseline firing rate could be apparent within 10 ms after the IN spike (0.71 ± 0.14 baseline-normalised PC rate in 0-10 ms bin after IN spike, n = 24 out of 56 pairs with significant inhibition, i.e. PC rate z-score of < -3). Moreover, in 6 pairs, an increase in PC rate could be observed starting 10 ms preceding the IN spike, indicative of co-activation of the IN and PC. This synchronous excitation stems from common granule cell input (Blot et al., 2016). Thus I confirm that spontaneous spiking activity of INs and PCs can exhibit cross-correlograms indicative of common excitatory input and monosynaptic inhibition (see Chapter 6 of this thesis).

INs are electrically coupled via gap junctions which can induce synchrony of coupled INs *in vitro* (Mann-Metzer and Yarom, 1999), and gap junction coupling has been shown to lead to synchronous spiking *in vivo*, albeit in Golgi cells, a different type of

interneuron in cerebellar cortex (van Welie et al., 2016) (also see Chapter 5 of this thesis). Thus, in my paired IN-PC recordings, the negative correlation between a given IN and a PC could theoretically result from the IN firing in synchrony with several other INs that inhibit the PC recorded from. Thus, to test whether the IN I recorded from can cause PC inhibition, it was necessary to induce single IN spikes in the interneuron. A technique for combining loose cell-attached stimulation and recording has been described previously, relying on a custom-designed patch-clamp amplifier allowing for large voltages (1-2 V) to be passed via the recording electrode (Barbour and Isope, 2000). In my experimental conditions, a standard electrophysiology amplifier (Multiclamp 700B) proved sufficient for single-cell stimulation, as application of the maximum voltage output (200 mV) for a duration of 0.2 ms could result in single action potentials in the IN recorded from (Fig 3.2b), owing to INs being electrotonically compact with high input resistances of > 500 MΩ (Häusser and Clark, 1997). The repolarizing phase of the induced spike was easily detectable, allowing for clear separation of successes and failures in spike induction (Fig 3.2b).

Upon successfully induced IN spikes, the PC exhibited a clear firing rate decrease within 10 ms, to a strikingly similar degree as upon spontaneous IN spikes (Fig 3.2e,f). Pairs in which the induced IN spike resulted in significant PC inhibition (pairs with a z-score of < -3 in the 0-10 ms bin after the IN spike, n = 6 out of 30 pairs, Fig 3.3a) were also pairs that exhibited PC inhibition upon spontaneous IN spikes. Furthermore, the baseline-normalised PC rates after induced and spontaneous IN spikes of all 30 pairs were correlated ($p = 0.024$, $R^2 = 0.168$, Fig 3.3a), and the values corresponding to the 6 pairs with significant PC inhibition after induced IN spikes were close to the unity line, indicating a strong correspondence between spontaneous and induced IN-PC effects. Accordingly, in these 6 pairs the PC rates after spontaneous and induced IN spikes were not significantly different (normalised PC rates of 0.58 ± 0.11 vs 0.62 ± 0.14, Fig 3.3b, $p = 1.00$), indicating that inducing single IN spikes can mimic the inhibitory effect of spontaneously occurring IN spikes. Finally, pairs in which single IN spike induction did not result in a significant PC rate decrease exhibited a much weaker spontaneous IN-PC effect on average than pairs in which induced IN spikes decreased PC firing significantly (normalised PC rates of 0.9 ± 0.16 vs 0.62 ± 0.14, Fig 3.3c, $p = 0.002$).

Do these sub-millisecond voltage pulses really activate single INs, or might they recruit the entire electrically coupled IN network? To address this concern, I tested the specificity of the spike induction protocol by recording from two nearby INs simultaneously, inducing spikes in one of the two INs (Fig 3.4a). Importantly, voltage pulses inducing spikes in one IN did not induce spikes in the other IN (Fig 3.4b), although under spontaneous conditions, their spiking activity exhibited synchrony indicative of gap-junction coupling (two peaks at ± 1 ms from 0 in the spike cross-correlogram, for detailed analysis of dual IN recordings see chapter 5 of this thesis) (Fig 3.4c). Although this experiment was only performed once, it suggests that this cell-attached stimulation protocol was highly specific to the stimulated IN, allowing me to test the direct influence of a single IN on PC spiking.

These results indicate that also *in vivo*, single INs can exert powerful influence over the spiking of postsynaptic PCs, and that functional connectivity between INs and PCs can be read out by cross-correlating spontaneous spikes.

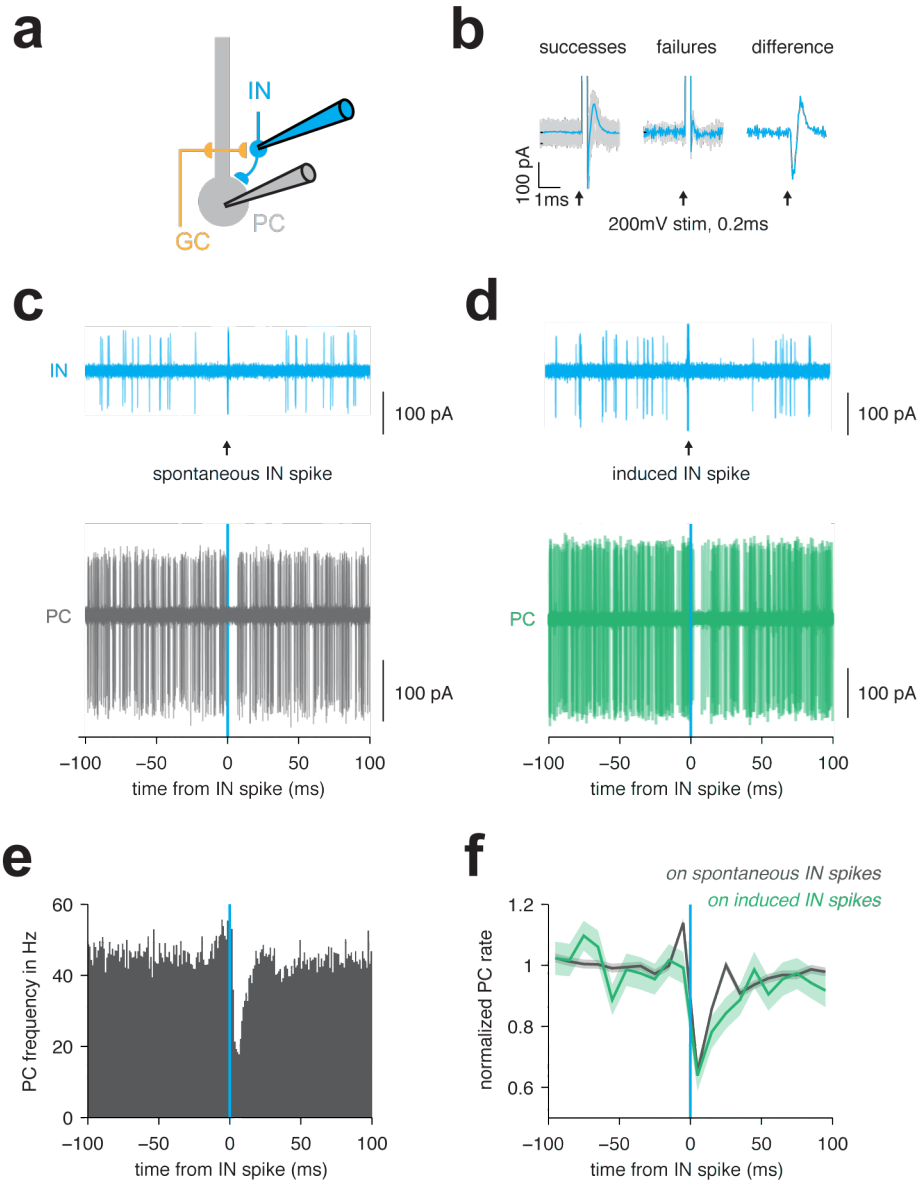

Fig 3.2 The effect of single IN spikes on PC activity in vivo

(a) Schematic of recording configuration and underlying circuitry. (b) Single IN spikes could be induced with a 200 mV 0.2 ms voltage pulse, with the repolarizing phase of the spike obvious after stimulus offset. (c) Raw IN trace triggered on 20 consecutive spontaneous IN spikes, below corresponding simultaneous raw PC recording (complex spikes removed). (d) Raw IN trace triggered on electrically induced IN spikes; below corresponding PC trace. (e) PC simple spike histogram triggered on spontaneous IN spikes (bin size = 1 ms). (f) Normalised PC spike rate triggered on spontaneous (grey) and induced (green) IN spikes (bin size = 10 ms). Shading denotes SEM. Panels c)-f) are from the same dual recording.

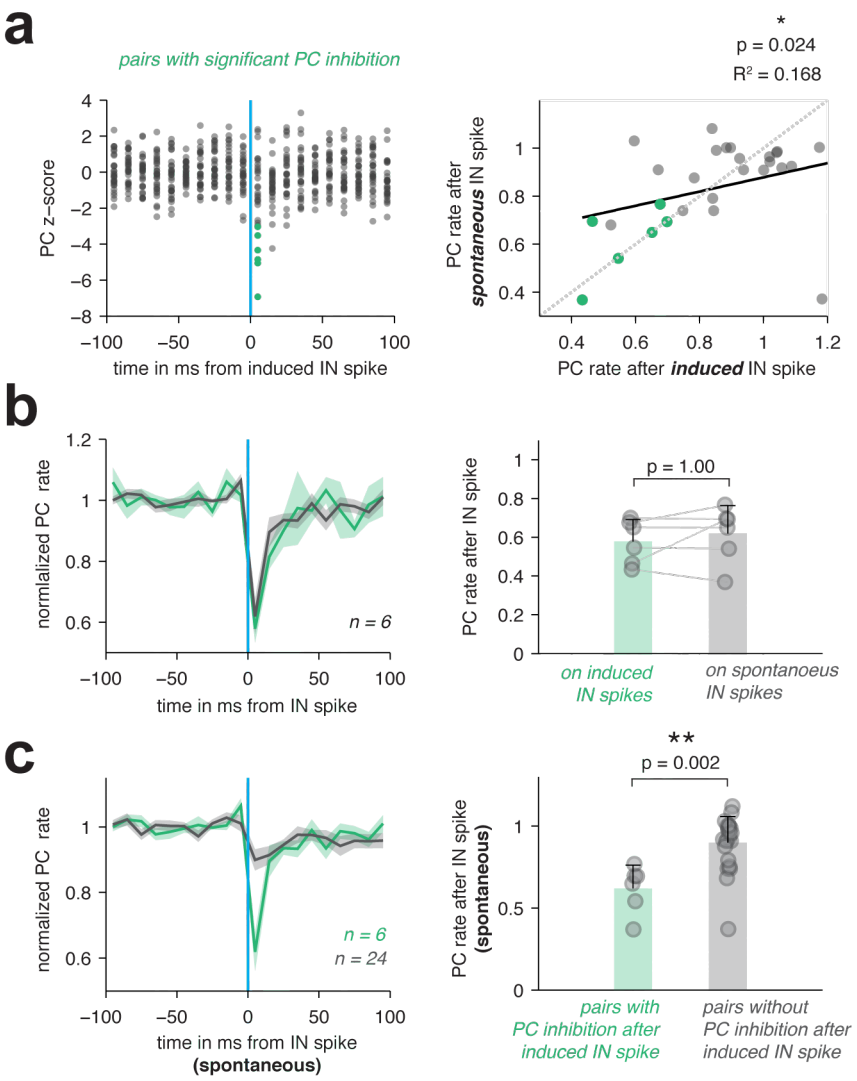

Fig 3.3 The effects of spontaneous and induced IN spikes on PC activity are similar

(a) Left: Z-scores of PC rates triggered on induced IN spikes (n = 30 pairs). PC inhibition was considered significant if a z-score threshold of -3 was crossed in the 0-10 ms bin post IN spike (n = 6, green) Right: Normalised PC rates after induced and spontaneous IN spikes are correlated (black: regression line, dotted line: unity line). Note that pairs with significant PC rate decreases after induced IN spikes are close to the unity line. (b) Left: Mean baseline-normalised PC rates triggered on spontaneous (grey) and electrically induced (green) IN spikes for pairs in which the induced IN spike resulted in significant PC inhibition (n = 6 out of 30 pairs). Right: The corresponding PC rates in the 0-10 ms bin after the IN spike are similar. (c) Left: Mean baseline-normalised PC rates triggered on spontaneous IN spikes for pairs in which induced IN spikes resulted in significant PC inhibition (green, n = 6) and pairs in which induced IN spikes did not inhibit PC spiking significantly (grey, n = 24). Right: The corresponding PC rates in the 0-10 ms bin after the spontaneous IN spike are different.

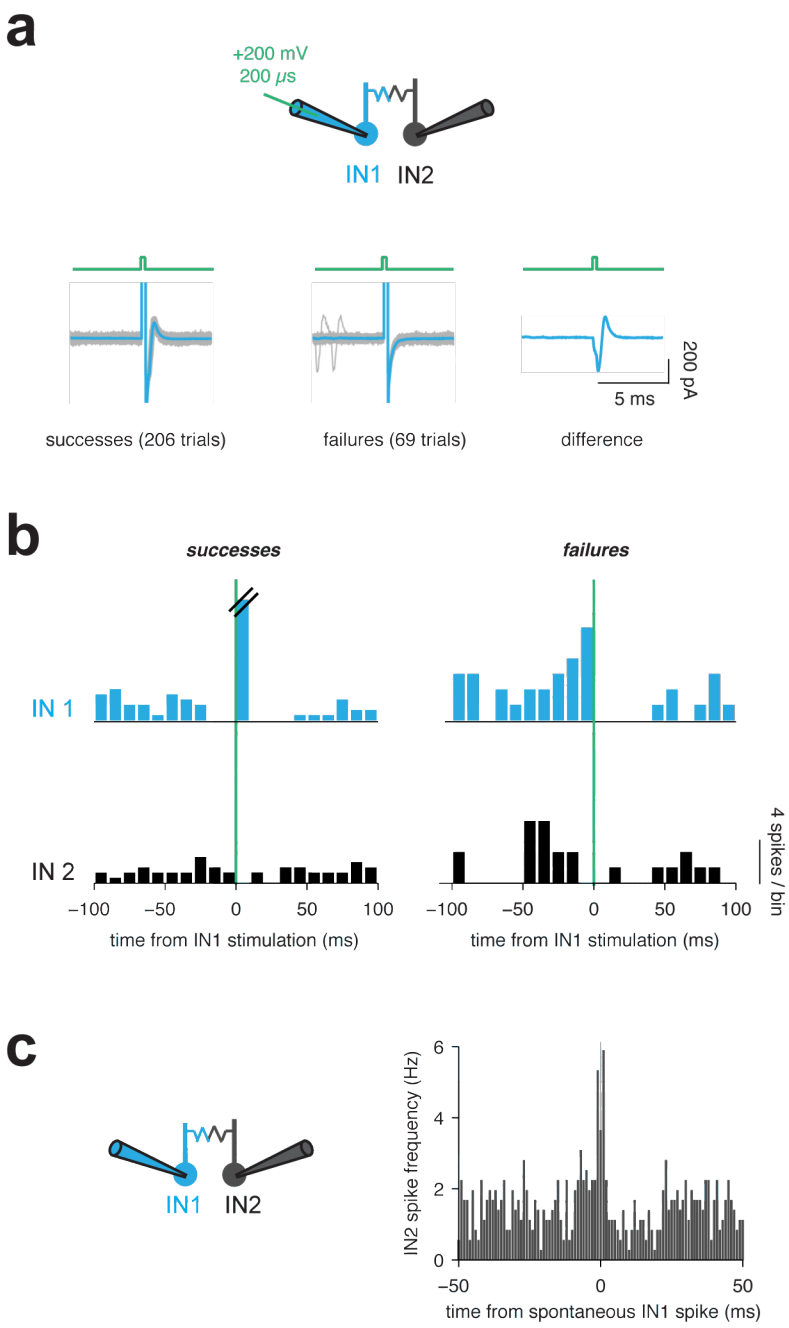

Fig 3.4 Spike induction in a single IN does not recruit a coupled IN

(a) Top: Configuration of a dual IN recording. IN1 was stimulated with 200 mV, 200 μs voltage pulses (green). Below: Voltage pulses could induce temporally precise single spikes in IN1, with the repolarizing phase of the spike obvious after stimulus offset. Left: Successful trials, middle: failure trials, right: Mean waveform difference between success and failure trials. (b) Top: Histograms of spikes in IN1 in success trials (left) and failure trials (right). Below: Histograms of simultaneously recorded spikes in IN2. Note that spike induction in IN1 did not induce spikes in IN2. Bin size = 10 ms. Green lines indicate time of IN1 stimulation. (c) Left: Configuration of recording. Spontaneous spikes were recorded in IN1 and IN2. Right: Histogram of IN2 triggered on spontaneous IN1 spikes. Note the peaks at ± 1 ms indicative of gap junction coupling between IN1 and IN2.

3.2.2 Spatial organisation of interneuron-Purkinje cell inhibition

I next assessed the spatial organisation of the functional IN-PC inhibition I observed *in vivo*. For 54 out of 56 paired recordings of spontaneous IN and PC activity, I could extract the positions of IN and PC somata from two-photon z-stacks (see Fig 3.1), and calculated intersomatic Euclidean distances with respect to the transverse, sagittal and vertical plane (see Fig 3.6a). My spatial sampling did not exhibit correlations between different planes (Fig 3.5, R^2 values of 0.008 – 0.012), allowing me to pool all recordings in analysing distance-dependence of IN-PC inhibition.

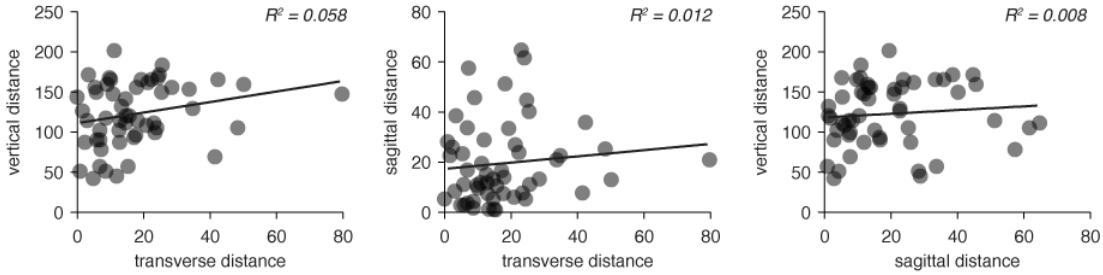

Fig 3.5 Spatial sampling of IN-PC pairs

Each data point corresponds to the Euclidean distance between a recorded IN and PC, n = 54. Left: Transverse versus vertical distances sampled. Middle: Transverse versus sagittal distances sampled. Right: Sagittal versus vertical distances sampled. Black: Linear regression lines. Low R^2 values throughout indicate that spatial sampling did not exhibit linear correlations between different planes.

I categorized the recordings into pairs with significant (blue colour code) and pairs without significant PC inhibition (grey colour code), based on the PC z-score in the 0-10 ms bin after the IN spike (z-score significance threshold of -3, Fig 3.6b). I sampled IN-PC pairs with distances up to 80 μm, 65 μm and 200 μm in the transverse, sagittal and vertical plane, respectively. I found that INs associated with PC inhibition were closer to the PC layer in vertical distance than INs without an effect (mean distance to PC: 106.3 ± 43.9 μm (n = 24) vs 135.8 ± 30.6 μm (n = 30), p = 0.006, Fig 3.6c, d, e top row).

While an unambiguous categorization of INs into the traditional ‘stellate’ and ‘basket’ cells seems problematic (Sultan and Bower, 1998), it is especially not indicated with

my dataset, given that I only have information about the IN soma locations and not the axonal projection patterns. My data does support the notion, however, that vertical distance of an IN from the PC layer is a determinant of the IN's capability to influence PC spike output. I further found that IN-PC pairs with significant inhibition were closer in transverse distance than pairs without inhibition (11.7 ± 7.6 μm vs 20.1 ± 17.0 μm, p = 0.010, Fig 3.6, d,e middle row). No relationship between IN-PC inhibition and distance within the sagittal plane (Fig 3.6d,e bottom row) was apparent. Given that a PC soma is ~25 μm in diameter (Palay and Chan-Palay, 1974; Roth and Häusser, 2001), these results illustrate that INs had to be in the same sagittal plane as a given PC in order to exhibit functional connectivity. This matches anatomical constraints on synaptic connectivity, as PC dendrites are planar and IN axons tend to run mainly parasagittally for up to 300 μm (Palay and Chan-Palay, 1974), a value much higher than the maximum sagittal distance that I sampled.

Given that I found a correspondence between PC inhibition after spontaneous and electrically induced IN spikes (Fig 3.2 and 3.3), one would expect PC inhibition in response to induced IN spikes to exhibit a similar spatial profile as after spontaneous IN spikes. Indeed, when sorting all IN-PC pairs with induced IN spikes (n = 30) by the IN's vertical distance from the PC layer and plotting the corresponding PC z-scores triggered on induced IN spikes, it became apparent that INs with significant inhibitory effects (PC z-score < -3, see Fig 3.2g) were positioned lower in the molecular layer than INs without significant inhibitory effects (Fig 3.7a and b left, mean vertical distances of 97.0 ± 23.9 μm (n = 6) versus 141.6 ± 30.1 μm (n = 24), respectively, p = 0.004). With respect to transverse distance, there was a trend of INs with inhibitory effects being closer than INs without inhibitory effects (15.9 ± 8.0 μm versus 22.2 ± 20.1 μm, p = 0.856). This difference was not statistically significant, but matches the spatial profile of spontaneous IN-PC inhibition in terms of values in the two groups, suggesting that a lower sample size (n = 30, 6 pairs with significant inhibition versus n = 56, 24 significant pairs) might be the reason for a non-significant difference. Again, there was no correlation between the transverse and vertical distances sampled (Fig 3.7c left, $R^2 < 0.001$), indicating that the dependence of IN-PC inhibition on vertical distance appearing in the pooled dataset does not stem from a systematic sampling bias.

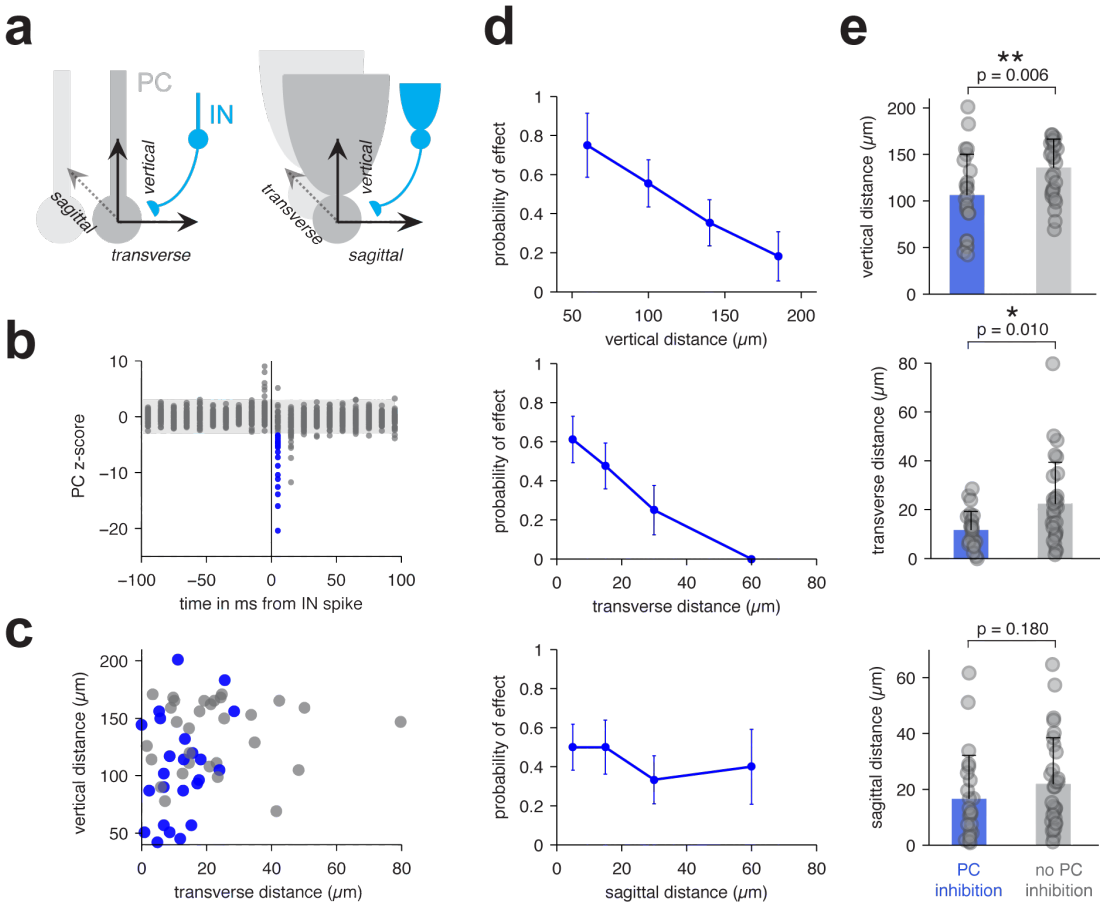

Fig 3.6 IN-PC inhibition depends on vertical and transverse distance

(a) Illustration of the different spatial planes in which IN-PC distance was measured as intersomatic Euclidean distance. The centre of the PC soma denotes 0 μm distance. (b) Z-scores of PC rates triggered on spontaneous IN spikes (n = 56 pairs). Significance threshold of -3 is indicated as a grey bar. Significant PC inhibition (z-score of <-3 0-10 ms after IN spike) is shown in blue. (c) Illustration of spatial sampling: transverse distances sampled are plotted versus vertical distances sampled, pairs with significant IN-PC inhibition are shown in blue. (d) Fraction of pairs with significant IN-PC inhibition across vertical (top), transverse (middle) and sagittal (bottom) distance. Error bars show SD based on bootstrap analysis. (e) Comparison of mean vertical (top), transverse (middle) and sagittal (bottom) IN-PC distances for pairs with (n = 24) and pairs without (n = 30) significant PC inhibition. Error bars denote SD.

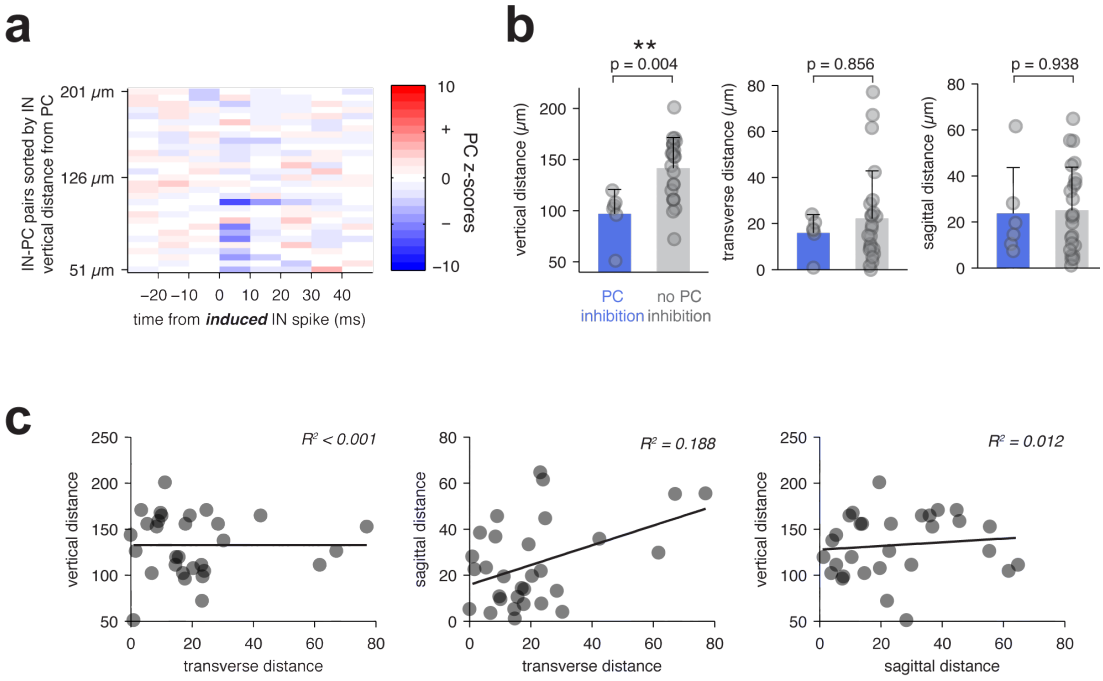

Fig 3.7 Inducing single spikes in INs with low vertical positions inhibits PCs

(a) Z-scores of PC rates triggered on electrically induced single IN spikes, sorted by IN distance from PC layer in vertical space (n = 30 pairs). PC z-score values are clipped at -10 and +10 for better visualization. (b) Comparison of vertical (left), transverse (middle) and sagittal (right) IN-PC distances for pairs with significant (blue) and pairs without significant (grey) PC inhibition after induced IN spikes. Error bars denote SD. (c) Spatial sampling of IN-PC pairs with induced IN spikes. Left: Transverse versus vertical distances sampled. Middle: Transverse versus sagittal distances sampled. Right: Sagittal versus vertical distances sampled. All distances are in units of µm. Black: Linear regression lines.

Finally, I asked if not only the presence, but also the amplitude of IN-PC inhibition depended on the IN's vertical distance from the PC layer. To address this question, I quantified the amplitude of inhibition by calculating the baseline-normalised average PC spike rate in the 0-10 ms bin after the IN spike. I limited this analysis to IN-PC pairs within 30 µm transverse distance, as I did not observe significant PC inhibition in pairs with greater transverse distances (see Fig 3.6), and to IN-PC pairs for which the average PC rate after the IN spike was below 1, i.e. below 100% of the PC's baseline firing rate, to specifically look for inhibition.

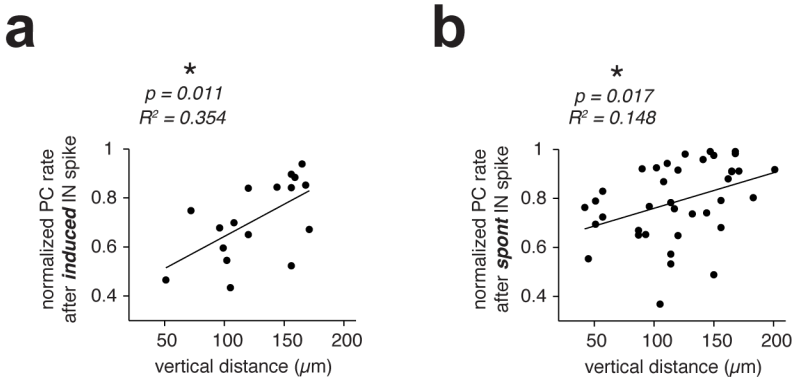

Fig 3.8 Relationship between IN-PC vertical distance and PC inhibition

(a) Vertical intersomatic IN-PC distance plotted versus average baseline-normalised PC rates in 0-10 ms bin after induced IN spike. Only IN-PC pairs within 30 μm transverse distance are shown. There is a significant correlation between IN-PC vertical distance and PC inhibition amplitude (p = 0.011, n = 17). Black line indicates linear regression. (b) Like (a), but for spontaneous, not electrically induced, IN-PC inhibition. The correlation between vertical IN-PC distance and PC inhibition is significant (p = 0.017, n = 38).

When looking at the amplitude of PC inhibition caused by electrically induced IN spikes, there was a significant correlation between the IN's position in the molecular layer and the amount of PC inhibition (Fig 3.8a): The lower the IN was positioned in the molecular layer, the bigger was the inhibitory effect of induced IN spikes on PC spiking ($p = 0.011$, $R^2 = 0.354$, $n = 17$). This relationship was also present, albeit weaker, between the IN's vertical position and the amount of PC inhibition when looking at spontaneous, and not induced, inhibitory IN-PC interactions (Fig 3.8b, $p = 0.017$, $R^2 = 0.148$, $n = 38$). The correlation between PC inhibition amplitude and vertical IN suggests that the position of the IN in the molecular layer does not only determine the presence, but also the size of PC spike rate inhibition. INs higher up in the molecular layer are more likely to contact distal branches of the PC dendritic tree as opposed to the soma (Palay and Chan-Palay, 1974), so a greater electrotonic distance from the spike initiation site would result in attenuation of the inhibitory postsynaptic potential and less influence on PC spike output. My data suggests that the size of PC spike output inhibition is graded with vertical IN distance.

In summary, I found that functional IN-PC inhibition *in vivo* is strongly restricted to the parasagittal plane, with a sharp drop-off with transverse distance, i.e. along the plane of the parallel fibres, matching the mainly parasagittal organisation of IN axonal projections. Moreover, the likelihood of an IN inhibiting PC spike output, as well as the amplitude of the inhibitory effect, were found to depend on the INs vertical position: INs with low vertical positions are more likely to inhibit PC spiking, in line with the dependence on vertical position for the generation of basket-type axonal projections (Sultan and Bower, 1998).

3.3 Discussion

In this chapter, I used dual two-photon targeted electrophysiological recordings to assess functional inhibition between pairs of INs and PCs *in vivo*. I found that single spontaneous spikes in INs could correlate with significant PC spiking inhibition on a timescale in line with monosynaptic connectivity. Furthermore, single electrically induced IN spikes could inhibit PC spiking to a similar degree, establishing a causal role for single INs in the inhibition of PC spike output *in vivo*. PC inhibition was restricted to a parasagittal plane with a transverse width of 30 μm, and INs with lower vertical somatic positions were more likely to cause PC inhibition. In conclusion, single INs can control PC spiking powerfully.

3.3.1 Functional IN-PC inhibition

It has been suggested that single IN spikes should have little effect on PC spike output, especially in the mature cerebellar cortex, as the amplitude of synaptic inhibition between IN-PC pairs decreases from up to 1 nA to tens of pA during maturation (Bengtsson et al., 2013; Pouzat and Hestrin, 1997). In contrast, in this chapter I provide, to my knowledge, the first evidence that single spikes in a single IN can inhibit principal cell spiking *in vivo*. While there are several studies reporting inhibitory interactions between spike trains of extracellularly recorded neurons in other brain areas as well as in the cerebellum (Barthó et al., 2004; Blot et al., 2016; Diba et al., 2014), they lacked the ability to stimulate the neuron supposedly causing the inhibition, thereby being restricted to reporting correlations. With cell-attached stimulation via the recording electrode (Barbour and Isope, 2000), I was able to

induce precisely timed single spikes in INs and compare the effect of spontaneous and induced IN spikes on PC firing. The strength of single interneuron inhibition I observed is surprising given that modelling studies have predicted that the impact of individual synaptic inputs should be substantially weakened *in vivo* (Bernander et al., 1991; Rapp et al., 1992), given the high level of synaptic input in the intact brain (Destexhe and Paré, 1999; Waters and Helmchen, 2006). Moreover, the timecourse of IN-PC inhibition, exhibiting decreases of PC rates for about 10 ms, is indicative that the inhibition is of synaptic, and not just of ephaptic nature: ephaptic inhibition, i.e. inhibition mediated by the electric field of IN axons surrounding the Purkinje cell axon initial segment, results in PC spiking inhibition of just 1 ms (Blot and Barbour, 2014).

The similarity of PC rate decreases upon spontaneous and induced IN spikes demonstrates that cross-correlograms of spontaneous IN and PC spikes allow the readout of functional connectivity between INs and PCs. While absence of a significant effect on spiking does not rule out a weak monosynaptic connection, or an electrotonically remote synapse on a PC distal dendrite, it demonstrates that the IN recorded from does not deliver strong inhibition to the PC in terms of spike output. Likewise, the presence of a significant IN-PC effect does not prove a monosynaptic connection, given that INs are electrically coupled and can fire synchronously (Mann-Metzer and Yarom, 1999) (Chapter 5 of this thesis), but it establishes the role of the IN functionally partaking in PC inhibition. Furthermore, the fact that PC rate decreases in response to spontaneous and induced IN spikes are similar suggests that IN-PC cross-correlograms likely do reflect monosynaptic connectivity in many cases, as recruitment of coupled INs seems negligible during sub-millisecond cell-attached stimulation.

3.3.2 Spatial profile of functional IN-PC inhibition

Inhibitory effects on PCs were observed for INs with certain spatial characteristics: INs with inhibitory effects were closer in transverse as well as in vertical distance than INs without significant inhibitory effects. The distance dependence of IN-PC interactions not exceeding 30 μm in the transverse plane matches the distance dependence of gap junctions between INs as well as their axonal transverse extent,

imposing morphological constraints on connectivity (Palay and Chan-Palay, 1974; Rieubland et al., 2014), supporting the view that INs deliver local inhibition within a given parasagittal plane. While IN axons do not cover large transverse distances, they can extend up to 300 μm parasagittally, allowing them to mediate lateral, "off-beam" inhibition (Dizon and Khodakhah, 2011; Sultan and Bower, 1998). Indeed inhibition onto a single PC has been shown to have a sagittal extent of up to 300 μm (Kim et al., 2014). Hence it is unsurprising that in my dataset where the maximum sagittal distance sampled was 65 μm, I did not see a decrement in functional inhibition with increasing sagittal distance. With my spatial recording configuration of small sagittal distances, I favoured the 'on-beam' as opposed to the 'off-beam' IN-PC arrangement, i.e. INs and PCs with similar distances to a given set of parallel fibres.

Furthermore, my data supports the notion that vertical distance from the PC layer is a determinant in a given IN's effect on PC spike output, as significant PC inhibition predominantly occurred after spikes in INs with lower vertical positions. These data are in agreement with Vincent and Marty, who found that activation of INs closer to the PC layer resulted in larger mean synaptic inhibitory currents in the postsynaptic PC (Vincent and Marty, 1996).

Moreover, I also observed a correlation between the amplitude of PC rate inhibition and the IN's vertical position, with INs closer to the PC layer having a stronger effect on PC output. How can these data inform the classical debate on IN categorization into stellate and basket cells?

In a detailed morphological analysis of INs, Sultan and Bower suggest that the vertical position of an IN's soma not only correlates with the size of the soma, but also with the number of basket-type axonal collaterals (Sultan and Bower, 1998). A small number of basket-type connections between a given IN-PC pair may result in significant, but relatively weak PC spike inhibition, whereas a larger number of basket-type collaterals would result in larger PC spike inhibition, as more GABAergic synapses on the PC soma would be activated simultaneously, yielding a larger inhibitory postsynaptic current. It is thus conceivable that the correlation between vertical IN position and PC spike inhibition observed *in vivo* reflects a varying number of IN-PC basket-type collaterals. My data therefore support the notion that IN characteristics vary continuously along the vertical extent of the cerebellar cortex, and does not support a binary categorization of INs into stellate and basket cells.

3.3.3 Functional implications

What are the functional implications of the finding that single INs in cerebellar cortex can potently inhibit PC spiking *in vivo*?

Between 5-10 INs have been estimated to converge on a single PC (Häusser and Clark, 1997; Kim et al., 2014; Palay and Chan-Palay, 1974). Like PCs, INs are spontaneously active in absence of excitatory inputs, so their tonic firing is bound to keep PC baseline firing levels below the PCs intrinsic rate. A transient change in the activity of a single IN may thus change PC activity levels bi-directionally: An increase in inhibition would cause PC rate decreases and vice versa. Single INs may therefore have effects on the dynamic range of PC firing rates. Spontaneous IN activity *in vitro* has been shown to make PC firing less regular (Häusser and Clark, 1997), and a chronic lack of IN-PC inhibition results in more regular PC firing *in vivo* (Wulff et al., 2009). My data demonstrating strong effects of INs on PC output *in vivo* are in line with these findings.

As electrical coupling increases the spatial convergence of inhibition onto PCs (Kim et al., 2014), it is further conceivable that other INs without direct impact on PC spiking, but electrically coupled to these powerful INs, might indirectly influence PC spike output. The great impact of single INs further suggests that in order to inhibit PC spiking, strong excitatory input onto a single IN might be sufficient. The spatiotemporal clustering of parallel fibre activity could provide the necessary focal excitation for this scenario (Wilms and Häusser, 2015). Alternatively, it has been suggested that basket-like INs could predominantly be targets of ascending granule cell axon synapses rather than parallel fibre synapses (Bower, 2010). Ascending granule cell inputs activate directly overlying PCs (Bower and Woolston, 1983), thus making this a possible source of excitation into single INs. Moreover, INs respond rapidly to small numbers of excitatory or inhibitory inputs (Carter and Regehr, 2002), therefore only a small number of synchronous inputs would be necessary to activate the IN.

The potent inhibition of PC spiking caused by single INs highlights their ability to control the timing of PC spikes and is reminiscent of basket cells in other neural circuits such as neocortex and hippocampus, also providing strong and rapid

somatic inhibition (Pouille and Scanziani, 2004, 2001). What role might more distal INs have then, if not directly inhibiting PC spiking?

As INs exhibit chemical connectivity among each other with a top-to-bottom organisation (Rieubland et al., 2014), more superficial INs might predominantly affect spiking of other INs below (see chapter 5 of this thesis). As to their effect on PC activity, they might have similar roles as some Somatostatin-positive cells in other cortical circuits (Tremblay et al., 2016): Targeting distal dendritic regions of the PC as opposed to the soma, their inhibitory effect could be local to the targeted dendritic compartment, providing inhibition that counteracts local excitation. While this inhibitory action may not directly be reflected in PC spike output, and therefore not measurable with my technique employed here, it could regulate dendritic voltages and / or calcium levels, sculpting dendritic non-linearities and plasticity induction (Callaway et al., 1995).

In order to further elucidate the functional role of inhibition by INs in the cerebellar molecular layer, it is essential to identify the rules of IN recruitment by excitatory input pathways *in vivo*. In chapters 4 and 6 of this thesis, I will present progress in addressing this issue.

4 Functional climbing fibre-interneuron connectivity

4.1 Introduction

Inhibition is known to have profound influence on the activity of principal neurons (Tremblay et al., 2016), so understanding how inhibition is activated is essential for advancing our knowledge of neural circuit function. Determining the wiring diagram of neural circuits is one important element in this process: With the so-called 'connectome' on the microscale, one would have information on all chemical and electric connections between all neurons, and could thus e.g. identify which interneurons may be activated by excitatory inputs into a circuit. However, several important pieces of information cannot be deduced from the connectome and require investigation of not just anatomy, but physiology: Firstly, the connectome of an isolated neural circuit does not provide the spatiotemporal activity patterns entering the circuit. Secondly, it cannot inform us on extrasynaptic transmission. In the latter case, also called volume transmission or spillover transmission, released neurotransmitters diffuse not only onto receptors located in the postsynapse, but also onto extrasynaptic receptors of the same postsynaptic neuron, or even onto receptors of other neurons in the vicinity (Oláh et al., 2009; Scanziani, 2000). Functional interactions between neurons and the resulting activity patterns in neural circuits therefore cannot be predicted by the wiring diagram alone.

In the cerebellar cortex, Purkinje cells (PCs) are under inhibitory influence of molecular layer interneurons (INs) that can strongly decrease PC firing rates (Häusser & Clark 1997, also see chapter 3 of this thesis). Apart from granule cells that form excitatory synapses with INs, INs have for a long time been suggested to also receive excitation from climbing fibres (CFs) (Palay and Chan-Palay, 1974), the axons of inferior olivary neurons thought to convey error signals guiding motor coordination and learning. While CFs run very closely to IN somata and dendrites as observed in early Golgi stain preparations, Palay and Chan-Palay themselves stated that "(…) apparent contacts seen in Golgi preparations do not necessarily signify the existence of synapses at these points. The Golgi method is simply not capable of defining the position of synapses (…)" (Palay and Chan-Palay, 1974). In electron microscopic images of cerebellar cortex, no chemical synapses have been found

between CFs and INs, but only membrane appositions. These appositions exhibit clusters of the potassium channel Kv4.3 in IN somata and dendrites, whose function remains unknown (Kollo et al., 2006). In line with the lack of chemical CF-IN connectivity despite proximity, Szapiro and Barbour demonstrated that CFs excite INs purely via glutamate spillover, by activating AMPA and NMDA glutamate receptors (Szapiro and Barbour, 2007). CF activity does not only cause IN excitation, but also inhibition, by inducing spikes in INs via glutamate spillover that in turn inhibit other INs via GABAergic transmission. Depending on whether a given IN is inside or outside the volume of glutamate diffusion from a given CF, it may thus respond to CF input with excitation, excitation and inhibition, or pure inhibition (Coddington et al., 2013). The activation of INs by CF input has been suggested to prolong PC post complex spike pauses, and also cause pauses in neighbouring PCs not directly innervated by the active CF (Mathews et al., 2012).

Although CF-IN signalling has been investigated in detail *in vitro*, *in vivo* data on this transmission remains limited. Already 50 years ago, Eccles et al demonstrated that by stimulating the inferior olive in cats electrically, single spikes in INs could be evoked (Eccles et al., 1966). More recently, similar experiments in decerebrate cats and rats report long duration excitatory sub- and suprathreshold IN responses to inferior olive electrical stimulation (Jirenhed et al., 2013; Jörntell and Ekerot, 2003). Thus, up to date, IN firing decreases in response to CF input have not been observed *in vivo*, causing incongruity between *in vitro* and *in vivo* data. Electrical stimulation likely imposes unnatural firing patterns on climbing fibres. Therefore, to assess how CF input affects IN activity in the intact circuit with physiological CF input levels it is necessary to study natural CF and IN activity simultaneously *in vivo*.

In this chapter, I address this issue by performing dual two-photon targeted cell-attached recordings from INs and PCs in anaesthetised mice, using the PC complex spike as a reliable readout of local CF input in order to cross-correlate CF and IN activity. I demonstrate that IN responses to local CF input are diverse: INs exhibit spike rate increases, delayed decreases, or both. Spike rate decreases show a time lag of about 10 ms from increases, in line with GABAergic signalling among INs causing inhibition upon CF input. Moreover, I find that there is a vertical structure to IN responses: INs throughout the vertical extent of the molecular layer show excitation, but INs with lower vertical positions show inhibition after CF input. In

contrast to predictions from *in vitro* studies, I thus show that inhibited INs are very close to the CF-innervated PC, and not further away. These spatiotemporal response patterns of INs to CF input have important implications for cerebellar cortical function.

4.2 Results

4.2.1 Functional CF-IN connectivity *in vivo*

To characterize functional interactions between climbing fibres (CF) and molecular layer interneurons (INs) *in vivo*, I performed simultaneous two-photon targeted cell-attached recordings from PCs and INs in isoflurane-anaesthetised mice. I used cross-correlation analysis techniques to quantify the activity of individual INs in relation to local CF input, taking advantage of the fact that CF input into a PC faithfully elicits the characteristic multiphasic PC spike waveform termed 'complex spike'. The analysis presented in this chapter is based on the same experiments used to characterise spontaneous IN-PC inhibition described in chapter 3.

Both IN spikes and complex spikes occur spontaneously at considerable rates (Chu et al., 2012; Eccles et al., 1966), allowing me to use spontaneous PC complex spike and IN activity to characterize physiological functional CF-IN connectivity. PC complex spikes and IN spikes occurred at mean rates of 1.18 ± 0.55 Hz and 8.02 ± 7.73 Hz, respectively (n = 56 pairs, see chapter 3.2.1 of this thesis). For each pair, I calculated IN average firing rates triggered on PC complex spikes, and computed IN rate z-scores based on shuffling PC complex spike times (see Methods).
When plotting IN rate z-scores triggered on complex spikes of all recorded pairs (n = 56, Fig 4.1a right), high positive z-scores after the time of the complex spike were apparent in some pairs, and a few negative z-scores were obvious afterwards. Looking at individual pairs, I identified three different IN response patterns to climbing fibre input: In 13 of 56 pairs, the IN exhibited a pure firing rate increase starting right after the complex spike and peaking at 10-20 ms (example in Fig 4.1b, z-score > 3 0-20 ms post complex spike, red colour code). This phenomenon is in line with *in vitro* data showing that INs are activated by climbing fibre input via glutamate spillover (Mathews et al., 2012; Szapiro and Barbour, 2007), as illustrated

in the schematic in Fig 4.1c. Another subgroup of INs (n = 8) exhibited a contrasting effect, namely a pure decrease in IN firing rate (Fig 4.1d-e, z-score <-3 10-30 ms post complex spike, blue colour code).

Pure IN inhibition upon climbing fibre input has been inducible *in vitro* with artificial climbing fibre stimulation, relying on the extrasynaptic activation of INs that in turn inhibit other INs supposedly positioned outside of the glutamate spillover diffusion limit (Coddington et al., 2013). A delay between rate increases in some and rate decreases in other INs makes it likely that in my *in vivo* recordings the same multi-synaptic signalling pathway was recruited (see Fig 4.1e). Finally, in 3 out of 56 pairs, I found a combination of IN rate increases and decreases, with the increase always preceding the decrease (example in Fig 4.1f-g, z-score > 3 0-10 ms, < -3 10-30 ms post complex spike). In these cases, the IN recorded from seems both directly excited by glutamate spillover and indirectly inhibited by other INs (see Fig 4.1g).

Thus I show that with physiological spontaneous climbing fibre activity, climbing fibres can elicit excitatory and/or inhibitory responses in INs, indicating that extrasynaptic transmission recruits the interneuron network to sculpt more diverse interneuron firing patterns than previously reported *in vivo*.

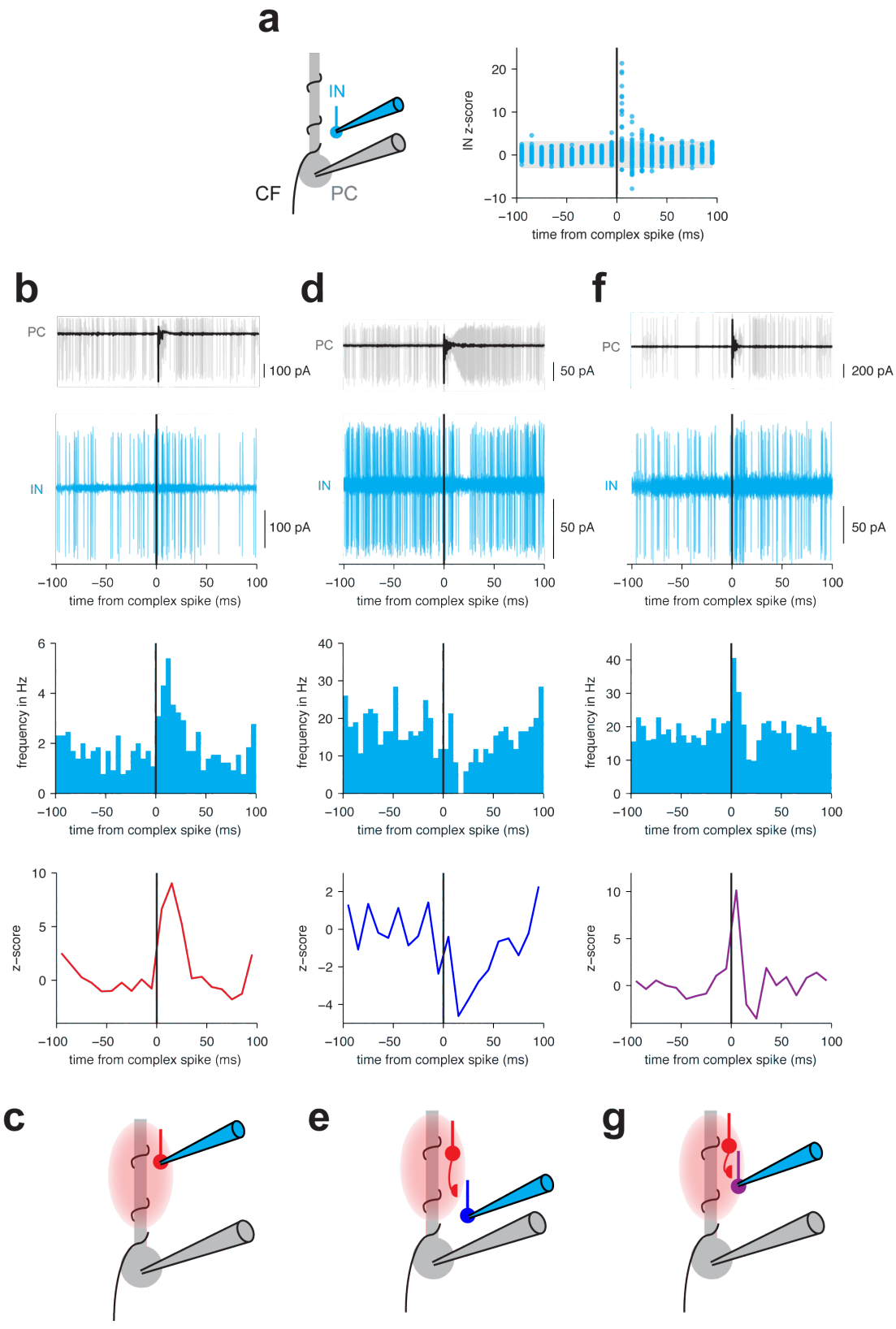

Fig 4.1 INs respond to CF input with rate increases, delayed decreases, or both

(a) Left: Schematic of the recording configuration. Right: IN z-scores triggered on PC complex spikes for all pairs (n = 56). Significance threshold of +3, -3 is indicated by grey shading. (b) Top: Raw PC trace triggered on 50 consecutive complex spikes. Below:

Corresponding IN trace triggered on 150 additional complex spikes. Below: IN histogram triggered on complex spikes (bin size = 5 ms). Below: Z-scores of IN rate triggered on complex spikes (bin size = 10 ms). The IN showed a pronounced rate increase up to 30 ms after the complex spike. (c) Schematic of circuitry underlying the complex spike – IN spike correlation illustrated above: IN excitation (red colour code) results from extrasynaptic IN activation upon CF input. (d,e): Analogous to (b,c), but for another dual IN-PC recording. PC and IN traces triggered on 76 consecutive complex spikes. The IN was inhibited 10-20 ms after the complex spike. Delayed IN inhibition (blue colour code) is caused by inhibition from another IN that is activated by CF input. (f,g) Another PC complex spike-IN spike example cross-correlogram. PC and IN traces triggered on 60 consecutive complex spikes. The IN showed sharper excitation at 10 ms followed by inhibition 20-30 ms after the complex spike. IN activation followed by inhibition (purple colour code) results from extrasynaptic climbing fibre IN activation followed by inhibition from another activated IN.

What is the exact timing relationship between excitatory and inhibitory effects of climbing fibre input on IN spiking? INs can fire at relatively low rates, and CF glutamate spillover is likely to induce rate changes without millisecond precision, making it difficult to measure spike rate changes precisely in histograms with small bin sizes. Therefore, I employed a different measure to address this question, namely the 'spike change', i.e. the cumulative spike count minus a linear fit to the pre-stimulus period (Mittmann and Häusser, 2007), the stimulus here being the PC complex spike. This measure yields the average number of added or omitted spikes over time in response to a stimulus, so if an IN fired one additional spike in response to CF input in 1 out of 10 trials, the absolute spike change value would be 0.1. The timing of the extra spike would manifest in a steep rate of rise of the spike change curve.

I calculated the IN spike change in response to CF input for pairs with significant IN rate increases (n = 13) and IN rate decreases (n = 8), to quantify excitatory and inhibitory IN response timecourses, respectively. The mean shape and absolute amplitude of the two curves were similar (Fig 4.2a), but the spike change of INs with rate decreases seemed to have a later onset than INs with rate increases. To quantify the timing of spike changes, I fit a logistic function of the following form to each IN spike change curve: $f(x) = \frac{a}{1+e^{b(-x+c)}}$, where a, b and c would yield spike change amplitude, steepness and midpoint, respectively (Fig 4.2b). These fits approximated the original spike change curves very well, as indicated by similarly

high R^2 values for the IN rate increase and decrease groups (R^2 = 0.959 ± 0.046 and 0.859 ± 0.159 for IN rate increases and decreases, respectively). The absolute IN spike change amplitude and steepness were similar for both groups (amplitude: 0.17 ± 0.10 versus 0.16 ± 0.16, p = 0.491; steepness: 0.28 ± 0.17 versus 0.47 ± 0.48, p = 0.587 for increases and decreases, respectively). However, the timing of IN spike changes differed between the two groups: IN spike change midpoints, i.e. 50% rise times, occurred earlier for the IN rate increase than for the decrease group (9.95 ± 7.18 ms versus 21.83 ± 11.64 ms, p = 0.012). As the spike change steepness and amplitude were similar for both groups, this 11.9 ms difference in midpoint timing can only be explained by a difference in response onset. This finding that inhibitory IN responses occurred after excitatory responses, with a lag on the order of 10 ms, supports the notion that inhibitory responses are caused by synaptic inhibition among INs.

I thus demonstrate that excitatory and inhibitory IN responses to local climbing fibre input can be approximated with a simple logistic function, and that inhibitory responses occur later, on a time-scale in line with chemical inhibition.

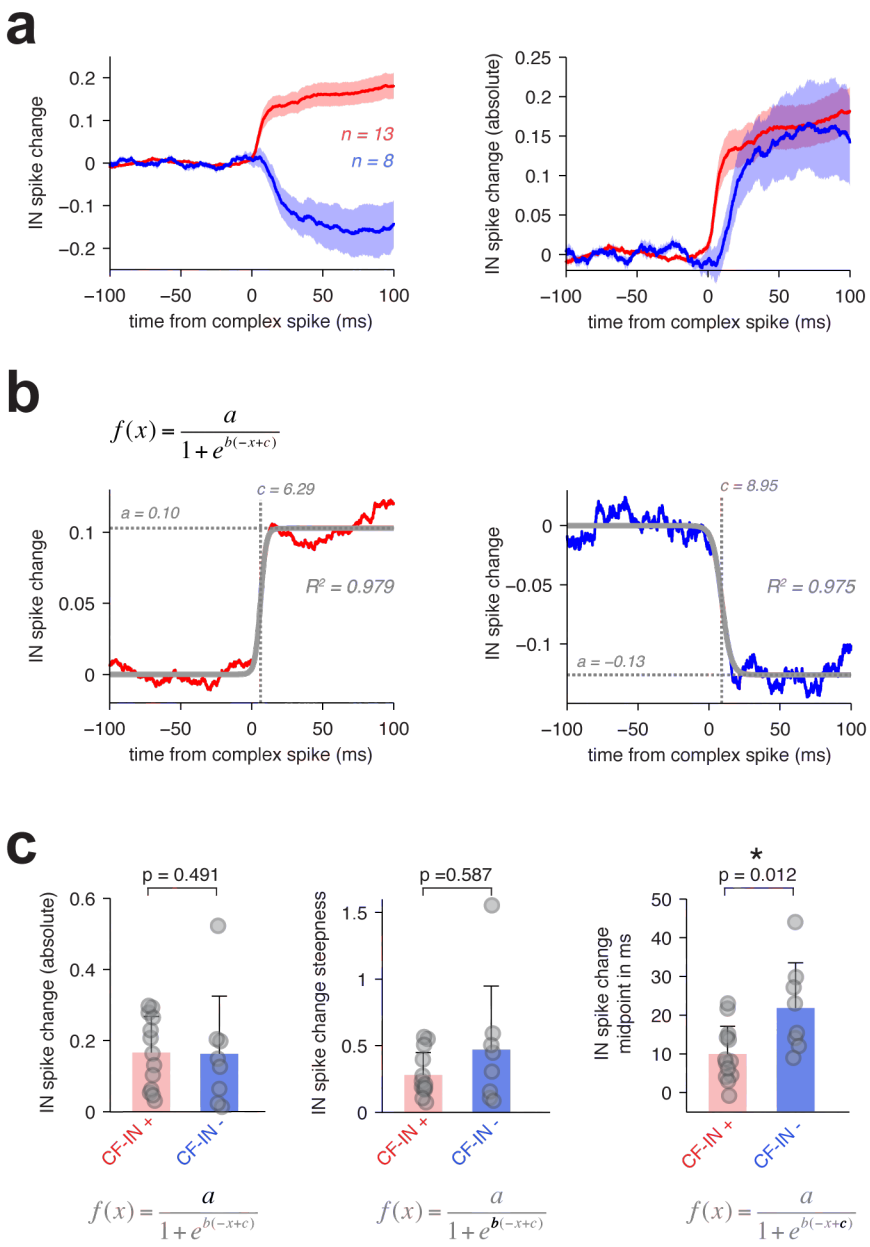

Fig 4.2 Amplitude and timecourse of IN responses to CF input

(a) Left: Mean IN spike changes upon CF input for INs with excitatory (red) and with inhibitory (blue) responses. Right: Same as left, but absolute IN spike changes. Note the difference in response onset between the two groups. Shadings denote SEM. (b) Logistic functions were fitted to IN spike changes upon CF input. Left: Example excitatory IN spike change and fit. Right: Example inhibitory IN spike change and fit. (c) Values of fitted parameters for CF-IN increase and decrease groups. Left: Absolute spike change amplitude. Middle: IN spike change steepness. Right: IN spike change midpoint in ms. Note that the midpoint occurred significantly earlier for the CF-IN increase than for the CF-IN decrease group.

4.2.2 Spatial organisation of climbing fibre – interneuron effects

What is the spatial organisation of the CF-IN effects described above? CF-IN excitation relies on glutamate spillover and thus might be spatially diffuse. CF-IN inhibition, on the other hand, might reflect recently uncovered structure within the IN network: GABAergic connectivity between INs exhibits a top-to-bottom organisation, with INs higher up inhibiting INs below (Rieubland et al., 2014) (also see chapter 5 of this thesis). To study spatial dependencies of CF-IN effects, I determined intersomatic IN-PC distances with respect to the vertical, transverse and sagittal plane. My spatial sampling did not exhibit correlations between different planes (see chapter 3.2.2 of this thesis), so I could pool all recordings for spatial analysis. I separated my paired recordings based on the IN response to CF input into pure IN rate increases, increases and decreases, and pure decreases (Fig 4.3a). Due to the low incidence of observing the mixed response in my dataset (IN rate increase followed by decrease, n = 3), the probability of observing this effect was not analysed further.

I found that the occurrence of IN rate increases was homogenous across vertical distance, whereas IN rate decreases were mainly observed in INs positioned low in the molecular layer (Fig 4.3b, c left), reflected in a decreasing probability of observing pure CF-IN inhibition with increasing IN-PC vertical distance (Fig 4.3c left). On average, INs with inhibition upon CF input were positioned closer to the PC layer than INs with excitation (78.4 ± 33.3 (n = 8) vs 126.5 ± 39.8 μm (n = 12), p = 0.038) or INs without an effect of CF input (78.4 ± 33.3 (n = 8) vs 132.5 ± 35.2 μm (n = 31), p = 0.008, Kruskal-Wallis test plus multiple comparison test). This relationship was furthermore obvious when sorting all pairs by the IN distance from the PC layer and plotting the corresponding IN rate z-scores triggered on CF input (Fig 4.3e)

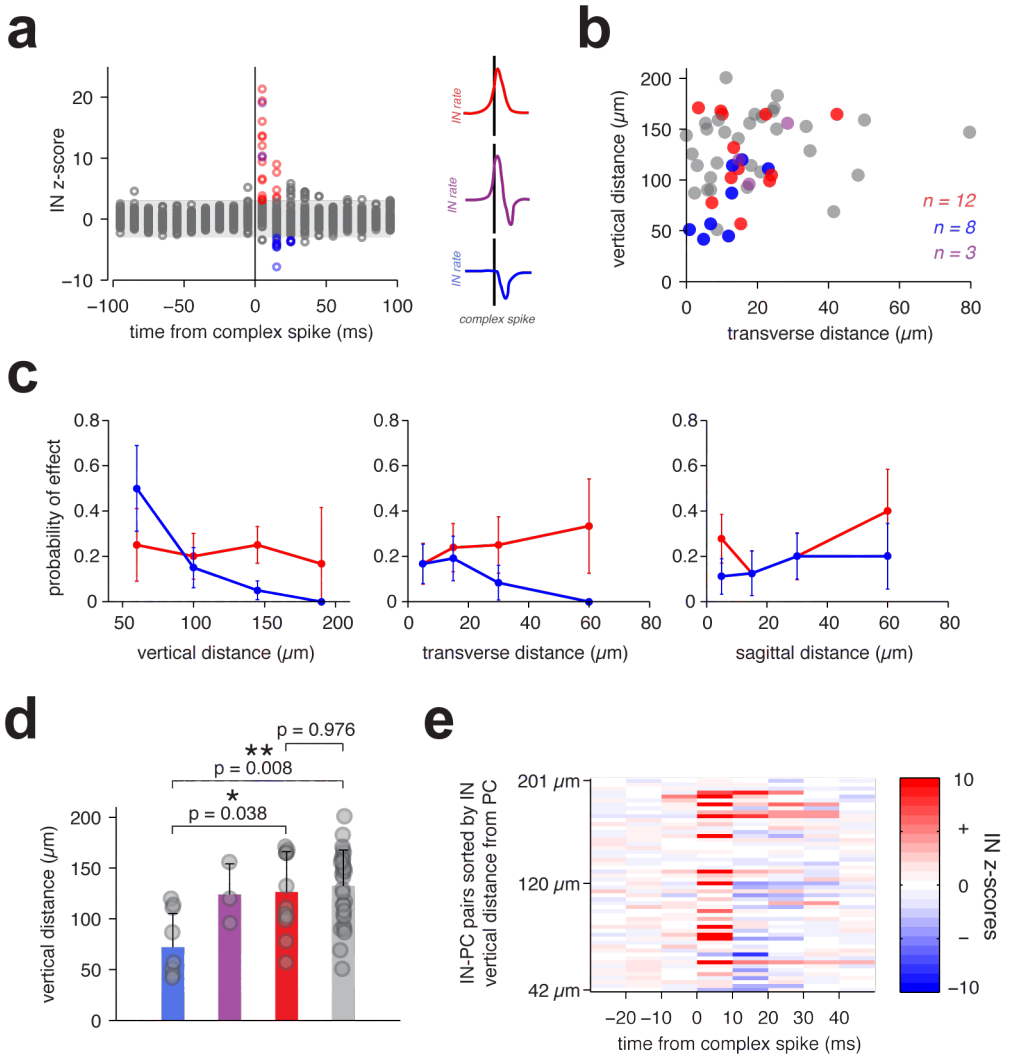

Fig 4.3 Climbing fibre–IN inhibition depends on vertical distance

(a) Z-scores of IN rates of all pairs triggered on complex spikes, colour-coded by response type: IN excitation in red, IN inhibition in blue, IN excitation and inhibition in purple. Grey shading denotes significance threshold of +3, -3. Same data as presented in Fig 4.1a right. (b) Transverse distances sampled are plotted versus vertical distances sampled, same colour code as in (a). (c) Fraction of pairs with significant CF-IN excitation (red) and inhibition (blue) across vertical (left), transverse (middle) and sagittal (right) distance. Error bars show SD based on bootstrap analysis. (d) Mean vertical IN-PC distances for CF-IN inhibition only (blue), excitation and inhibition (purple), excitation only (red), and no effect (grey). Error bars denote SD. P-values stem from a Kruskal-Wallis test plus a multiple comparison test. (e) Z-scores of IN rates triggered on PC complex spikes sorted by vertical IN-PC distance. Z-score heat-map values are clipped at -10 and +10 for better visualization.

There was no striking dependence of CF-IN effects on distance in the transverse plane (Fig 4.3c middle) or sagittal plane (Fig 4.3c right) across the distances sampled. This could result from the fact that CF activity is synchronized in parasagittal microbands that include multiple PCs along the transverse plane (Ozden et al., 2009). It is noteworthy that in the transverse plane, INs inhibited upon CF input were not further away from the active CF than INs excited upon CF input, as might have been expected based on simple assumptions of glutamate volume transmission and no knowledge of directional IN interconnectivity in parasagittal planes (Coddington et al., 2013).

I thus revealed a vertical segregation of IN activity upon CF input, with INs throughout the vertical extent being excited and lower INs being inhibited with a delay, likely by other excited INs.

4.3 Discussion

In this chapter, I present the first data on opposing modulation of molecular layer interneuron (IN) activity by climbing fibre input *in vivo*. Using dual targeted electrophysiological recordings from interneurons and Purkinje cells in anaesthetised mice, I showed that interneurons can exhibit firing rate increases and/or delayed decreases shortly after climbing fibre activity. Inhibitory IN responses occurred with a delay and preferentially in INs positioned lower in the molecular layer, suggesting that purely inhibitory IN responses stem from chemical inhibition between INs directed from top to bottom in the cerebellar cortex.

These diverse spatiotemporal IN activity patterns upon climbing fibre input have interesting implications for the role of extrasynaptic transmission in the cerebellar cortex.

4.3.1 Spatiotemporal patterns of functional CF-IN connectivity *in vivo*

The nature of climbing fibre-interneuron transmission has been puzzling for decades. Despite the lack of evidence for synaptic connections between climbing fibres and molecular layer interneurons, many early anatomical and physiological studies on the cerebellar cortex stated that climbing fibres provided excitatory input into INs (Eccles et al., 1966; Palay and Chan-Palay, 1974). The finding that CF-IN

excitation is mediated purely by glutamate spillover from CF terminals onto INs (Szapiro and Barbour, 2007) seemed to resolve this conundrum, but did not address the question of how relevant this form of transmission was *in vivo*: Is the manifestation of CF-IN transmission measurable in physiological, ongoing activity in the intact cerebellar network?

By cross-correlating spontaneous IN spiking activity and CF input, as measured by PC complex spikes, I demonstrated that indeed, interneuron firing after CF input *in vivo* can show strong bidirectional modulation, i.e. rate increases and/or decreases. Excitatory IN responses to electrical stimulation of the inferior olive have been reported before (Jirenhed et al., 2013; Jörntell and Ekerot, 2003). However, electrical stimulation likely introduces artificial levels of synchronization in the inferior olive, thereby resulting in synchronous glutamate release from more CFs simultaneously than would be observed under physiological conditions. On the other hand, with minimal electrical stimulation in the cerebellar granule cell layer *in vitro*, activation of supposedly single CFs has been used to quantify CF-IN interactions (Coddington et al., 2013; Szapiro and Barbour, 2007). The natural level of CF synchrony lies in between these two extremes: CFs exhibit high degrees of synchronous activity (with cross-correlation coefficients of up to 0.8) within parasagittally oriented bands with a transverse width of tens of microns (Ozden et al., 2009). Moreover, glutamate uptake is likely to be more powerful under physiological conditions than *in vitro* (Asztely et al., 1997; Auger and Attwell, 2000; Dzubay and Jahr, 1999), working against spillover transmission *in vivo* and making it difficult to directly extrapolate from the slice to the *in vitro* situation. By recording spontaneously occurring complex spikes in PCs instead of activating CFs artificially, I was able to measure the natural functional connectivity between CFs and INs. I confirmed the finding that INs can exhibit rate increases after CF input, and moreover found delayed inhibitory IN responses *in vivo*.

One confound of my approach, however, could theoretically be CF activity correlating with the other excitatory input into INs, namely granule cell inputs. In other words, might the correlation between CF and IN activity in my dataset be a spurious relationship, stemming from granule cell input into INs that are co-active with CF input? Several considerations make this hypothesis unlikely. Firstly, sensory-evoked granule cell input into INs is reported to elicit short-latency

excitatory responses consisting of a single spike with very low temporal jitter (Chu et al., 2012), contrasting the slower and broader time-course of excitatory CF-IN responses in my dataset. Moreover, granule cell input into INs is known to recruit feed-forward inhibition in INs, i.e. excitation quickly followed by inhibition (Mittmann et al., 2005). While this response pattern was qualitatively found in 3 out of 56 CF-IN spike cross-correlograms in my dataset, it cannot account for purely inhibitory IN responses to CF input that I more frequently observed (n = 8). On the other hand, purely inhibitory responses have been induced by CF stimulation *in vitro* (Coddington et al., 2013). Finally, Chu et al. found short-latency excitatory IN responses to granule cell input across the vertical extent of the cerebellar cortex, with lower INs responding even faster than more superficial ones (Chu et al., 2012). Hence it is unclear how granule cell inputs would cause purely inhibitory responses in INs of lower vertical depth, like I observed in my CF-IN spike cross-correlograms. Although the relationship between spontaneous and sensory-evoked granule cell activity on the population level has not been studied in detail, these discrepancies between known granule cell-mediated IN activity and the CF-IN correlations described here suggest that the latter ones indeed reflect IN responses to local CF input.

Excitatory IN responses to CF input occurred after PC complex spikes, with a mean 50% IN spike change rise time of roughly 10 ms after PC complex spikes. This delay is in line with glutamate volume transmission, and not synaptic transmission, between CFs and INs, as synaptic transmission between CFs and PCs causes earlier PC than IN excitation (Szapiro and Barbour, 2007).In addition to excitatory IN rate changes upon CF input, I also observed inhibitory IN responses, highlighting that CF input can bidirectionally modulate IN activity *in vivo*.

4.3.2 The source of delayed interneuron inhibition after CF input

What is the nature of the inhibitory IN responses to CF input described here? One candidate mechanism that might be suggested is depolarisation-induced suppression of inhibition (DSI): Upon strong depolarisation, PCs release endocannabinoids that diffuse onto presynaptic CB1 receptors on interneurons, which in turn activates interneuron potassium channels, leading to a reduction of IN

firing rates (Kreitzer et al., 2002). This form of retrograde PC-IN signalling, however, has only been demonstrated on much longer time-scales than the CF-IN interactions on the order of tens of milliseconds described here: The PC was depolarized to 0 mV for 5 seconds via a whole-cell recording pipette, thus the stimulation protocol was orders of magnitudes stronger than natural CF input, depolarising the PC for several milliseconds. The resulting IN firing inhibition lasted tens of seconds, again much longer than the IN responses described here. Moreover, in another study on DSE, i.e. depolarisation-induced suppression of excitation, single CF bursts were found to be insufficient to decrease the amplitude of parallel-fibre inputs into PCs (Brenowitz and Regehr, 2005; Safo et al., 2006), suggesting that CF burst inputs are too weak to induce levels of PC endocannabinoid release that are necessary to strongly affect presynaptic activity. Taking these considerations on retrograde endocannabinoid signaling into account, DSI alone seems like an improbable substrate for the CF-IN interactions described here.

On the other hand, GABAergic synaptic inhibition among the IN network seems to be the most probable underlying cause for several reasons. Firstly, IN inhibition occurred later than IN excitation, with a mean difference in spike change midpoints of roughly 11 ms. This delay suggests the involvement of an additional synapse in generating IN inhibition. Crucially, *in vitro*, IN spike pauses have also been reported in response to electrical CF stimulation, and were found to result from GABAergic transmission among INs, as they were abolished by application of a $GABA_A$ receptor antagonist (Coddington et al., 2013).

If GABAergic signalling within the IN network was causing indirect IN inhibition upon CF input, one would expect that the spatial structure of chemical IN connectivity would be reflected in the spatial organisation of delayed CF-IN inhibition. Chemical inhibition between INs is organised vertically, directed from top to bottom in the molecular layer (Rieubland et al., 2014), and indeed, I found CF-IN inhibition primarily in INs with low vertical positions. This spatial organisation of delayed CF-IN inhibition makes it plausible that INs that are directly excited by CF glutamate spillover in turn inhibit INs below them, inducing either feed-forward inhibition or pure inhibition in INs below. A demonstration of functional IN inhibition showing a top-to-bottom directionality in the molecular layer *in vivo* would further substantiate this claim (see chapter 5 of this thesis for experimental data addressing this issue).

How come INs lower in the molecular layer exhibit pure inhibition without prior excitation upon CF input? It is conceivable that due to CF morphology, synapse distribution and/or non-random overlap with INs (Brown et al., 2012), INs positioned low in the molecular layer get excited less efficiently by glutamate released from CFs, and / or are inhibited too quickly and strongly for diffusing glutamate to affect spiking. Future investigations into the role of specialized membrane appositions between CFs and INs containing a specific A-type potassium channel (Kollo et al., 2006) might further elucidate the mechanisms giving rise to segregated IN activity upon CF input.

4.3.2 Functional implications

What might be the function of climbing fibre–interneuron transmission in the cerebellar network? Direct regulation of PC spike output has been suggested as the predominant function in several studies: INs are excited by glutamate spillover from CF activity, and may inhibit the same PC that received the CF input. IN activation then prolongs the post-complex spike pause of PC firing and generates anti-correlations between PC complex spikes and simple spikes. This effect could also cause inhibition of neighbouring PCs not directly innervated by the CF, increasing contrast in the PC population (Marshall and Lang, 2009; Mathews et al., 2012; Wulff et al., 2009). For this scenario to be the dominant CF-IN function, however, the INs activated by CF input should be able to inhibit PC spike output powerfully. Specifically INs positioned lower in the molecular layer have strong inhibitory effects on PC spike output (see chapter 3 of this thesis) (Sultan and Bower, 1998; Vincent and Marty, 1996). Interestingly, the data presented here show that lower INs are not predominantly excited, but often inhibited upon CF input. Excited INs are found throughout the vertical extent of the cerebellar cortex, also at superficial IN positions where INs are unlikely to affect PC spike output. This novel spatial CF-IN organisation challenges the notion that IN activation by CF input causes strong feed-forward inhibition of PC spike output.

Alternatively, CF-IN transmission might play an important role in plasticity. For decades, theories of cerebellar function have relied on the concept that CF input acts as a teaching signal for granule-cell-PC plasticity (Marr, 1969). As early as

1971, Albus hypothesized that CF input also drives granule cell-IN plasticity, and that different INs, depending on their connectivity patterns with granule cells and PCs, should exhibit opposite learning rules upon CF input (Albus, 1971), increasing the overall computational capacity of the network. By demonstrating that different INs are activated and inhibited by CF input *in vivo*, my data suggest opposite changes in somatic IN voltage levels following CF input as a possible candidate for the implementation of such opposing learning rules. As CF glutamate spillover onto INs activates not only AMPA, but also NMDA receptors on INs (Coddington et al., 2013; Szapiro and Barbour, 2007), it is likely that not only somatic voltage levels, but also calcium levels are the substrate of CF-dependent plasticity. CF input has been implicated in shaping IN and PC receptive fields (Jörntell and Ekerot, 2002), and somatic voltage levels after granule cell input have been shown to affect plasticity in INs, with somatic depolarisation favouring LTP over LTD (Rancillac and Crépel, 2004), supporting the notion that indeed CF input can result in granule-cell IN plasticity.

In order to further elucidate the role of CF-IN transmission in cerebellar cortex, it is essential to study the effect that INs segregated by CF input exert on PC spike output directly. In chapter 6 of this thesis, I address this issue by quantifying the impact of identified INs on PC spike output as well as their recruitment by climbing fibre input, directly testing whether functional feed-forward inhibition is a dominant motif in this microcircuit.

5 Inhibition and synchrony within the molecular layer interneuron network *in vivo*

5.1 Introduction

Understanding how circuit structure supports neural computation represents a central goal in neuroscience. Cortical computations are performed by neurons that are broadly categorized into two classes: principal (often excitatory) neurons that propagate information within and across different circuits, and local inhibitory interneurons that can gate and sculpt signal propagation (Tremblay et al., 2016). To elucidate the exact role of inhibition, uncovering connectivity principles both between interneurons and principal cells as well as within interneuron networks, and linking these to network activity, is essential. In the cerebellar cortex, the activity of Purkinje cells (PCs), the projection neurons of the circuit, is predominantly influenced by one (as of now) molecularly uniform interneuron class: molecular layer interneurons (INs). These INs do not only inhibit PCs, but also each other, via GABAergic synapses (Häusser and Clark, 1997). In addition, they are connected by electrical synapses, consisting of Connexin-36 containing gap junctions (Van Der Giessen et al., 2006). This causes electrical coupling within the interneuron network (Alcami and Marty, 2013; Mann-Metzer and Yarom, 1999). Both inhibition and coupling are confined to the parasagittal plane (Kim et al., 2014; Rieubland et al., 2014), and a given IN pair can be connected both electrically and chemically. Moreover, inhibitory connections form transitive patterns with top-to-bottom directionality in the molecular layer (Rieubland et al., 2014).

While our understanding of anatomical connectivity in this inhibitory network is thus quite advanced, it is still unclear what the functional consequences of these anatomical motifs are. Electrical coupling can lead to synchronization of spiking (Mann-Metzer and Yarom, 1999; van Welie et al., 2016), but has also been shown to promote de-synchronization with sparse inputs *in vitro* (Vervaeke et al., 2010). Inhibition can delay spikes in postsynaptic neurons *in vitro* (Häusser and Clark, 1997) and can lead to synchrony and rhythmicity with appropriate modelling parameters (Wang and Buzsáki, 1996). A recent study reported positively correlated

firing of IN pairs *in vivo* (Blot et al., 2016), but did not report unidirectional inhibitory interactions in their albeit small dataset of dual IN recordings (n = 5). The spatiotemporal activity patterns emerging from chemical and electrical connectivity in the IN network *in vivo*, with physiological excitatory background activity from granule cells and climbing fibres, thus remain to be examined more thoroughly.

To address this issue, I performed dual two-photon targeted patch-clamp recordings from IN pairs in anaesthetised PV-GFP mice, recording spontaneous spiking activity. I found that cross-correlograms of IN spikes were highly variable across pairs. In one pair, spiking activity exhibited synchrony with millisecond precision indicative of gap-junction coupling. In a subset of pairs with small vertical intersomatic distances, synchronous spiking without inhibition was observed. In other pairs, cross-correlograms showed fast spike rate decreases in line with synaptic inhibition. These inhibitory interactions were organised vertically from top to bottom in the molecular layer. The activity of the IN network *in vivo* thus reflects the complexity of interactions between electrical coupling, inhibitory transmission, and excitatory inputs.

5.2 Results

5.2.1 Variety of interactions between interneurons

In dual two-photon targeted recordings from pairs of INs *in vivo* (n = 28, example in Fig 5.1a, b), spontaneous firing rates of INs varied from 0.5 Hz up to 30 Hz, with a mean rate of 7.3 ± 7.3 Hz (Fig 5.1c, n = 56), in line with IN rates recorded in cell-attached mode *in vitro* (Häusser and Clark, 1997), and slightly higher than average rates recorded in whole-cell mode *in vivo* (Chu et al., 2012).

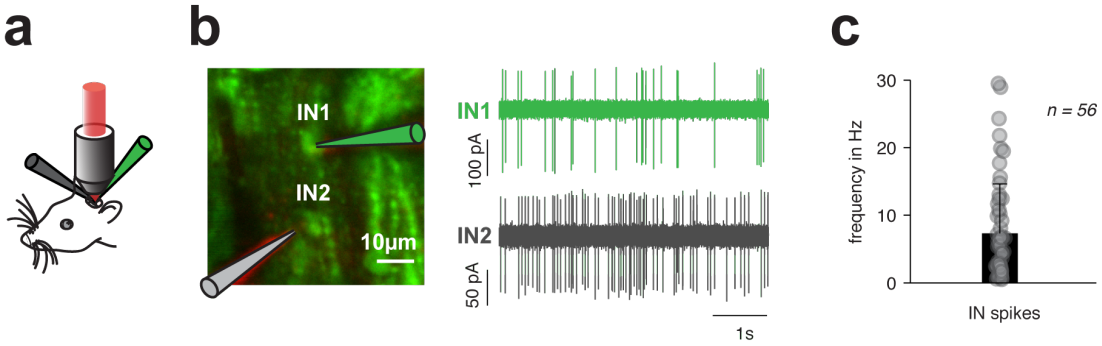

Fig 5.1 Dual IN recordings in vivo

(a) Two-photon targeted patch-clamp recordings were performed in anaesthetised mice. (b) Left: Two-photon average intensity projection showing the simultaneous cell-attached recording configuration of two INs at similar depths in the molecular layer. Right: 5 s segment of simultaneously recorded raw IN traces, corresponding to two-photon fluorescence image on the left. (c) Spontaneous firing rates of 56 INs (n = 28 pairs), mean + SD.

I sampled IN pairs with distances up to 35, 62 and 57 *µ*m in the transverse, sagittal, and vertical plane, respectively (Fig 5.2). There was no correlation between the distances sampled in different planes, as indicated by low R^2 values ranging from 0.01 to 0.03 (Fig 5.2b), allowing me to pool all pairs when analysing distance-dependence of interactions. To characterize the functional interactions of IN pairs, I calculated the average firing rate histogram of one IN triggered on spikes of the other IN, and computed IN rate z-scores for each bin based on a spike-shuffling method. When plotting the resulting IN rate z-scores of all pairs (n = 28, Fig 5.3.), some high positive z-scores close to time 0 were obvious (in the ± 2.5 – 7.5 ms bins), flanked by highly negative z-scores on each side (± 7.5 – 12.5 ms bins). Pairs of INs *in vivo* can thus exhibit precise correlated firing as well as anti-correlated firing on short time scales.

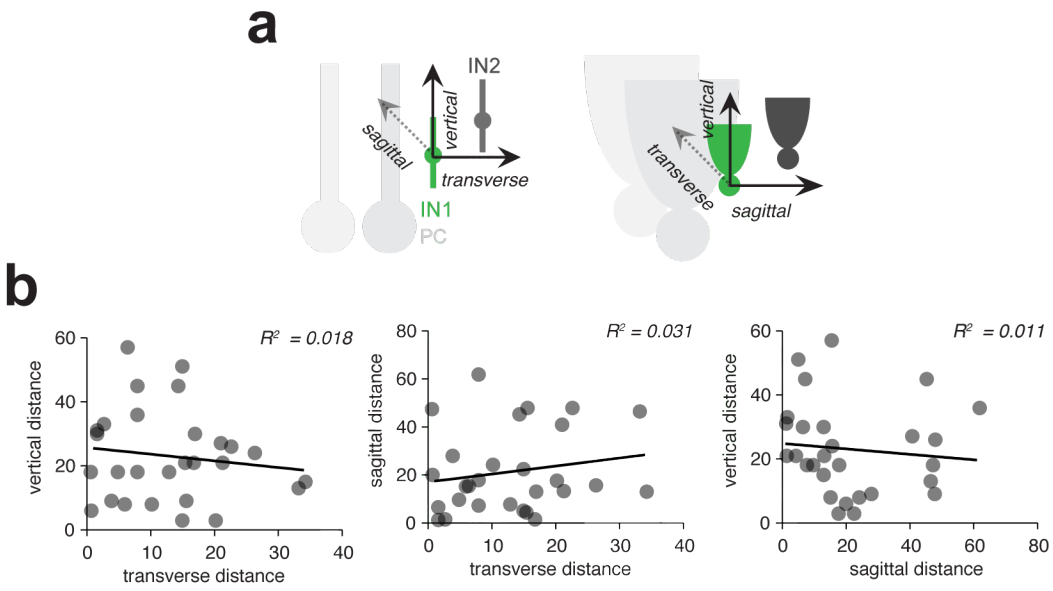

Fig 5.2 Spatial sampling of IN pairs

(a) Illustration of the different spatial planes in which IN-IN distance was measured as inter-somatic Euclidean distance. (b) Each data point corresponds to the distance between a pair of INs. Left: transverse versus vertical distances sampled. Middle: transverse versus sagittal distances sampled. Right: Sagittal versus vertical distances sampled. All distances are given in µm. Low R^2 values (0.01 - 0.03) throughout indicate that spatial sampling did not exhibit correlations between different planes.

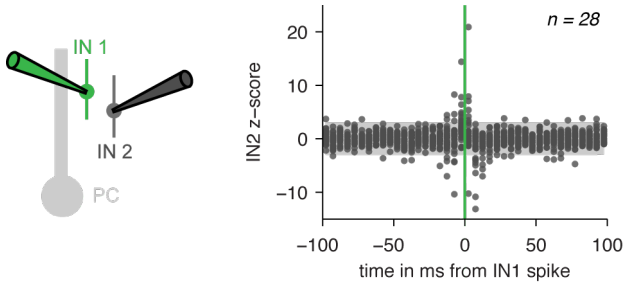

Fig 5.3 Correlated and anti-correlated activity in IN pairs

Left: Illustration of recording configuration. Right: Firing rate z-scores of IN2 triggered on IN1, n = 28 pairs, bin size = 5 ms. Grey shading represents z-score threshold of ± 3.

INs have been shown to exhibit 'dual connections', i.e. both chemical and electrical connections, but chemical or electrical connectivity can also occur in isolation on the pair level (Rieubland et al., 2014). In order to investigate whether functional synchrony and inhibition can be observed independently of each other *in vivo*, triggered IN rate z-scores of individual pairs were plotted, and were found to exhibit large variability in shape across different pairs (Fig 5.4). In 5 out of 28 pairs, IN

spiking was positively correlated within ± 2.5 ms, without significant inhibitory interactions (example in Fig 5.4a). In another set of IN pairs (8 out of 28 pairs), cross-correlograms exhibited unidirectional inhibition, as in Fig 5.4b, in line with unidirectional GABAergic chemical connectivity. Finally, in a single pair, I observed bidirectional inhibitory interactions, i.e. the firing rates of both neurons were significantly decreased after spikes in the respective other neuron (Fig 5.4c). This cross-correlogram is in line with GABAergic synaptic connections between the neurons, resulting in mutual inhibition.

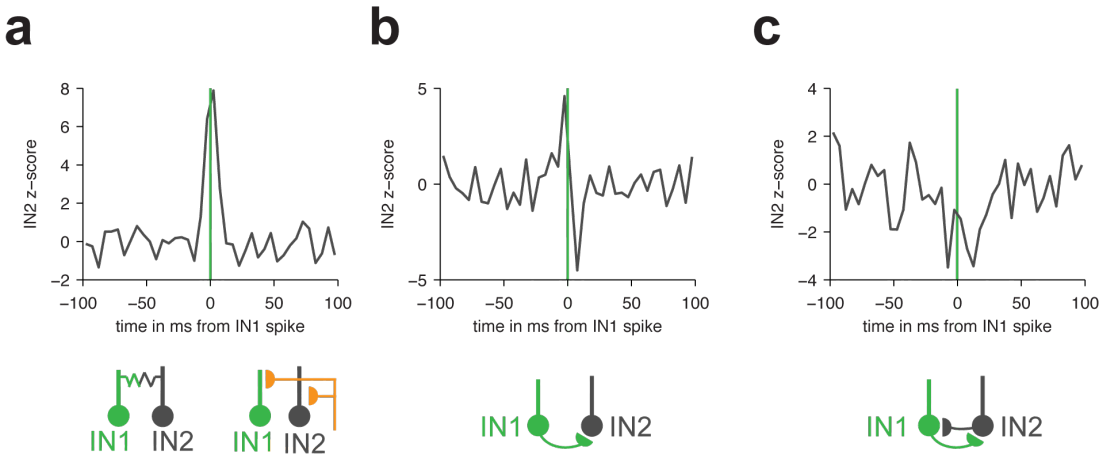

Fig 5.4 Variability of functional connectivity between IN pairs

(a) Top: Example rate z-scores of one IN triggered on spikes of another IN. In this pair, IN activity was positively correlated within ± 2.5 ms. Bottom: Hypothesized underlying connectivity based on cross-correlogram: INs could be synchronized through gap junctions (left) and/or common excitatory input (right). (b) As (a), but different example with different IN interaction. Top: Spiking of IN2 is significantly decreased after spikes in IN1. Before the decrease, an increase indicative of co-activation is obvious. Bottom: The cross-correlogram is in line with IN1 monosynaptically inhibiting IN2. (c) Another example. Top: Activity in both INs is decreased after spikes in the other IN recorded from. Bottom: INs could exhibit bidirectional GABAergic connectivity, inhibiting each other. Bin size = 5 ms for all IN z-scores.

Synchronous activity could stem from gap-junction coupling (Fig 5.4a), resulting in equalization of membrane potential and transmission of spikelets (van Welie et al., 2016), but could also stem from highly synchronous common input. In synchronously active electrically coupled cells, negatively correlated firing at longer time lags of > ± 2.5 ms might be a result of the transmission of the action potential after-hyperpolarisation via gap junctions, but in that case one would expect negative

z-scores not just in one, but in both directions, i.e. at both positive and negative lags from the peak of correlated firing (unless the gap junctions between a pair of neurons allowed current to only flow in one direction, which has not been found experimentally). It is therefore very likely that unidirectional inhibitory interactions as seen in Fig 5.4b reflect unidirectional chemical inhibitory connectivity between IN pairs, despite these pairs also exhibiting co-activation before inhibition.

I thus find that pairs of INs can exhibit a variety of functional interactions *in vivo*, including temporally precise correlated activity as well as inhibition, likely reflecting different combinations of possible underlying synaptic connectivity and common excitatory input.

5.2.2 Synchrony between interneurons

Gap-junction coupled neurons fire synchronous spikes with a well-defined temporal profile: Cross-correlograms exhibit symmetrically spaced peaks with lags of ± 1 ms from 0 ms (Brivanlou et al., 1998; van Welie et al., 2016), illustrating that spikes in one neuron can either occur shortly before or after spikes in the other neuron, with very high temporal precision.

To investigate whether IN interactions *in vivo* show similar temporal profiles, I constructed spike-triggered histograms of IN rates at higher temporal resolution, i.e. with a bin width of 0.5 ms. In 1 pair, this approach yielded a cross-correlation with obvious symmetrically positioned peaks at ± 1ms lag, reminiscent of functional interactions between gap-junction coupled neurons. Data from this paired recording is shown in Fig 5.5. The peak at +1 ms was larger than the peak at -1 ms, indicating that spikes in one cell (IN1) tended to lead spikes in the other (IN2). Asymmetry in IN-IN cross-correlograms has been reported previously, albeit not at such a narrow time scale (Mann-Metzer and Yarom, 1999). The synchrony of spontaneous spiking in this pair was already evident when inspecting the raw simultaneous electrophysiological recording (Fig 5.5a). At longer lags up to ± 20 ms, correlated firing was significantly decreased as evidenced by negative z-scores flanking the positive peak (Fig 5.5b). This feature has been observed in pairs of electrically coupled Golgi cells before, and was found to be a consequence of the hyperpolarising junction potential of spikelets transmitted via gap junctions (van Welie et al., 2016).

Spontaneous suprathreshold activity of IN pairs *in vivo* can thus show correlations indicative of electrical coupling via gap junctions, resulting in synchronous spiking activity with millisecond precision and anti-correlated firing at longer lags of tens of milliseconds.

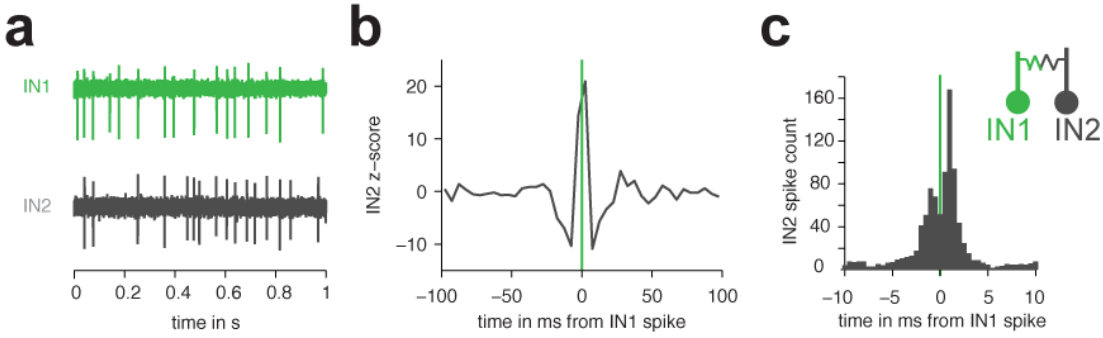

Fig 5.5 Synchrony of IN firing indicative of gap junction coupling

(a) Raw electrophysiological traces from a dual IN recording in loose-patch mode. (b) Z-scores of IN2 rate triggered on IN1 spikes. The cross-correlogram exhibits peak at ± 2.5 ms lag and negative values in both directions up to ± 20 ms lag. Bin size = 5 ms. (c) Left: IN2 rate histogram triggered on IN1 with bin size = 0.5 ms shows two peaks at ± 1ms. Right: INs are electrically coupled via gap junctions.

In another 5 pairs, INs exhibited positive correlations within ± 5 ms (Fig 5.6a), but no negative correlations at longer lags. These pairs also did not show symmetrically positioned peaks at ± 1ms lag when constructing cross-correlograms at higher time resolution, unlike the IN pair example in Fig 5.5. These purely positive correlations at narrow time scales might be the result of common excitatory input into both INs: Common input in the absence of gap junction coupling has been shown to lead to synchronized spiking without the double peak in the cross-correlogram that is characteristic of gap junction-mediated synchronization (van Welie et al., 2016). Interestingly, these INs were closer in vertical distance than INs that did not show significant interactions (11.6 ± 7.6 μm (n = 5) vs 23.6 ± 11.2 μm (n = 13), mean ± SD, p = 0.032), This finding is in line with anatomical constraints from parasagitally oriented IN dendrites and perpendicular parallel fibre inputs, making INs more likely to share a large number of parallel fibre inputs if their dendrites have similar vertical extents.

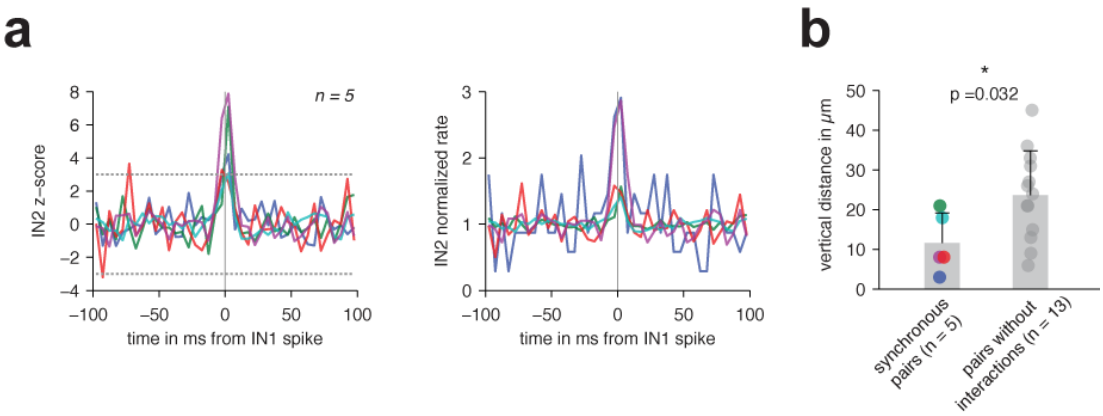

Fig 5.6 IN synchrony without inhibitory interactions

(a) Left: IN rate z-scores triggered on spikes in the other, simultaneously recorded IN, for n = 5 pairs with significant positive firing correlations within ± 2.5 ms lag, but no negative correlations at longer lags. Each pair is represented by a different colour. The dotted lines indicate the z-score threshold of 3. Right: Corresponding normalised IN rate histograms. Bin size = 5 ms. (b) IN pairs with purely positive correlations in firing were closer in vertical distance than IN pairs without significant functional interactions. Colours in b correspond to the traces in (a).

Pairs of INs can therefore exhibit different forms of spike synchrony: they can show synchronous spikes precisely offset by ± 1 ms and decreased spiking thereafter, and they can show synchronous spikes within ± 5 ms. These different forms of synchrony likely result from gap junction coupling and common excitatory input.

5.2.3 Inhibition between interneurons

INs are not only connected electrically, but also via chemical GABAergic synapses, leading to inhibition within the interneuron network. By recording spontaneous spiking activity of two INs simultaneously, I found unidirectional inhibitory interactions in 8 out of 28 IN pairs, as indicated by significant firing rate decreases of one IN triggered on spikes of the other IN (see Fig 5.4b, example in Fig 5.7a, average in Fig 5.7b), but not vice versa. To analyse the spatial organisation of inhibition, for each pair I defined a ‘trigger’ and ‘target’ IN: The IN whose spikes correlated with a spike rate decrease in the other IN was considered the trigger IN, and the IN whose spike rate was decreased as the target IN. Interestingly, I found that the position of the trigger INs was further away from the PC layer in vertical

distance than the position of the target INs (Fig 5.7c, normalised molecular layer positions of 0.74 ± 0.07 vs 0.59 ± 0.13, p = 0.020, n = 8, 0 denotes the position of the PC layer, distances from PC layer were normalised to overall depth of molecular layer in μm). Indeed, it has previously been observed that there is a preference for chemical connections projecting downward in the molecular layer, i.e. down from the pia towards the PC layer (Rieubland et al., 2014). The data presented here demonstrate that this rule of top-to-bottom chemical connectivity is reflected in the functional impact among INs *in vivo*.

In the majority (6 out of 8) of spike cross-correlograms of IN pairs with inhibitory interactions, inhibition of the target IN was preceded by significant co-activation of both INs so that the average rate z-score of the target INs showed a positive deflection in advance of the inhibition (Fig 5.7b). At low temporal resolution, this activity pattern is reminiscent of cross-correlograms between IN and PC spikes (Blot et al., 2016), (see chapters 3 and 6 of this thesis), where the source of co-activation preceding inhibition is synchronous granule cell input into the IN and PC. Thus, it is plausible that here the same phenomenon is observed, where synchronous granule cell input into both INs leads to synchronization before inhibition, forming a motif of feed-forward inhibition (Mittmann et al., 2005).

However, could it instead stem from weak electrical coupling between the INs, resulting in a fraction of spikes being synchronous? To address this issue, I investigated IN co-activation in these 8 pairs with inhibitory interactions at higher temporal resolution, i.e. with cross-correlation bin sizes of 0.5 ms. I found that in 1 out of 8 pairs, precisely timed spikes around 0 ms were apparent (Fig 5.8a). This pair showed an excess of synchronous spikes specifically at +1 ms (Fig 5.8b), a delay which is in line with transmission of spikes via gap junctions.

In summary, signatures of unidirectional inhibition between interneurons were observed in the spiking activity of INs *in vivo*, and exhibited a top-to-bottom anatomical organisation in the molecular layer. Co-activation of INs preceding inhibition likely stems from shared excitatory input, as well as from weak electrical coupling between INs.

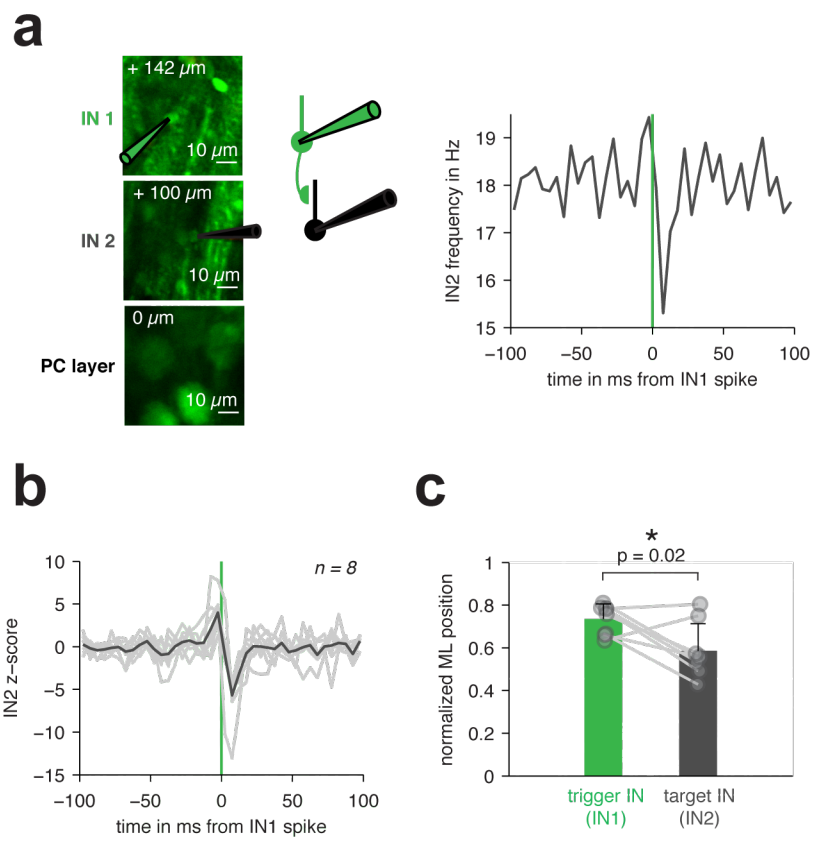

Fig 5.7 Inhibition within the IN network is vertically organised

(a) Example dual IN recording. Left: Two-photon average intensity projections showing the simultaneous dual IN cell-attached recording configuration, with IN2 (middle) and IN1 (top) positioned 100 µm and 142 µm above the PC layer, respectively. Middle: Schematic of inferred recording configuration. Right: Histogram of IN2 spikes triggered on spikes in IN1 (bin size = 5 ms). (b) Z-scored cross-correlograms of dual IN recordings with significant unidirectional inhibitory interactions (n = 8, bin size = 5 ms). (c) Normalised molecular layer positions of trigger INs are higher than the ones of target INs.

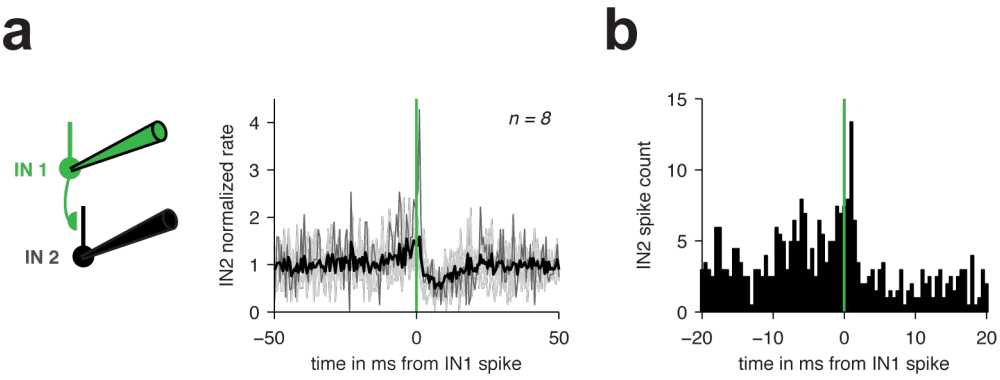

Fig 5.8 Inhibition can co-occur with precise synchrony

(a) Left: Schematic of recording configuration. Right: Histograms of IN2 spikes triggered on spikes in IN1 (bin size = 0.5 ms, n = 8). Grey lines show single pairs, dark grey line shows pair with synchronous spikes around 0 ms, black line shows average. (b) Zoomed in version of the dark grey histogram in (a), showing synchronous spikes at +1 ms.

5.3 Discussion

By performing dual loose-patch clamp recordings from IN pairs *in vivo*, I provide evidence for correlated as well as anti-correlated spontaneous IN activity with high temporal resolution. I observed that functional interactions of INs, as measured by cross-correlating spikes, showed high qualitative variability across pairs, consisting of different combinations of co-activation and inhibition. INs could exhibit synchronous spiking activity with millisecond precision and bidirectional inhibition, or synchronous spiking without inhibition, in which case IN somata were close in vertical distance. INs also showed unidirectional inhibitory interactions. In these cases, IN somata were spatially segregated in vertical distance, with IN inhibition occurring lower in the molecular layer.

5.3.1 The relationship between IN connectivity and cross-correlograms of IN spike trains

While anatomical connectivity has been studied in detail in many networks, the spatiotemporal activity patterns emerging from specific local connectivity motifs and

long-range input into circuits are less understood. INs exhibit both electrical and chemical connections that can co-occur in a single IN pair, and both electrical and chemical connectivity are clustered in the parasagittal plane (Rieubland et al., 2014). Both electrical and chemical connectivity have been suggested to lead to synchronization and de-synchronization of spiking under different conditions (Häusser and Clark, 1997; Karnani et al., 2016; Mann-Metzer and Yarom, 1999; Vervaeke et al., 2010; Wang and Buzsáki, 1996). It thus appears non-trivial to predict spatiotemporal firing patterns of the IN population *in vivo* based on connectivity alone, necessitating direct measurements of functional connectivity in the intact circuit. Now that I have presented such measurements in this chapter, how can the functional interactions observed be explained by underlying connectivity?

The knowledge about anatomical connectivity can be combined with existing dual recordings of other neuron types *in vivo* as well as with simulations to interpret the observed IN-IN cross-correlograms. Short-latency anti-correlations in firing have been observed between INs and PCs *in vivo* (Blot et al., 2016) (see chapters 3 and 6 of this thesis), i.e. PC spiking decreases within 5-10 ms after the occurrence of IN spikes. Often, these cross-correlograms also show positive correlations right before the spike decrease, indicating common excitatory granule cell input. In the dataset of 28 dual IN recordings presented here, 8 cross-correlograms presented a very similar shape consisting of a short-latency unidirectional decrease in firing, often proceeded by a narrow increase. As it is established that INs can form unidirectional GABAergic connections and that INs receive fast excitatory inputs from granule cells, it is likely that these cross-correlograms reflect qualitatively similar underlying connectivity as in the IN-PC case, i.e. feed-forward inhibition (Mittmann et al., 2005). Moreover, I found a difference in vertical IN position in these cases: The IN whose spikes correlated with inhibition of the other simultaneously recorded IN had a higher vertical position than the inhibited IN. This rule of top-to-bottom functional connectivity matches *in vitro* data on directionality of GABAergic connections among INs (Rieubland et al., 2014), further supporting the notion that the IN cross-correlograms described here reflect inhibitory chemical connectivity.

Might the synchronization of spiking before the inhibition reflect electrical coupling instead of common excitatory input? Gap junction coupling leads to very characteristic spike train cross-correlograms, showing narrow peaks of correlated

firing at ± 1 ms and anti-correlated firing afterwards for tens of ms (Brivanlou et al., 1998; Dugué et al., 2009; van Welie et al., 2016). Electrical coupling results in the transmission of so-called spikelets: After an action potential occurs in one cell, a filtered version of this action potential, the spikelet, can be measured with a delay in the somatic sub-threshold voltage recording of another electrically coupled cell (Dugué et al., 2009; Mann-Metzer and Yarom, 1999; van Welie et al., 2016; Vervaeke et al., 2010). Recent modelling work makes it possible to distinguish between the effect of the depolarising and the hyperpolarising junction potentials of these spikelets on spike train cross-correlations and the associated cross-correlograms: The depolarising junction potential was found to underlie the two narrow peaks, whereas the hyperpolarising junction potential generates symmetric negative troughs at longer latencies, but only when the action potential after-hyperpolarisation was large and long as measured in Golgi cells (van Welie et al., 2016). Because INs exhibit large after-hyperpolarisations as well (Chu et al., 2012; Midtgaard, 1992b), it is plausible that strongly electrically coupled INs would show cross-correlograms that are qualitatively equivalent to those of Golgi cells. Accordingly, if an IN pair were strongly electrically coupled, one would expect inhibitory interactions not only in one, but in both directions of the cross-correlogram, unlike in the cases of unidirectional inhibition described above. Precisely synchronous spikes were only observed in one of the eight cases, with a lag of +1 ms. It is thus more likely that in the majority of cases, common excitatory input predominantly generates the observed co-activation preceding inhibition.

In one IN-IN pair cross-correlogram, I found narrow peaks at ± 1 ms and broader troughs on both sides afterwards, indicative of gap junction coupling. Theoretically, the troughs might also be caused by bidirectional chemical inhibition in addition to transmission of the after-hyperpolarisation via gap junctions. However, this connectivity motif consisting of bidirectional GABAergic connections as well as electrical coupling between a single pair is very rare, as it was only found twice in 420 pairs in an *in vitro* study (Rieubland et al., 2014).

Finally, another functional connectivity motif I identified in 5 pairs consisted of a positive correlation within ± 5 ms, but not precisely at ± 1 ms, and no negative interactions at longer lags. Positive spiking correlations on short time-scales in the absence of inhibitory interactions can result from common excitatory input, as a

neuronal modelling study demonstrated (van Welie et al., 2016). Furthermore, these IN pairs exhibited lower vertical inter-somatic distances than pairs without this functional connectivity profile. This finding suggests that common excitatory input might stem from parallel fibres: INs with similar positions in the molecular layer likely have similar vertical dendritic extents (Rieubland et al., 2014; Sultan and Bower, 1998), maximizing the likelihood of sharing parallel fibre input that runs perpendicularly to the parasagittal dendritic IN plane. Alternatively, common excitatory drive might stem from climbing fibre glutamate spillover, leading to depolarisation of nearby INs (see chapter 4 of this thesis).

5.3.2 Functional implications

While top-to-bottom directionality of chemical connectivity has been described before, it remained unclear whether this would lead to vertically oriented anti-correlated firing of INs *in vivo*, given that INs exhibit gap junction coupling clustered in the parasagittal plane. The finding that indeed, pairs of INs can show inhibitory interactions with vertical organisation suggests that despite parasagittal gap junction coupling, the IN network might consist of functional subnetworks with different vertical positions. Focal excitatory input at a higher vertical position could lead to excitation of superficial INs, which in turn would inhibit INs with lower positions, resulting in IN subnetworks with oppositely modulated rates. The observed co-activation on narrow time-scales of INs with similar vertical positions makes this scenario plausible. Vertical segregation of IN activity has been observed upon CF input (see chapter 4 of this thesis), implying that chemical connectivity between INs can result in opposite IN responses to long-range excitatory input. This in turn could create differential levels of dendritic versus somatic PC inhibition, with opposite effects on PC spike output and dendritic plasticity.

Molecularly distinct classes of interneurons in neocortex have been demonstrated to promote co-activation within a given interneuron class through gap junction coupling and disinhibition, via preferential inhibition of other interneuron classes (Karnani et al., 2016). Through directional chemical inhibition, INs in the cerebellar cortex might similarly create different subgroups with differential activity. Finally, electrical coupling as well as feed-forward inhibition in the IN network both seem to promote

precise IN spike timing, resulting in precise patterns of PC inhibition ultimately controlling movement.

6 Differential recruitment of feed-forward inhibitory networks by granule cell and climbing fibre input

6.1 Introduction

The activity of cortical networks depends on the precise interplay of synaptic excitation and inhibition (Isaacson and Scanziani, 2011), thus understanding the rules by which inhibition onto principal cells is recruited by different excitatory inputs is crucial to understand neural circuit function. In the cerebellar cortex, Purkinje cells receive synaptic inhibition from molecular layer interneurons (INs), and the circuit gets two different excitatory inputs: granule cells (GCs) provide highly diverging and converging input, with ~200,000 GCs synapsing onto a single PC. GCs also synapse onto INs, resulting in a feed-forward inhibition motif (Andersen et al., 1964; Mittmann et al., 2005).

The other excitatory afferent to the cerebellar cortex are climbing fibres (CFs), the axons of inferior olivary neurons, that are thought to relay instructive signals driving cerebellar learning by modifying the efficacy of granule cell inputs and PC intrinsic excitability (Albus, 1971; Johansson et al., 2015; Marr, 1969; Medina and Lisberger, 2008). Each PC is contacted by a single CF via hundreds of synapses widespread on the dendritic tree. CFs are in close apposition to IN somata and dendrites, yet excite INs solely via glutamate spillover (Szapiro and Barbour, 2007). Recently, it has been shown *in vitro* that CFs can also inhibit INs disynaptically, exciting INs that in turn inhibit other INs supposedly further away from the active CF (Coddington et al., 2013). It has thus been suggested that CF input results in local feed-forward inhibition and more distant disinhibition of PCs via INs. Finally, chemical and electrical connectivity within the IN network itself has been shown to exhibit structure in the sagittal plane (Rieubland et al., 2014), but how this structure affects the recruitment of INs remains elusive.

Despite the abundance of *in vitro* data, our understanding of how excitatory input pathways recruit the IN network *in vivo*, and how the resulting IN activation impacts PC dynamics, remains limited. To study the principles governing the recruitment of

INs and their targets simultaneously, I performed dual two-photon targeted patch-clamp recordings of INs and PCs in mice *in vivo*, using cross-correlation analysis of PC complex spikes, simple spikes, and IN spikes. I found that synchronous granule cell input to INs and PCs is always observed in concert with powerful IN-PC inhibition, demonstrating functional feed-forward inhibition on the level of single IN-PC pairs. I further demonstrate that INs with opposite responses to climbing fibre input do not equally affect PC spike output: INs excited by CF input often have no detectable effect on PC spike output, arguing against a CF-IN-PC feed-forward inhibition motif controlling PC spiking. Accordingly, in preliminary experiments in which IN firing was inhibited optogenetically, I found no evidence for IN activity prolonging the pause in PC firing after CF input. INs inhibited by CF input, on the other hand, often have inhibitory effects on PC firing, thereby forming a local motif of CF-IN-PC feed-forward disinhibition. My data demonstrate differential recruitment of functional IN-PC connectivity by different excitatory pathways, with important implications for the dynamic role of inhibition in the cerebellar network.

6.2 Results

6.2.1 Interneuron-Purkinje cell inhibition: The recruitment by granule cell input

In order to study the recruitment of functional inhibition by excitatory input pathways *in vivo*, I performed dual patch-clamp recordings from INs and PCs in vermis and Crus II of isoflurane-anaesthetised PV^{+}-GFP mice under two-photon guidance. Analysis presented in sections 6.2.1 and 6.2.2 of this chapter is based on the same experiments as described in chapters 3 and 4. Cross-correlograms of spontaneous IN and PC simple spikes revealed signatures of shared granule cell input as well as of IN-PC inhibition (see chapter 3 of this thesis): In the -10-0 ms bin preceding the IN spike, PC rates could be significantly increased (PC rate z-score > 3), indicating co-activation of the IN and PC by granule cell input. In the 0-10 ms bin after the IN spike, PC rates could be significantly decreased (PC rate z-score < -3), indicative of inhibition from INs (Fig 6.1a, data previously shown in Fig 3.6b).

Are the presence of shared granule cell input and inhibition in a given IN-PC pair independent of each other? To address this question, I quantified the occurrences of common excitatory input and inhibition in my dataset of spontaneous IN-PC spike cross-correlograms. In 56 pairs I recorded, I observed 6 instances in which PC spiking significantly increased 10-0 ms prior to the IN spike, and 24 instances in which PC spiking was significantly decreased after the IN spike. Importantly, in all 6 pairs with IN-PC co-activation, I also observed inhibition, showing that the occurrences of common input and inhibition are not independent of each other (Fig 6.1b, Fisher's exact test, $p = 0.004$). In accordance with (Blot et al., 2016), I thus find that IN-PC pairs that share excitatory granule cell input are connected, demonstrating the implementation of feed-forward inhibition on the level of individual IN-PC pairs receiving spontaneous granule cell inputs. I did not detect significant common granule cell input in 18 out of 24 pairs with PC inhibition, which might be explicable by low levels of spontaneous granule cell activity (Chadderton et al., 2004; Wilms and Häusser, 2015) or by some connected IN-PC pairs not sharing a substantial amount of granule cell excitation. The average normalised PC rate after the IN spike was similar for both groups (Fig 6.1c), and the correlation between amplitudes of common input and inhibition (i.e. between the normalised PC rates pre and post IN spike) was weakly significant across all pairs (linear regression, $R^2 = 0.095$, $p = 0.020$).

INs with significant inhibitory impact on PC spiking are positioned lower in the molecular layer (see chapter 3 of this thesis). Within this group of IN-PC pairs exhibiting significant PC inhibition, however, I found no evidence for the spatial position of an IN inhibiting a given PC determining the presence of common granule cell input (Fig 6.1e).

In summary, by showing that all IN-PC pairs receiving common granule cell input also show IN-PC inhibition, I establish that granule cell input recruits functional feed-forward inhibition, highlighting the role of INs in limiting excitation of PCs in time.

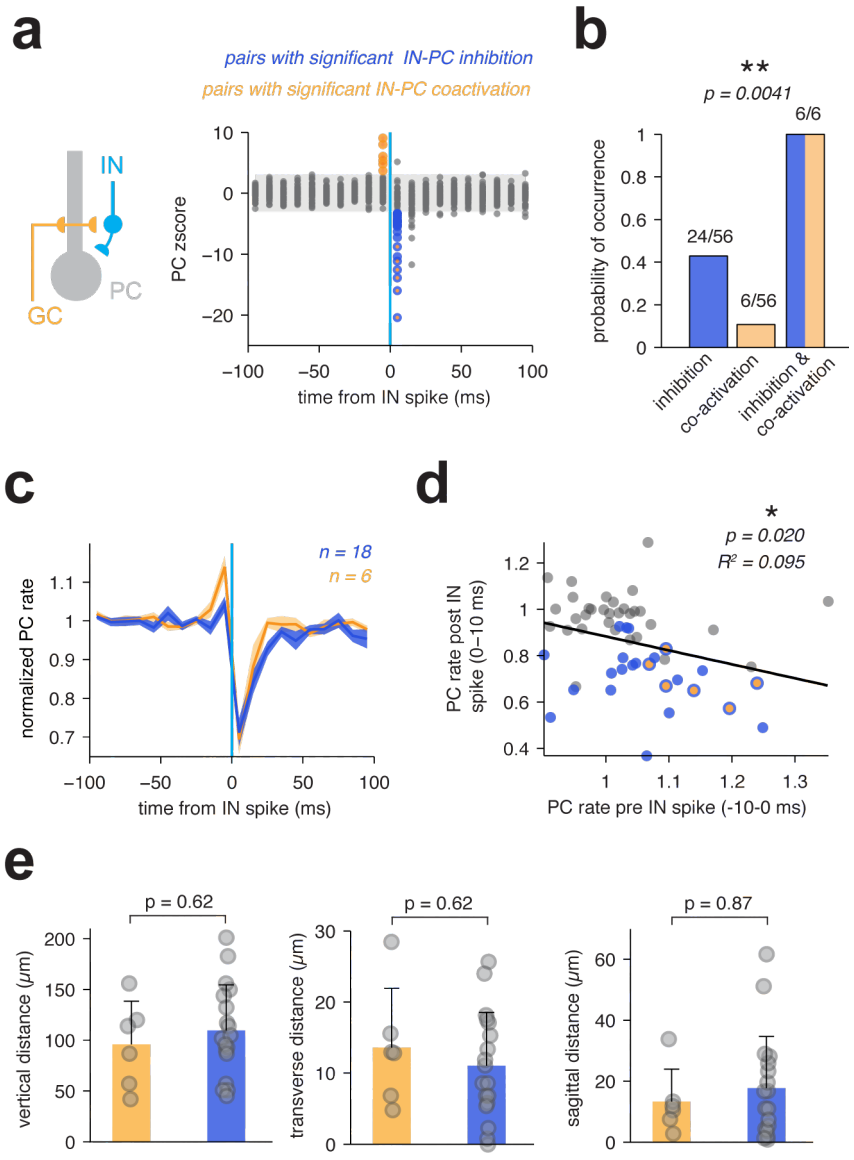

Fig 6.1 IN-PC pairs with common granule cell input are connected

(a) Left: Illustration of relevant microcircuit. Right: Z-scores of PC rates triggered on spontaneous IN spikes (n = 56 pairs). Significance threshold of 3 is indicated as grey bar, significant PC co-activation with IN (z-score > 3 -10-0 ms from IN spike) is shown in orange, PC inhibition (z-score < -3 0-10 ms from IN spike) in blue. The overlap of both effects is shown as an orange circle with a blue outline. Same data as shown in Fig 3.6b. (b) The probability of observing IN-PC inhibition (blue) is 100% in pairs with significant IN-PC co-activation (orange). The association between IN-PC inhibition and co-activation is significant (Fisher's exact test). (c) Normalised PC rates for pairs with significant co-activation (orange) and pairs with significant inhibition only (blue) are similar after the IN spike. Shading denotes SEM. (d) Normalised PC rates before the IN spike negatively correlate with PC rates after the IN spike (black: regression line, n = 56). Same colour code as in a. (e) Vertical (left), transverse (middle), and sagittal (right) Euclidean intersomatic IN-PC distances are similar

for pairs with significant IN-PC co-activation (orange) and pairs with significant IN-PC inhibition only (blue).

6.2.2 Interneuron-Purkinje cell inhibition: The recruitment by climbing fibre input

Molecular layer interneurons can respond to local climbing fibre input with rate increases and/or delayed decreases *in vivo*, as I have described in chapter 4 of this thesis. In order to understand how this segregated IN activation upon CF input affects PC activity, it is essential to investigate how differentially influenced INs signal to the PC receiving the CF input: Do INs and their targets receive common excitatory CF input, forming a motif of feed-forward inhibition (Fig 6.2a), or do INs and their targets receive opposing CF input (inhibition and excitation, respectively), resulting in a motif of feed-forward disinhibition (Fig 6.2b)?

To address this question, I separated my dual recordings into pairs with significant CF-IN excitation only (n = 13), CF-IN inhibition only (n = 8), and pairs without CF-IN effects (n = 32, Fig 6.2c). I then assessed the average effect of spikes in these INs on the simultaneously recorded PC simple spikes (Fig 6.2d). The average effect on PC spiking was significantly bigger in the CF-IN inhibition than in the CF-IN excitation group, as seen in a greater PC spike rate decrease (normalised PC rate of 0.70 ± 0.13 vs 0.90 ± 0.21 after IN spike, p = 0.018) (Fig 6.2d right). Moreover, the probability of observing significant IN-PC inhibition in a given pair did not seem to depend on the presence of CF-IN excitation (3 out of 13 pairs with CF-IN excitation exhibited significant IN-PC inhibition, p = 0.13, Fig 6.2e), whereas the probability of observing IN-PC inhibition was highly increased in CF-IN inhibition pairs (7 out of 8 pairs, p = 0.01, Fisher's exact test). This result is consistent with the anatomical inhibitory routes described in chapters 3, 4 and 5 of this thesis: INs lower in the molecular layer are inhibited upon CF input, and lower INs are more likely to inhibit PC spiking.

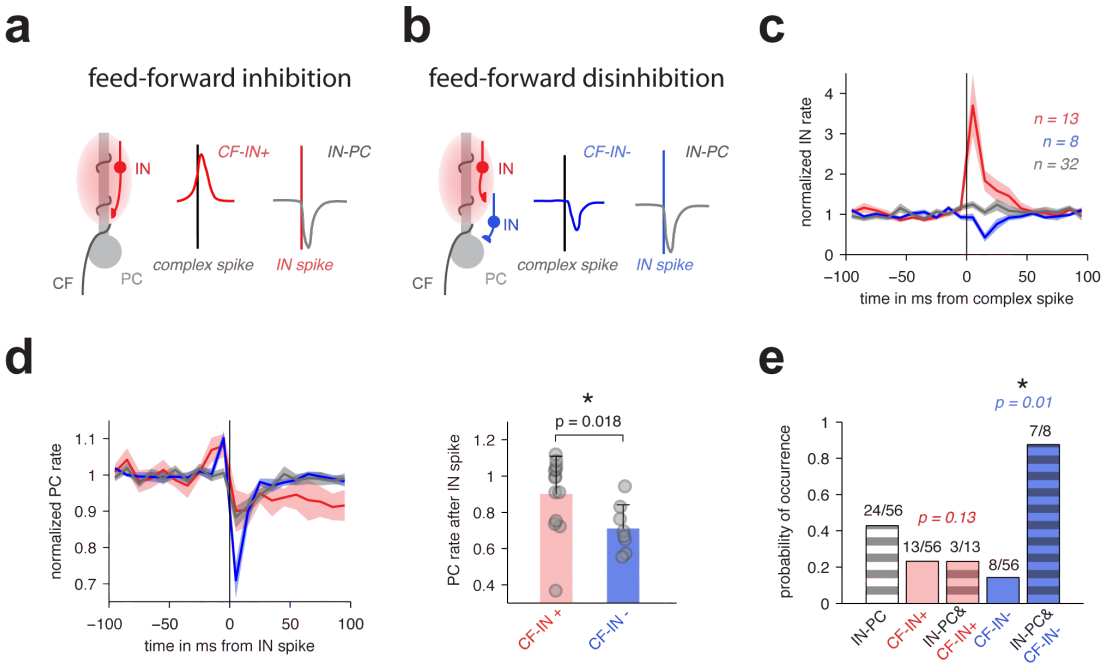

Fig 6.2 Climbing fibre input inhibits INs with impact on PC spiking

(a) Schematic of a CF-IN-PC feed-forward inhibition circuit (left). A preference for this motif would manifest in CF-IN excitation (CF-IN+, middle) co-occurring with IN-PC inhibition (right) in the same IN-PC pairs. (b) Schematic of a CF-IN-PC feed-forward disinhibition motif: A preference for this circuit would manifest in CF-IN inhibition (CF-IN-, middle) co-occurring with IN-PC inhibition (right). (c) Normalised mean IN rates triggered on complex spikes. INs are grouped based on whether they respond to CF input with significant excitation (red), inhibition (blue) or no rate change (grey). (d) Left: Normalised PC rates triggered on IN spikes, same grouping as in (c). Shadings denote SEM. Right: Normalised PC rates 0-10 ms after the IN spike were significantly lower in CF-IN- pairs than in CF-IN+ pairs. (e) The absolute probabilities of observing significant IN-PC inhibition (grey stripes), CF-IN+ (red), CF-IN- (blue), and the conditional probabilities of observing IN-PC inhibition given CF-IN+ or CF-IN- in a given IN-PC pair are shown. The association between the occurrence of IN-PC inhibition and CF-IN+ is not significant, whereas the association between IN-PC inhibition and CF-IN- is (two tailed Fisher's exact test).

Contrary to predictions from *in vitro* studies, I thus reveal that INs activated by glutamate spillover from local CF activity show little direct effect on PC spike output, arguing against a crucial role of CF-PC feed-forward inhibition via INs in regulating PC spiking. On the other hand, I demonstrate that the INs indirectly inhibited upon CF input have strong impact on PC spike output, revealing a preference for a local CF-PC feed-forward disinhibition motif via INs.

In contrast to granule cell input that activates both INs and their targets (see Fig 6.1), CF input modulates strongly connected IN-PC pairs in opposite directions, exciting the PC, but inhibiting INs with strong inhibitory effects on the same PC. These opposing IN recruitment pathways are especially apparent when considering the full functional connectivity matrix, illustrating the probability of co-occurrences of all measured CF-IN and IN-PC effects in a given pair (Fig 6.3a): The most common co-occurrence was given by CF-IN inhibition coinciding with IN-PC inhibition and common granule cell input (probability of 5/6 = 0.83). Thus, GC and CF inputs have opposite effects on these INs that deliver powerful inhibition to PCs. The resulting anatomical opposing routes of GC feed-forward inhibition and CF feed-forward disinhibition are summarized in the circuit diagram in Fig 6.3b.

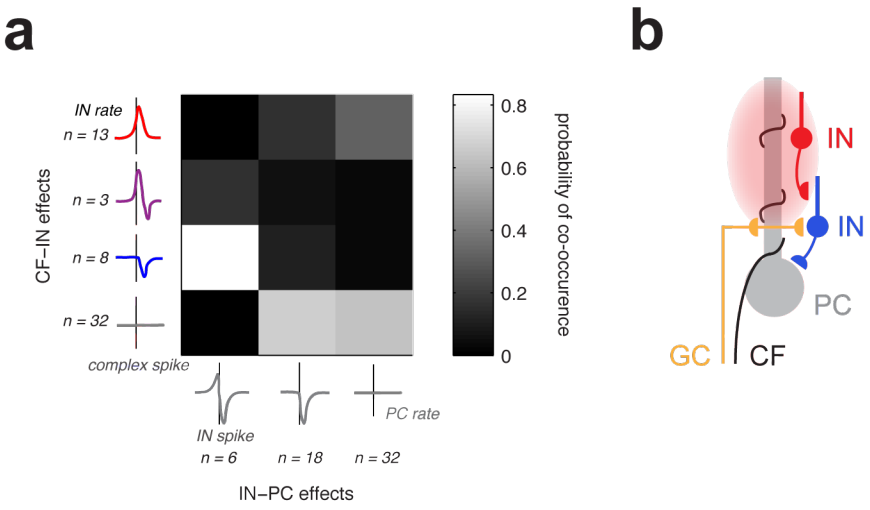

Fig 6.3 Opposing recruitment of IN feed-forward circuitry by granule cell and climbing fibre inputs

(a) Functional connectivity matrix illustrating the probability of co-occurrence of all possible CF-IN and IN-PC effects in a given pair. Note that CF-IN inhibition strongly co-occurs with IN-PC inhibition preceded by common excitatory granule cell input. (g) Diagram of the resulting microcircuit motif.

6.2.3 The effect of INs on PC spiking after CF input

Activation of INs by climbing fibre glutamate spillover has been suggested to mediate feed-forward inhibition onto PCs, prolonging the pause in PC simple spiking often observed after a PC complex spike (Mathews et al., 2012). My data, however, show that spikes in single INs with excitatory responses to CF input often do not inhibit PC spiking, and demonstrate a feed-forward disinhibition circuit motif. This discrepancy prompts the question: What is the net effect that IN recruitment by CF input has on PC spiking? Is there evidence of PC disinhibition upon CF input, and do the timecourses of IN and PC responses to CF input match? To address these questions, I first quantified the change of PC spiking after CF input and compared its timecourse to the dynamics of IN spiking upon CF input (described in detail in chapter 4 of this thesis).

Fig 6.4a shows an example of a PC simple histogram triggered on complex spikes: After the initial post complex spike pause, an increase in PC firing rate above baseline was observed, with two clear peaks indicating two precisely timed simple spikes following a complex spike. This delayed increase in PC firing sometimes termed 'simple spike facilitation' has been documented previously (De Zeeuw et al., 2011) and also appeared in the median of all normalised PC rate histograms triggered on complex spikes, peaking at 17.5 ms (n = 56, Fig 6.4b). To assess whether the recruitment of the IN network might contribute to this PC facilitation, I visualized the timecourse of IN and PC responses to CF input by plotting the net spike changes (Fig 6.4c). On average, PCs fired one extra spike in response to CF input. The absolute changes in INs responding with pure increases (n = 13) or pure decreases (n = 8, see circuit diagram on right) were smaller (means of 0.18 and -0.16 respectively). After CF input, PCs showed decreases in spiking for as long as excited INs showed increases. Afterwards, PCs exhibited spike increases that appeared delayed to the spike decreases of INs inhibited by CF input.

These data illustrate that upon CF input, PCs show a bidirectional modulation of simple spiking, consisting of a decrease followed by an increase. The timecourses of segregated IN excitation and inhibition upon CF input match the timecourses of PC inhibition and facilitation. Based on the timing of modulation in spiking, it thus

seems plausible that the structured IN network could sculpt changes of PC spiking after CF input, resulting in pauses and facilitation of PC firing.

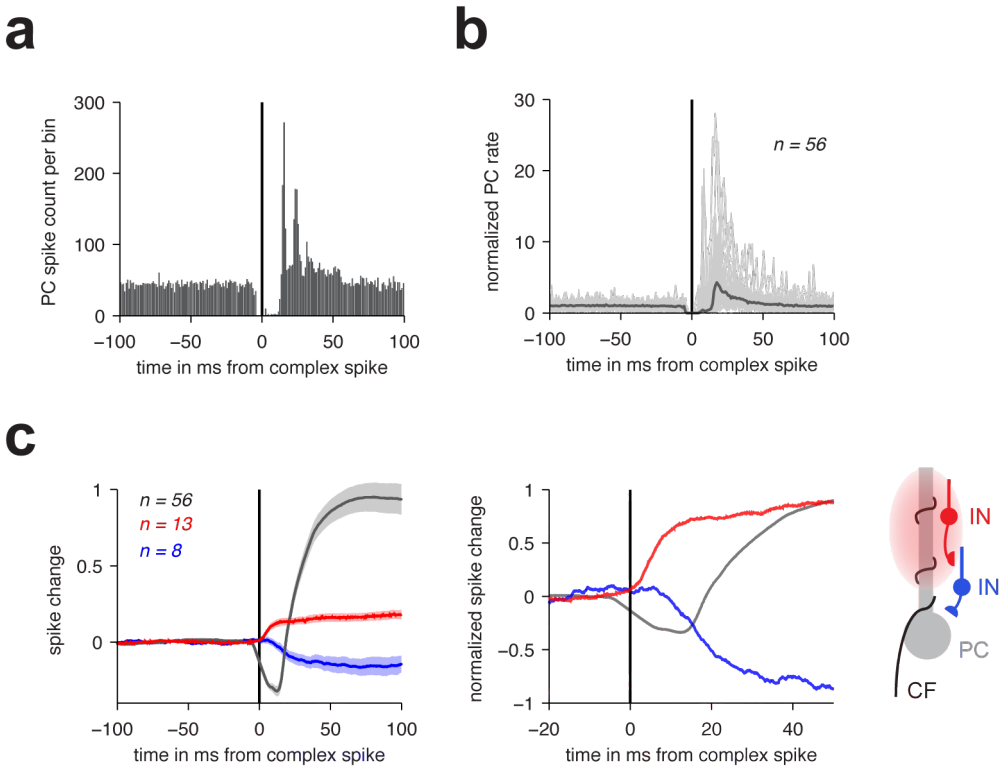

Fig 6.4 Timecourse of IN and PC responses to climbing fibre input

(a) Example of a PC simple spike histogram triggered on complex spikes, bin size = 1ms. (b) Normalised PC rates triggered on complex spikes (light grey: single PCs, dark grey: median of 56 PC recordings). (c) Left: Mean spike changes triggered on complex spikes for all PCs (grey, n = 56), INs exhibiting pure increases (red, n = 13) and INs exhibiting pure decreases (blue, n = 8). Shadings denote SEM. Middle: Zoom of left figure with expanded x-axis and mean spike changes normalised to their extreme values for better comparison of timecourses. Right: Schematic of underlying circuit.

While the correspondence between IN and PC response timecourses is highly suggestive, it is still a pure correlation and does not demonstrate a causal relationship between IN and PC responses to CF input. To directly assess how INs contribute to PC spiking, a method to prevent IN recruitment by CF input is necessary.

I therefore infected INs specifically with the optogenetic silencer ArchT (Han et al., 2011), using an nNOS-Cre-ER mouse line and a virally delivered floxed version of the opsin fused to GFP (Fig 6.5a). 4 weeks post virus injection into the cerebellum and 3 weeks after induction of expression with tamoxifen (Hayashi and McMahon, 2002), GFP expression was obvious in IN membranes with two-photon microscopy *in vivo* (Fig 6.5b). I performed two-photon targeted loose-patch recordings of GFP-expressing INs (Fig 6.5c,d). Illumination of the cerebellar cortex with an amber LED (595 nm) resulted in robust inhibition of IN spiking (Fig 6.5d) (from 3.38 ± 2.56 Hz to 0.01 ± 0.05 Hz, $p = 1.71*10^{-6}$, n = 30 trials, Wilcoxon signed-rank test), followed by a brief period of IN rebound firing upon LED offset. An unlabelled PC, identified by the size of the soma shadow under 2-photon microscopy (Kitamura et al., 2008) as well as by the presence of complex spikes, showed the opposite change in firing rate: During LED illumination, PC simple spike frequency significantly increased (Fig 6.5e) (from 21.95 ± 3.82 Hz to 27.10 ± 3.86 Hz, $p = 1.2*10^{-5}$, Wilcoxon signed-rank test, 85 trials) and then transiently decreased below baseline after LED offset. These data demonstrate that by transfecting INs with ArchT, specific IN silencing can be achieved, removing tonic inhibition from PCs and thereby resulting in PC disinhibition.

With this tool at hand, I could then investigate the contribution of INs to PC firing modulation after CF input. In each PC recorded from, I first verified that LED presentation resulted in PC spiking disinhibition, as shown in Fig 6.5e. In the 3 PCs I was able to record from, simple spike rates did increase significantly during LED illumination by 12-30% of baseline rates, indicating that INs synapsing onto the PCs recorded from were expressing ArchT and successfully inhibited.
I then analysed PC spiking after complex spikes during control and IN inactivation conditions, respectively. If IN activation upon CF input led to strong feed-forward inhibition of PC spiking, one would expect to see stronger PC spiking inhibition in the LED off than in the LED on condition, e.g. in the form of a prolonged post-

complex spike pause of PC spiking or in an overall reduction of PC spiking in the first tens of milliseconds after complex spike onset.

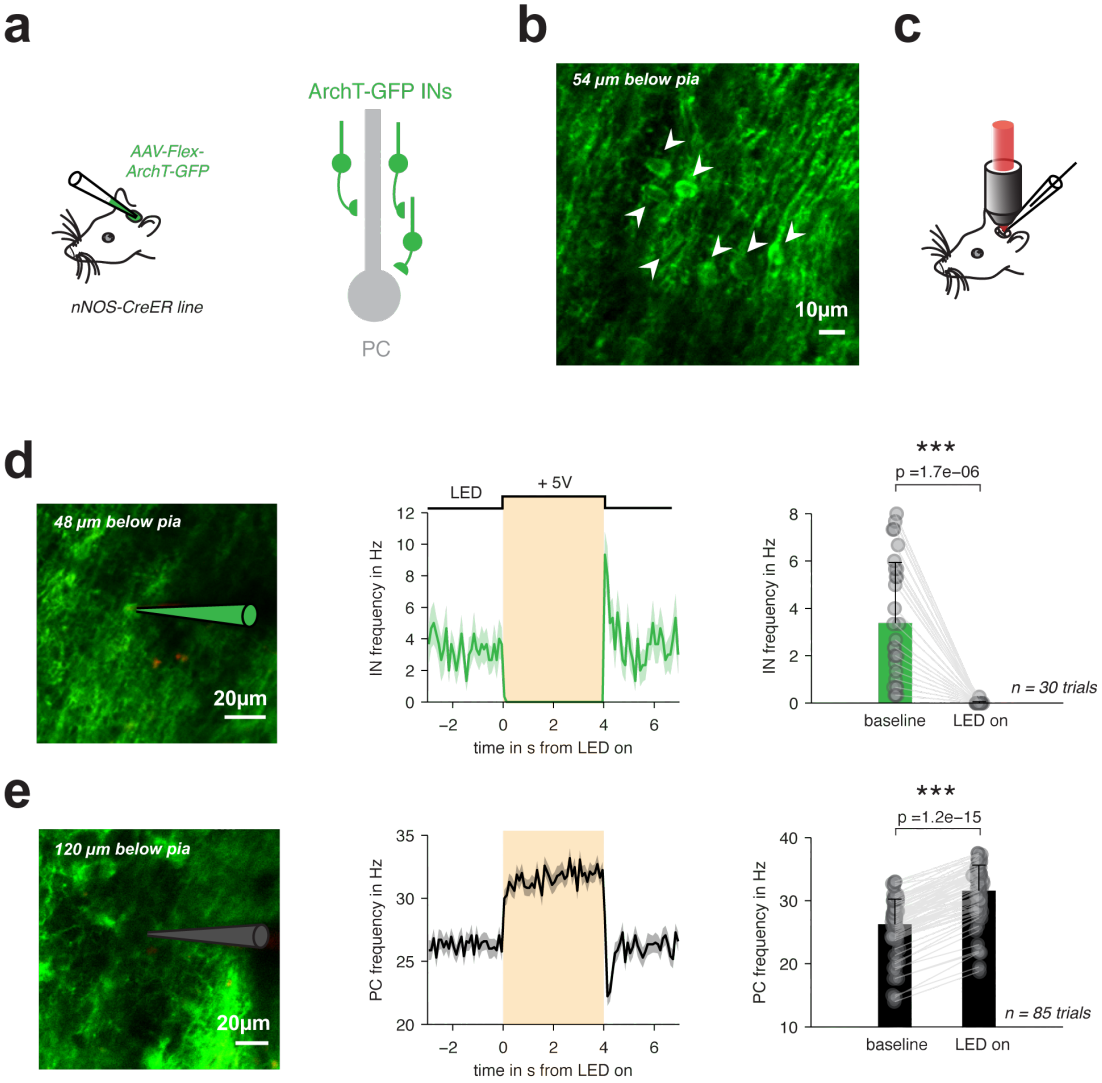

Fig 6.5 Optogenetic inhibition of INs disinhibits PCs

(a) Left: Mice of the nNOS-CreER line were injected with AAV-Flex-ArchT-GFP, to achieve ArchT-GFP expression in molecular layer interneurons (right). (b) 2-photon average intensity projection of cerebellar cortex 54 µm below the pia. Arrows indicate somata of INs expressing ArchT-GFP. (c) Two-photon targeted recordings were performed in nNOS-CreER mice injected with ArchT-GFP. (d) Left: 2-photon average intensity projection of IN recording expressing ArchT-GFP. Middle: Average IN firing rate before, during and after illumination with a 595 nm LED. Right: IN firing was significantly reduced during illumination. (e) Left: 2-photon image of PC recording in the same animal. PCs were not labeled. Middle: Average PC simple spike rate before, during and after illumination. Right: PC simple spike frequency was significantly increased during illumination.

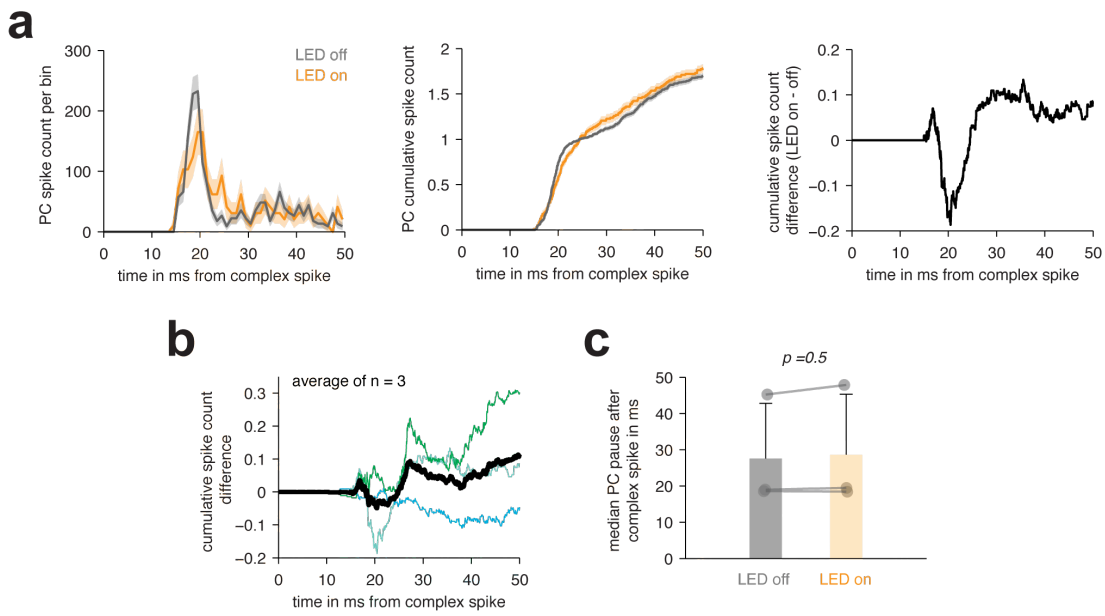

Fig 6.6 Effects of IN inactivation on PC post complex spike activity

(a) Left: Histogram of PC simple spikes triggered on PC complex spikes during control (LED off, grey) and during optogenetic IN inactivation (LED on, orange). Bin size = 2 ms. Middle: Average cumulative PC simple spike count triggered on PC complex spikes, same colour code as left. Shading denotes mean ± SEM. Right: Difference of mean PC cumulative spike count between both conditions (LED on minus LED off condition). (b) Same as (a) right, but for n = 3 PCs. Coloured lines represent individual PCs, black trace represents the average. (c) Median duration of pause in PC simple spiking after complex spikes during control (left) and IN inactivation (right). n = 3 PCs.

However, IN inactivation via optogenetic inhibition only had subtle effects on PC spiking after climbing fibre input, as the example in Fig 6.6a illustrates. The spike histograms and cumulative spike counts after complex spikes were similar for both conditions, with PC simple spiking resuming at roughly 14 ms after complex spike onset. There was no sign of stronger PC inhibition in the 'LED off' condition in the first 20 ms after the complex spike. In fact there were slightly more PC spikes in this time window without optogenetic inhibition of INs, which is most obvious when looking at the difference in mean PC cumulative spike counts between the 'LED on' and 'off' conditions (Fig 6.6a right). At longer delays, there were more PC spikes in the 'LED on' condition, consistent with PCs being disinhibited by optogenetically hyperpolarising tonically active INs. The summary data for all three recorded PCs

revealed inconsistent effects (Fig 6.6b): The other two PCs showed opposite cumulative spike count differences between the two conditions, one exhibiting a net increase and one a net decrease of PC spiking after complex spikes due to IN inactivation. Moreover, the pause of PC spiking after complex spikes was not significantly and consistently altered (Fig 6.6c).
In summary, in my small dataset of n = 3 PC recordings, I did not find evidence for IN activation by CF input increasing the PC post-complex spike pause, as reported in other studies.

Unfortunately, in mice expressing ArchT in INs, PCs could be visualized and recorded from very rarely. Upon slicing the cerebellum and staining for neuron somata with a red Nissl stain, it became obvious why: In areas where INs expressed ArchT, no PC somata were seen in the underlying PC layer (Fig 6.7). Instead, green fluorescent elongated aggregates were visible, probably being autofluorescent remnants of dead PCs. In the same cerebellum, in areas with no ArchT expression in INs, PC somata were clearly identifiable (Fig 6.7), indicating that the loss of PCs was specific to areas of IN-ArchT expression. It therefore appeared that expression of the proton pump ArchT in INs lead to degeneration of underlying PCs, preventing a systematic assessment of PC spiking dynamics during IN inactivation with the current method.

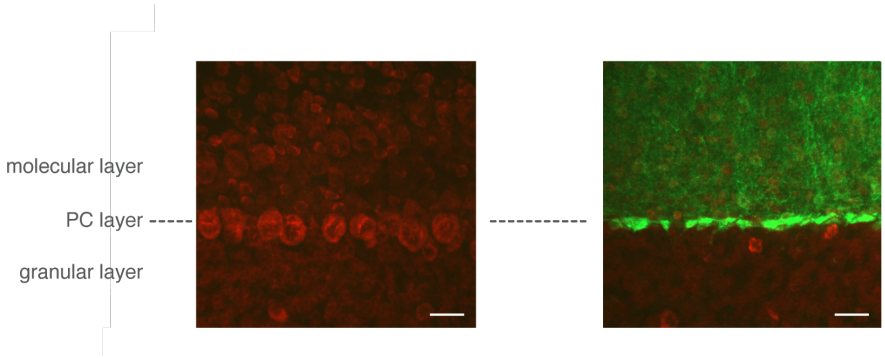

Fig 6.7 ArchT expression in INs co-occurs with PC degeneration

Confocal images of cerebellar slices (80µm) of an nNOS-CreER ArchT mouse treated with a red Nissl stain. Left: An area of the cerebellum without ArchT-GFP expression in INs in the molecular layer shows an intact PC layer. PC layer position is indicated by dotted grey line. Right: An area of the same cerebellum with ArchT-GFP expression in INs shows no intact PC cell layer, but green fluorescent aggregates instead. Scale bars indicate 20 µm.

6.3 Discussion

My experiments presented in this chapter provide the first *in vivo* assessment of higher-order functional connectivity involving synaptic and extrasynaptic pathways. By recording spiking activity of identified INs and PCs simultaneously, I measured functional inhibitory connectivity between INs and PCs as well as between excitatory inputs and their targets. I revealed that granule cell and climbing fibre input recruit functional feed-forward inhibitory networks differently: While granule cell input recruits both INs and their targets, resulting in feed-forward inhibition, CF input often activates INs with no detectable influence on PC firing, but indirectly inhibits powerful INs with a delay, forming a motif of feed-forward disinhibition. This segregation of IN activity highlights that the function of INs is dynamic, depending on the excitatory input pathway activating the circuit.

6.3.1 Granule cell input recruits PC feed-forward inhibition via INs

It has previously been suggested that under physiological conditions, connected IN-PC pairs are not likely to be activated by the same excitatory granule cell inputs (Jörntell et al., 2010). However, in my dataset, all IN-PC pairs that were co-activated by shared excitatory input also showed inhibitory functional connectivity,

demonstrating an overrepresentation of the IN-PC feed-forward inhibition motif. The implementation of feed-forward inhibition on the microcircuit scale has been suggested before based on slice studies (Mittmann et al., 2005), but in these cases, granule cell inputs were stimulated electrically, likely leading to unnatural levels of synchrony in parallel fibre activity. By cross-correlating spontaneous IN and PC spikes *in vivo*, in contrast, I could assess whether INs and PCs were co-activated by synchronous spontaneous granule cell input, i.e. by the activity of natural granule cell ensembles. This method does not render evidence that co-activated IN-PC pairs were activated by inputs from the exact same granule cells, as in theory, different granule cells could fire in synchrony and contact only INs or PCs separately, thereby creating correlations in the activity of INs and PCs. However, spontaneous granule cell activity levels are very low, especially under isoflurane anaesthesia (Wilms and Häusser, 2015), making it likely that in my dataset, co-activated INs and PCs indeed do share a substantial amount of the same granule cell inputs.

What exactly is the nature of the shared inputs into INs and PCs? Studies on granule cell population activity so far have mostly been restricted to field potentials, as granule cells are too densely packed and too small for individual cells to be identified with multi-unit extracellular recordings. In these studies, it was found that spatially restricted activity in the granule cell layer correlates positively with activity of PCs overlying the active granule cell cluster (Bower and Woolston, 1983; Lu et al., 2005). This vertical organisation of both spontaneous as well as sensory-evoked granule cell and PC activity lead to the suggestion that the excitatory effect of granule cells on PC spiking is primarily exerted via ascending granule cell axons, rather than via parallel fibres. On the other hand, measuring sensory-evoked activity of parallel fibres using axonal calcium imaging revealed spatial clustering of co-active parallel fibres (Wilms and Häusser, 2015), suggesting that spatially clustered parallel fibre input could give rise to specific PC and IN activation.

The fact that I did not see positive correlations of IN and PC spiking at large transverse distances, but only within the IN-PC population exhibiting inhibition at small transverse distances of 30 μm or less, suggests that maybe in my dataset, common excitatory input into INs and PCs might indeed stem from ascending granule cell axons and/or from synapses of parallel fibres close to the axonal bifurcation point (Pichitpornchai et al., 1994). While ultrastructure studies on the

ascending axon to PC synapse exist, supporting the notion that ascending axons indeed have strong excitatory influence on PC spiking (Gundappa-Sulur et al., 1999; Pichitpornchai et al., 1994), no such information is available for possible ascending axon to IN synapses. Recent advances in automated ultrastructure image reconstruction (Helmstaedter et al., 2013) may facilitate future efforts of generating detailed connectivity maps of the cerebellar cortex, illuminating the relative contributions of parallel fibres and ascending axons to shared excitation between IN and PC pairs.

What is the functional significance of this feed-forward inhibition motif? I observed a weak, yet significant correlation between the amplitudes of common excitatory input and inhibition across the entire dataset, implying that excitation and inhibition in IN-PC pairs might scale together: It seems that the greater the common input of a given IN-PC pair, the greater the IN inhibits the PC. A fine balance of excitation and inhibition *in vivo* has been described in other sensory cortices before (Haider et al., 2006; Okun and Lampl, 2008), and has been implied in regulating excitability and timing of principal cells. Feed-forward inhibitory connectivity has been demonstrated to increase the dynamic range of network responses, preventing early saturation (Pouille et al., 2009), and to regulate the exact timing of principal neurons, narrowing the time window for summation of excitatory inputs and spike output (Gabernet et al., 2005; Mittmann et al., 2005; Pouille and Scanziani, 2001). The overrepresentation of feed-forward inhibition on the microcircuit level described here indicates that this motif is a core feature of cerebellar computation. It highlights that INs have a crucial role in limiting excitation of PCs following granule cell input, and puts INs in a position to precisely regulate the timing of PC output in response to granule cell input. Given the role of the cerebellum in fine-tuning movement during sensorimotor tasks, INs are likely important circuit features enabling precision of spike timing and behaviour.

6.3.2 A circuit motif of climbing fibre-PC disinhibition via INs

To date, the effect of extrasynaptic CF-IN transmission on local PC activity has mostly been considered in a feed-forward inhibitory framework where activated INs inhibit the local PC, prolonging post complex spike pauses in simple spiking

(Marshall and Lang, 2009; Mathews et al., 2012; Wulff et al., 2009). The recruitment of chemical interactions within the IN network upon CF input has been hypothesized to mediate disinhibition of more distant PCs not innervated by the active CF (Coddington et al., 2013). My data present structured overlap between functional CF-IN and IN-PC interactions, revealing a novel microcircuit in which INs inhibited upon CF input inhibit spiking of the local PC, thereby forming a circuit motif of local delayed PC disinhibition upon CF input.

What is the consequence of this motif for PC dynamics following CF input? Activation of vertically distant INs might provide dendritic inhibition to PCs that I could not assess by recording somatic PC spikes, thereby providing feed-forward inhibition with little effect on PC spike output. As IN activity powerfully regulates dendritic calcium levels of PCs (Callaway et al., 1995), the observation that inhibition regulates variability of CF-triggered dendritic calcium levels (Kitamura and Häusser, 2011) is in line with this hypothesis. CF and IN axon morphology could favour compartmentalized inhibition within the PC dendritic tree, as CF and IN synapses at branch points might represent 'strategic places in the complex PC dendritic tree', possibly allowing to 'tune in or out whole sectors of the dendritic tree' (Palay and Chan-Palay, 1974). The fact that INs inhibiting PCs powerfully were not activated, but rather inhibited upon CF input, makes the IN population a less likely candidate to precisely regulate the pause of PC spikes following CF input, a phenomenon that might rather be the result of dynamic, complex interactions between somatic and dendritic PC currents (Jaeger et al., 1997).

6.3.3 Effects of optogenetic IN inhibition

By optogenetically silencing INs and observing PC firing rate increases as a result, I confirmed that *in vivo*, PCs are under tonic inhibition from INs. This result is in line with previous studies using pharmacological manipulations of GABAergic signalling, reporting PC rate increases *in vitro* and *in vivo* upon application of $GABA_A$ receptor blockers (Blazquez and Yakusheva, 2015; Häusser and Clark, 1997).
Given that INs responded to CF input, showing excitation and delayed inhibition (also see chapter 4 of this thesis), and that INs had strong effects on PC spiking (also see chapter 3 of this thesis), one would expect the recruitment of INs by CF

input to affect PC spiking. Accordingly, previous studies reported shortened pauses in PC spiking after climbing fibre input when preventing PC $GABA_A$ receptor activation with pharmacological or genetic manipulations (Mathews et al., 2012; Wulff et al., 2009), suggesting that IN recruitment by CF input prolonged the pause in PC spiking.

In my dataset, however, PC spiking after CF input was rather similar during control conditions and during optogenetic IN inactivation, with no change in the duration of the PC post-complex spike pause. This lack of IN effect is in line with my finding that INs activated by CF input often do not noticeably inhibit spiking of PCs receiving that CF input, providing further support for the notion that the CF-IN-PC feed-forward inhibition motif is not crucial for regulating PC spiking. On the other hand, my preliminary data suggest that IN recruitment by CF input might even cause additional PC spikes around 20 ms after CF input. This time-course intriguingly matches the timing of inhibitory IN responses to CF input, suggesting that this effect might be due to PC disinhibition via INs. However, a larger dataset would be necessary to study the temporal dynamics of IN effects on PC spiking beyond the first spike after CF input more carefully.

Why did most PCs appear to have degenerated in areas where INs expressed ArchT, evidenced by missing PC somata and autofluorescent aggregates in the PC layer? The hyperpolarising action of ArchT relies on pumping protons out of the neuron upon illumination (Han et al., 2011), which may result in acidification of the extracellular medium. Changes in intracellular and extracellular pH levels affect neuronal excitability (Ruffin et al., 2014), especially in PCs: PC membranes contain acid-sensing ion channels that are activated by extracellular pH levels below 6.8 resulting in inward current (Allen and Attwell, 2002). With high levels of ArchT expression in INs, there might be some baseline ArchT activity even without illumination, either transiently or persistently, creating an acidic extracellular medium in which PCs cannot maintain their metabolically demanding activity levels and degenerate. The vulnerability of PCs to alcohol consumption, also resulting in lower pH levels, fits this hypothesis (Ramadoss et al., 2008).

To achieve sufficient levels of hyperpolarising opsin expression in INs while maintaining intact PCs, employment of a different hyperpolarising opsin might be more fruitful. Halorhodopsin, an inward chloride pump, or recently developed light-

guided anion channels could be suitable alternatives (Chuong et al., 2014; Govorunova et al., 2015; Gradinaru et al., 2010).

6.3.4 Functional implications

In his 'theory of cerebellar function', Albus suggested that subgroups of INs show opposite forms of plasticity at the parallel fibre-IN synapse, instructed by climbing fibre input. The sign of plasticity, he conjectured, should depend on a given IN's connectivity pattern with granule cells and its target PCs: INs that do not receive the same granule cell input as the PCs that they target were said to exhibit granule cell-IN LTD, whereas INs receiving common granule cell input with their target PCs were said to exhibit granule cell-IN LTP. 'Thus (those INs sharing granule cell input with their target PCs) are conjectured to change in the opposite direction from all the other variable synapses under the same coincidence conditions.' (Albus, 1971). Albus thereby predicted that whether a given IN delivers granule cell feed-forward inhibition onto PCs should determine the sign of its CF-dependent plasticity. In a feed-forward inhibitory network, LTD of the granule-cell IN synapse would then work synergistically with LTP at the granule-cell PC synapse.

My data show that indeed, there is a relationship between an IN's participation in functional granule cell feed-forward inhibition onto PCs and its response to CF input: Specifically INs receiving common granule cell input with their PC targets are inhibited upon CF input, while many other INs are excited upon CF input.

What is the functional significance of this arrangement? Paired granule cell and excitatory CF input into INs may lead to LTP (Jörntell and Ekerot, 2002; Rancillac and Crépel, 2004), as opposed to LTD at granule cell-PC synapses. In INs mediating granule feed-forward inhibition, however, no depolarisation upon CF input occurs, so that specifically in these INs, CF input likely does not lead to LTP. As a result, paired granule cell and CF input may not lead to diverging weight changes of granule cell input into INs and PCs, as would be the case given opposite learning rules at granule cell-IN and granule cell-PC synapses. The weight ratio of granule cell-IN and granule cell-PC synapses may rather remain constant even across learning, ensuring that a given set of granule cell inputs would recruit INs and their

targets with similar efficiency. Therefore, hyperpolarisation of a subset of INs by CF input might be crucial for the maintenance of granule cell feed-forward inhibition, serving a homeostatic function.

7 Functional interneuron-Purkinje cell connectivity during sensory processing

7.1 Introduction

Integrating sensory and motor information to optimize motor output is a key function of the central nervous system. The cerebellum is a crucial structure for sensorimotor integration: lesions of cortical projections to the cerebellum impair a rat's ability to use whisker-related sensory information to guide movements (Jenkinson and Glickstein, 2000). Moreover, cortical sensory and motor inputs converge in the cerebellar cortex, whose activity in turn influences motor cortex firing patterns as well as whisking behaviour, demonstrating functional sensorimotor cortico-cerebellar loops (Proville et al., 2014).

One critical aspect of sensorimotor integration is the representation of sensory information itself,. The relevance of the cerebellum as a sensory structure is highlighted by the extent of its tactile input: the cerebellar hemispheres contain an enormous tactile representation of perioral surfaces and whiskers (Shambes et al., 1978; Woolston et al., 1981). Tactile information is conveyed via several pathways involving projections from the trigeminal nucleus to cerebellar cortex directly, to the pontine nuclei, the inferior olive, and thalamo-cerebro-pontine loops (Bosman et al., 2011). Direct projections as well as projections from the pons activate the mossy fibre-granule cell pathway into the cerebellar cortex, whereas projections via the inferior olive activate the climbing fibre pathway.

In the cerebellar cortex, these pathways converge at the level of Purkinje cells (PCs). Accordingly, PC responses to tactile input are multifarious, consisting of fast simple spike responses from granule cell activation, and slower complex spike responses from climbing fibre activation (Bosman et al., 2010; Brown and Bower, 2001). PC sensory responses also exhibit inhibitory components, reflecting activation of molecular layer interneurons (INs) inhibiting PCs via GABAergic synapses (Chu et al., 2011a; Santamaria et al., 2007). As INs have powerful effects on PC spike output (Blot and Barbour, 2014; Häusser and Clark, 1997, also see chapter 3 of this thesis), understanding how INs and their targets are recruited by

afferent pathways during sensory processing is critical to elucidate cerebellar sensory representations.

INs, like their targets, receive excitatory inputs from granule cells. With electrical stimulation of granule cell axons *in vitro*, INs have been shown to narrow the time window of excitatory PC responses, resulting in higher precision of PC spiking in time and highlighting a role of INs in feed-forward inhibition (Mittmann et al., 2005). In line with rapidly recruited granule cell inputs, INs exhibit fast and precise excitatory responses to tactile stimulation (Chu et al., 2012; Duguid et al., 2012). It has been suggested, however, that during sensory processing, INs and their postsynaptic PCs have a low chance of being activated by the same granule cell inputs conveying tactile information from a specific skin area, arguing against a functional role of feed-forward inhibition (Jörntell et al., 2010). Whether synaptically connected IN-PC pairs both respond to sensory-evoked granule cell input, as well as the timing relationship between IN and PC recruitment, thus remain unclear.

Recent *in vitro* studies have demonstrated that INs also receive input from the climbing fibre pathway. Climbing fibre-IN transmission is extrasynaptic, relying purely on glutamate spillover (Szapiro and Barbour, 2007). In contrast to the diversity of tactile responses in PCs, however, only fast excitatory responses have been reported in INs so far (Chu et al., 2012), preceding sensory-evoked climbing fibre input into cerebellar cortex. The relevance of physiological climbing fibre input into INs during sensory processing thus remains elusive.

In order to elucidate sensory representations in cerebellar cortex, I have studied functional IN-PC connectivity on the pair level during spontaneous and sensory-evoked activity. Not only PCs, but also INs exhibited fast and delayed excitatory responses to tactile stimulation. After fast excitation, PC firing was often decreased. Fast responses in PCs preceded fast IN responses, and sensory-evoked IN spikes correlated with PC spike increases followed by decreases, in line with recruitment of feed-forward inhibition. I found that IN recruitment by granule cell input was graded with vertical IN distance from the PC layer. Finally, I identified specificity in the recruitment of INs by different excitatory input pathways during sensory processing: INs that were excited by spontaneous climbing fibre input showed small granule cell-evoked responses and larger delayed responses in trials with sensory-evoked local

climbing fibre input. In contrast, INs that were inhibited by spontaneous climbing fibre input showed larger granule-cell mediated responses and no delayed excitatory responses.

These results demonstrate that already at the level of INs, sensory-evoked afferents of different origins generate complex sensory representations, expanding our understanding of sensory processing in the cerebellar cortex.

7.2 Results

7.2.1 Sensory responses of Purkinje cell simple spikes, complex spikes, and interneurons

In this chapter, I present data on simultaneously recorded activity of INs and PCs in Crus II during tactile stimulation of the ipsilateral whisker field and / or perioral region with a 60 ms airpuff (60 PSI). INs and PCs were targeted under two-photon guidance as described previously (Kitamura et al., 2008; Margrie et al., 2003, also see chapters 3, 4 and 6 of this thesis). IN-PC pairs had intersomatic Euclidean distances of up to 77 μm, 65 μm and 186 μm in the transverse, sagittal and vertical plane, respectively, without any correlations in sampling between different planes (n = 25, R^2 values of 0.02 – 0.10, p values of 0.12 – 0.47). Crus II is known to receive tactile projections both via the mossy fibre-granule cell pathway and via the climbing fibre pathway (Brown and Bower, 2001). Accordingly, PCs exhibited short-latency excitatory simple spike responses as well as complex spike responses, illustrated by the example in Fig 7.1a. PC complex spike responses occurred at longer and more variable latencies, as reported previously (Brown and Bower, 2001). In a simultaneously recorded IN, short-latency excitatory responses were observed with similar timing as fast responses in PCs. In other dual recordings, PC simple spikes showed additional delayed excitatory responses, a phenomenon that has been observed previously (Bosman et al., 2010). Importantly, I also found delayed excitatory responses in some INs, as shown in the example recording in Fig 7.1b. These late responses could occur independently of late responses in PCs. I further quantified sensory responses in terms of the spike change introduced by the sensory stimulus, i.e. the absolute number of extra or omitted spikes over time (Mittmann and Häusser, 2007) (Fig 7.1c, d). On average, IN sensory responses

exhibited a precisely timed fast and a more broadly timed slow component (n = 26). The slow component had a remarkably similar timecourse to PC complex spike responses (Fig 7.1d). Sensory stimulation therefore induced rapid and delayed IN responses: the former type is in line with rapid recruitment by sensory-evoked granule cell input, whereas the latter one occurs on similar timescales as sensory-evoked PC complex spikes, indicating climbing fibre input.

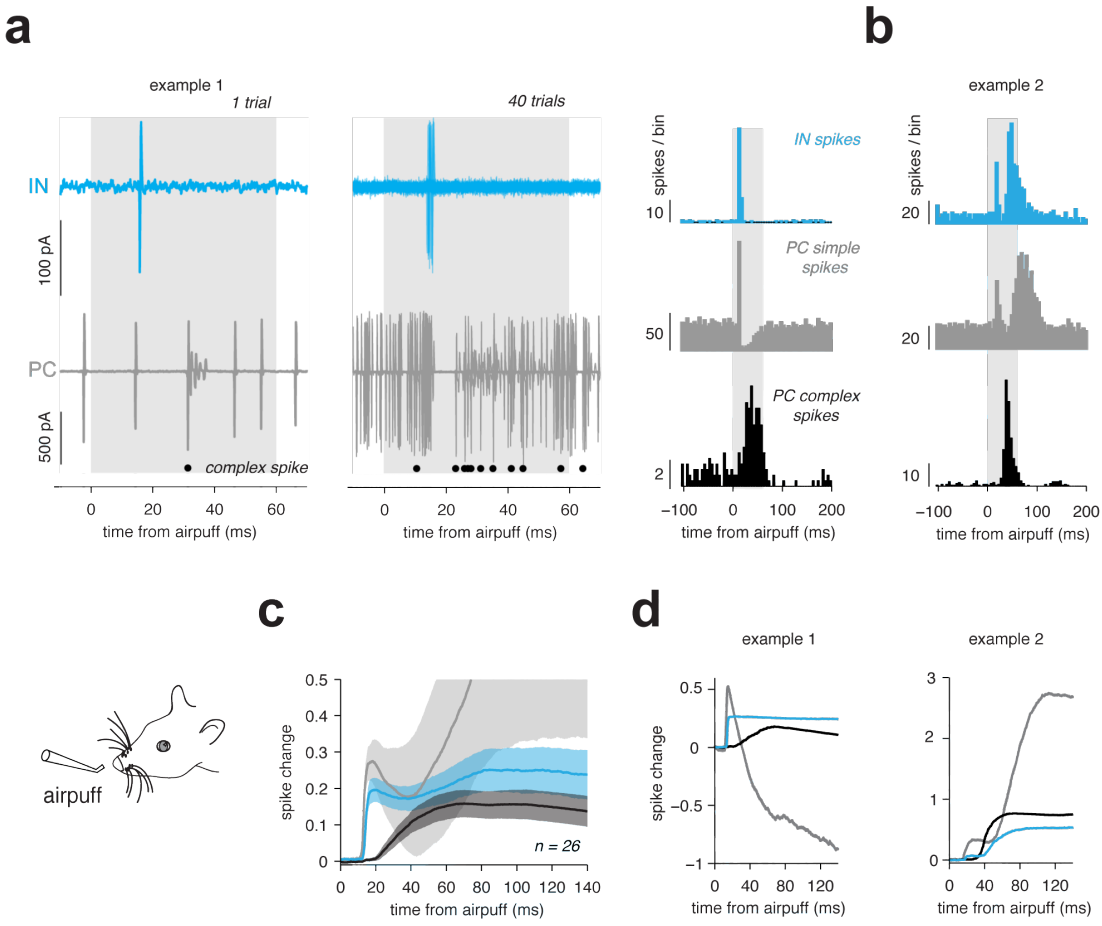

Fig 7.1 Sensory stimulation induces rapid and delayed responses in INs and PCs

(a) Example of simultaneously recorded IN and PC responses to an airpuff (60 ms, 60 PSI) directed at the ipsilateral whisker pad. Left: Raw recording of IN (top) and PC (bottom) activity. A single trial is shown. Grey rectangle indicates airpuff duration. Black circles indicate PC complex spikes. Middle: Same as left, but 40 consecutive trials overlaid. Right: PSTHs of IN spikes (top), PC spikes (middle), and PC complex spikes (bottom). Bin size = 5 ms. (b) PSTHs of a different IN-PC pair. (c) Mean sensory-evoked spike changes of IN spikes (blue), PC simple spikes (grey), and PC complex spikes (black) for all paired recordings (n = 26). Shadings denote ± SEM. (d) Sensory-evoked spike changes for the two examples shown above in (a, left) and (b, right).

What is the exact timing relationship between fast sensory-evoked responses in INs and PCs? To address this question, I calculated distributions of latencies from sensory stimulus onset to the first spike in INs and PCs. The distributions of response latencies across all pairs revealed that on average, fast PC simple spike responses preceded fast IN responses by about 1 ms, as the peaks of response latency distributions for PC simple spikes and IN spikes were positioned at 13 and 14 ms, respectively (Fig 7.2a, n = 26). PC complex spike response latencies did not show a narrow peak, but a broad increase from 20 – 60 ms, reflecting slower and more variable response times. To further analyse fast IN and PC response latencies on the pair level, I measured the maxima of response latency distributions for pairs with distinct peaks in the response latency distributions in both the IN and the PC (maxima had to be at least 4 standard deviations above mean, n = 15). Plotting PC versus IN response latencies revealed that in the majority of these pairs, the IN response lagged the PC response, as evident by most points being above the unity line (n = 12/15). Accordingly, mean PC response latencies were smaller than mean IN response latencies (13.7 ± 1.1 ms versus 14.8 ± 0.6 ms for PCs and INs, respectively, p = 0.003, n = 15).

These data reveal that in nearby IN and PC pairs, INs and PCs often both get rapid sensory-evoked granule cell input from tactile stimulation, and that INs and PCs are recruited near-simultaneously, with IN responses lagging PC responses by about 1 ms.

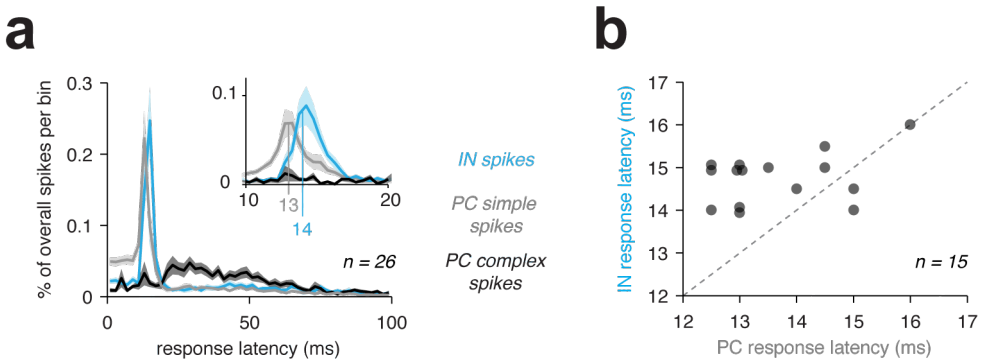

Fig 7.2 Rapid PC responses precede rapid IN responses by 1 ms

(a) Mean distributions of latencies from stimulus onset to first spike for IN spikes, PC simple spikes and PC complex spikes. Bin size = 2 ms. Inset: Bin size = 0.5 ms for better visualization of lag between PC simple spike and IN spike responses. Shadings denote ± SEM. (b) PC response latencies are plotted versus IN response latencies. Values represent

maxima of response latency distributions (bin size = 0.5 ms) for pairs in which for both INs and PCs, maxima of response latency distributions exceeded 4 standard deviations of mean values, allowing a reliable estimate of fast response latencies (n = 15/26 pairs).

The position of the IN in the molecular is an important factor in IN recruitment by CF input (see chapter 4 of this thesis), as well as in the IN's ability to influence PC spike output (see chapter 3 of this thesis). I therefore asked whether vertical IN-PC distance could explain IN sensory response variability. The amplitude and timecourse of IN sensory responses were variable (Fig 7.3a). When sensory-evoked IN spike changes were sorted by vertical intersomatic IN-PC distance (Fig 7.3b), it became apparent that rapid IN activation, i.e. within 20 ms after stimulus onset, was predominantly found in INs with low vertical positions. Indeed, the amplitude of fast IN spike changes within 20 ms showed an inverse correlation with IN-PC distance (Fig 7.3c left, $R^2 = 0.324$, $p = 0.003$), demonstrating that the closer the IN to the PC layer was, the stronger its activation by rapid sensory-evoked granule cell input. This result was not explicable by a difference in recruitment of the region recorded from in general, i.e. by activation of a different tactile area, as the responses of simultaneously recorded PCs did not vary systematically as a function of vertical IN-PC distance ($R^2 = 0.048$, data not shown). Moreover, the interneuron baseline rate did not correlate with vertical IN position ($n = 54$, $p = 0.911$, $R^2 = 0.911$) or with the amplitude of rapid IN spike changes ($n = 26$, $p = 0.265$, $R^2 = 0.051$).

In contrast to fast IN responses, the amplitude of the delayed IN spike change, i.e. the difference in IN spike change amplitude between the delayed 50 – 120 ms time window and the early 0–20 ms time window, did not significantly correlate with IN-PC vertical distance (Fig 7.3c right, $R^2 = 0.109$, $p = 0.107$). These data show that similar to spontaneous CF-IN excitatory effects, delayed sensory-evoked IN responses in INs do not depend on the IN's position in the molecular layer.

In summary, my data demonstrate that not only PCs, but also INs exhibited fast and delayed excitatory responses. Fast responses in INs inversely scaled with vertical IN-PC distance and occurred within about 1 ms after fast PC responses. What is the consequence of this fast IN recruitment for PC spiking?

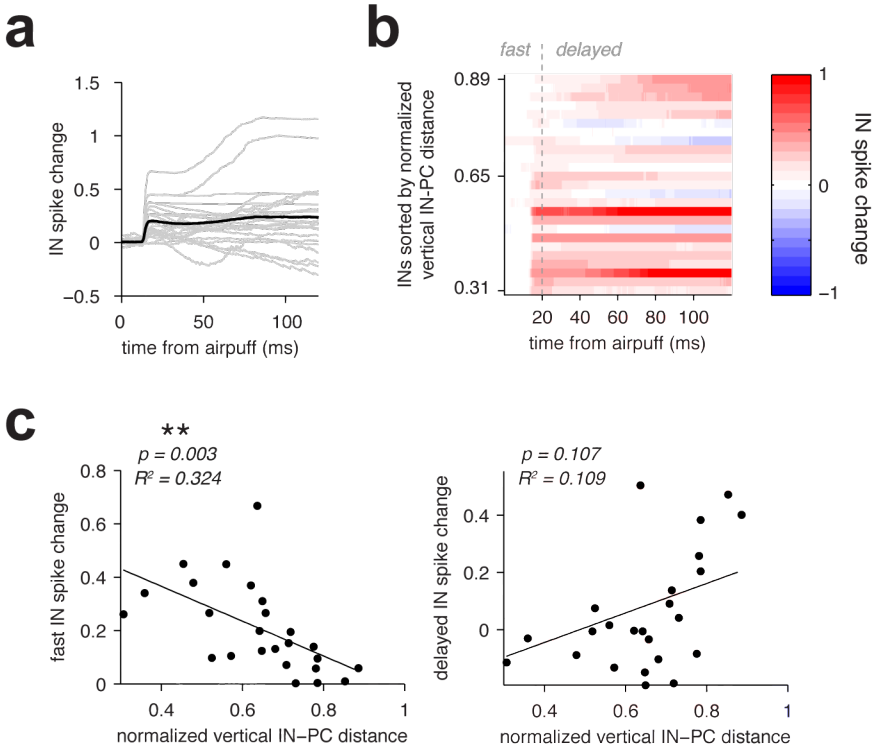

Fig 7.3 Rapid IN responses depend on vertical IN position

(a) Individual (grey) and mean (black) sensory-evoked IN spike changes, n = 26. (b) IN spike changes sorted by vertical IN distance from PC layer normalised to overall extent of molecular layer. Spike change values are displayed from -1 to 1 for better visualization. The vertical grey dotted line indicates the time window of fast sensory-evoked IN spike changes (0-20 ms from stimulus onset), after which in some cases, delayed IN spike changes are apparent. (c) Left: The amplitude of fast IN spike changes (maximum spike change in 0-20 ms from stimulus onset) is plotted versus normalised vertical IN-PC distance. Right: The amplitude of delayed IN spike changes (maximum spike change in 50-120 ms from stimulus onset minus fast IN spike change amplitude) is plotted versus vertical IN-PC distance. n = 25 IN-PC pairs. Black lines indicate linear regression lines.

7.2.2 Interneuron-Purkinje cell inhibition during sensory processing

It has been suggested that during sensory processing, synaptically connected IN-PC pairs may not get the same granule cell input conveying information from a specific tactile region, but that connected IN-PC pairs may be driven by different sets of granule cells (Jörntell et al., 2010). Yet feed-forward inhibition from granule cells onto PCs via INs has been repeatedly suggested as a key feature of cerebellar computation (Blot et al., 2016; Mittmann et al., 2005; Santamaria et al., 2007). To

address this discrepancy, I analysed the relationship between spontaneous and sensory-evoked IN-PC cross-correlations.

By recording spontaneous spiking activity of IN and PC pairs, inhibitory effects of INs on PCs can readily be identified, likely reflecting monosynaptic GABAergic connectivity (Blot et al., 2016, also see chapter 3 of this thesis). What is the relationship between these spontaneous IN-PC interactions described earlier, and sensory-evoked IN-PC recruitment and inhibition? To address this, I grouped dual recording pairs according to the presence of spontaneous IN-PC inhibition into functionally connected and unconnected pairs (Figure 7.4a, recordings with sensory-evoked PC inhibition, a minimum of 20 trials with sensory-evoked IN spikes, and enough spontaneous IN-PC spikes for cross-correlation analysis (minimum of 200 spontaneous IN spikes), n = 10, trials with sensory-evoked complex spikes were removed). I then calculated normalised PC rates triggered on IN spikes evoked by sensory-driven fast granule cell inputs, i.e. on IN spikes occurring within 20 ms after stimulus onset.

For these groups, the normalised PC rates triggered on fast sensory-evoked IN spikes (i.e. IN spikes within 20 ms of stimulus onset) were remarkably similar, exhibiting sharp PC activation preceding the IN spike and prolonged PC inhibition afterwards (Figure 7.4a right). The sharp IN-PC cross-correlogram peak in both groups signified that both connected and unconnected IN-PC pairs were recruited near-simultaneously by sensory-evoked granule cell input. The following sensory-evoked IN-PC inhibition was of similar amplitude in both groups (mean baseline-normalised PC rate in 5-10 ms window post IN spike of 0.30 ± 0.29 (n = 6 pairs with spontaneous IN-PC inhibition) versus 0.45 ± 0.44 (n = 4 pairs without spontaneous IN-PC inhibition), p = 1). Accordingly, sensory-evoked IN-PC inhibition was larger than spontaneous IN-PC inhibition across pairs (mean baseline-normalised PC rates after IN spike of 0.36 ± 0.34 versus 0.71 ± 0.29 for evoked and spontaneous IN-PC effects, respectively, n = 10, p = 0.0195, Figure 7.4b). This was also evident by the majority of data points (5/6) lying below the unity line in a comparison of spontaneous versus sensory-evoked IN-PC inhibition amplitudes (Fig 7.4b).

Moreover, sensory-evoked inhibition appeared prolonged in time, as PC spiking was inhibited up to 40 ms after the IN spike, whereas spontaneous IN-PC inhibition lasted up to 10 ms after the IN spike (Figure 7.4a). Thus, during sensory processing, both connected and unconnected IN-PC pairs exhibit interactions indicative of feed-

forward inhibition, suggesting that sensory stimulation synchronizes large numbers of INs and PCs, with synchronous IN activation resulting in larger and prolonged PC inhibition.

My data suggest that inhibitory connectivity between a given IN-PC pair does not decrease its likelihood of receiving common sensory-driven granule cell input. Rather, sensory-evoked IN-PC spike cross-correlograms exhibited signatures of feed-forward inhibition consisting of fast co-activation followed by inhibition. The fact that this relationship between IN and PC spikes was also apparent in unconnected pairs indicates that tactile stimulation introduced precisely timed correlations among a large number of INs and PCs, so that sensory-induced synchrony between INs inhibiting different PCs created inhibitory correlations between unconnected IN-PC pairs.

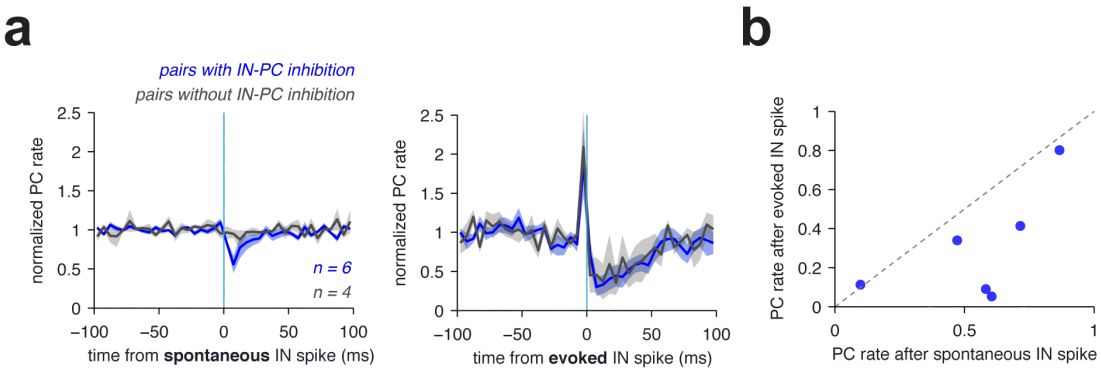

Fig 7.4 Relationship between spontaneous and sensory-evoked IN-PC cross-correlograms

(a) Left: IN-PC pairs were categorized into connected (blue, n = 6) and unconnected (grey, n = 4) pairs based on baseline-normalised PC rates triggered on spontaneous IN spikes. Right: For the same groups, mean baseline-normalised PC rates triggered on IN spikes recruited by rapid granule cell input, i.e. within 20 ms of stimulus onset, are shown. Shadings denote SEM. Bin size = 5 ms. (b) Amplitudes of spontaneous and sensory-evoked IN-PC inhibition plotted against each other for each connected pair. Amplitudes are measured as mean baseline-normalised PC rates 5-10 ms post IN spike. Dotted line represents the unity line, n = 6.

Across cortical areas, trial-to-trial variability in the responses of single neurons as well as on the population level has been observed (Faisal et al., 2008). In my dataset, average sensory-evoked spike changes below the value of 1 (see Fig 7.1c and 7.3a) indicate that in INs and PCs, spikes were not evoked on every single trial, but only in a fraction of trials. This phenomenon prompted me to analyse whether on a trial-by-trial basis, IN and PC recruitment were independent of each other, and to investigate the effect of sensory-evoked spikes on PC activity: Are synaptically connected IN-PC pairs predominantly recruited on the same trials, and can the inhibitory effect of the presynaptic IN be identified specifically in these trials?

To address this question, in an IN-PC pair with spontaneous IN-PC inhibition (Fig 7.5a), I sorted sensory stimulation trials into trials with and trials without fast granule cell-evoked IN responses (Fig 7.5b). Fast excitatory PC responses were identical in trials with and trials without IN recruitment, indicating that recruitment of the IN and PC were independent of each other on a trial-by-trial basis (Fig 7.5c).
The following inhibitory PC response component, however, could be larger in trials with evoked IN spikes, reflecting an additional inhibitory effect presumably stemming from the IN recorded from (mean normalised PC rate in 20-35 ms window after airpuff of 0.13 ± 0.48 (n = 275 trials without IN spike) versus 0.02 ± 0.17 (n = 100 trials with IN spike), p = 0.018, significant difference observed in 2 out of 6 connected and 0 out of 4 unconnected IN-PC pairs). Thus, although several synchronously active INs generate the large PC inhibition upon sensory stimulation, the recruitment of a single presynaptic IN on a given trial can correlate with even larger PC inhibition, highlighting the crucial influence of single INs on PC output.

In summary, the recruitment of INs and PCs by sensory-driven granule cell input did not appear to co-vary on a trial-by-trial basis. In some instances, sensory-driven IN activation co-occurred with larger inhibitory sensory responses in PCs, which was only found in pairs with spontaneous IN-PC inhibition. These data suggest that variability of the fast excitatory sensory response stems from INs and PCs themselves, whereas variability of the inhibitory PC sensory response is partly related to variability of IN recruitment.

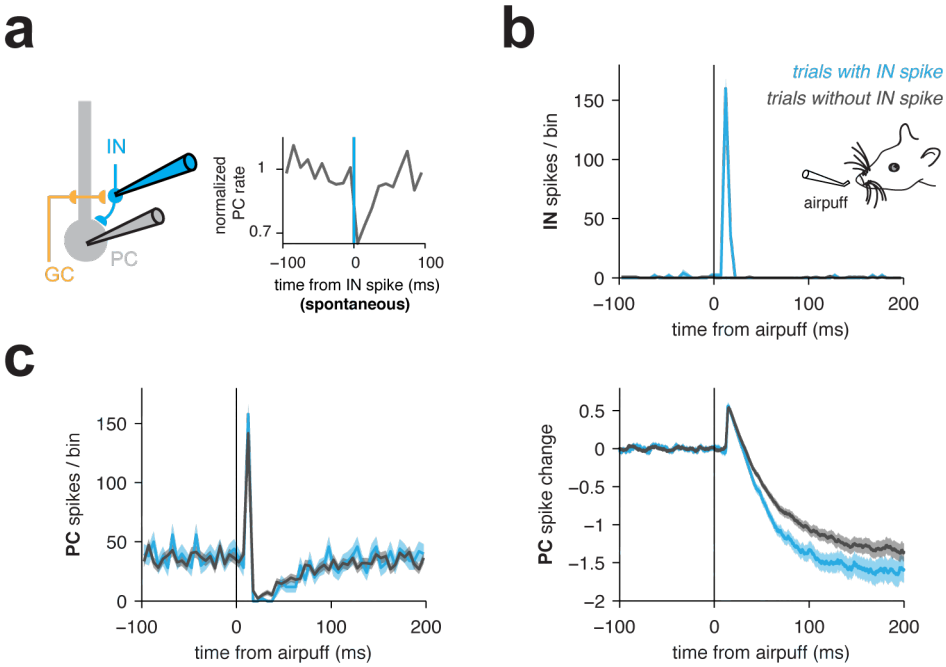

Fig 7.5 The effect of IN spikes on PC sensory responses

(a) Left: Recording configuration showing the underlying circuitry. Right: Normalised PC rate triggered on spontaneous IN spikes showing IN-PC inhibition. (b) PSTHs of IN spikes. Sensory stimulation trials were sorted into trials with (blue) and trials without (grey) rapid sensory-evoked IN spikes (occurring within 20 ms of stimulus onset reflecting granule cell activation). (c) Left: Corresponding PSTHs of PC simple spikes. Bin size = 5 ms. Right: Corresponding sensory-evoked mean PC simple spike changes. Shadings denote ± SEM.

7.2.3 Pathway-specific recruitment of INs during sensory processing

In the previous sections, I presented data on how INs are recruited by rapid sensory-driven granule cell input, but how does the other excitatory input pathway, i.e. climbing fibre input, recruit INs during sensory processing? Is the segregation of INs by spontaneous climbing fibre input (see chapter 4 of this thesis) also reflected in the sensory responses of INs?

Given in that some IN-PC pairs, delayed IN responses to sensory stimulation occurred with similar timecourses as sensory-evoked climbing fibre input (see Fig 7.1), I further investigated the relationship between climbing fibre and IN activity after sensory stimulation. In pairs with recordings of both sensory-evoked spikes

and enough spontaneous spikes for cross-correlation analysis (minimum of 200 IN spikes within ± 100 ms of PC complex spikes), I again categorized INs according to their rate modulation upon spontaneous CF input into INs responding with rate increases (n = 5) and with rate decreases (n = 3) (Fig 7.6a). The average sensory response in these respective groups exhibited stark differences (Fig 7.6b): INs with spontaneous CF-IN inhibition responded strongly with a fast excitatory component, whereas INs with CF-IN excitation showed weaker fast activation (maximum of mean IN spike change within 20 ms after airpuff onset of 0.289 ± 0.045 (n = 3) versus 0.091 ± 0.035 (n = 5), p = 0.036). Moreover, the CF-IN excitation group showed an additional slow excitatory response component.

To unmask the contribution of CF input to sensory responses in these IN groups, I quantified sensory responses of INs in trials with and without sensory-evoked local CF input, measured by the presence of PC complex spikes. Fig 7.6c shows two examples of such an analysis, one in an IN with spontaneous CF-IN excitation and one in an IN with spontaneous CF-IN inhibition. In the former one, while the fast response of the IN was not affected, the slow response was bigger in trials with sensory-evoked CF input, indicating that during sensory processing, CF input was involved in secondary excitatory responses in INs. The fact that the second component was smaller, but still present in trials without complex spikes in the simultaneously recorded PC suggests that the IN may pool from several CFs (Szapiro and Barbour, 2007) that did not all respond to sensory stimulation in a given trial. In the other example shown with spontaneous CF-IN inhibition, IN responses did not differ between trials with and without local sensory-evoked CF input. Overall, the difference in IN spike change between trials with and without local CF input was positive for pairs with spontaneous CF-IN excitation, but not for pairs with CF-IN inhibition (Fig 7.6c right, mean differences of 0.230 ± 0.115 (n = 5) versus –0.032 ± 0.086 (n = 3) for CF-IN increase and decrease groups, respectively, p = 0.036), highlighting the role of CF input in segregating IN activity during sensory processing.

In line with this differential recruitment of INs by CF input, sensory-evoked CF-IN cross-correlograms were different for the two groups (Fig 7.6d left): INs with spontaneous CF-IN activation also showed rate increases after sensory-evoked CF activity, whereas INs with spontaneous CF-IN inhibition showed activation preceding CF input, reflecting recruitment by the faster granule cell pathway.

Finally, how does sensory-evoked IN activation via these different pathways affect the sensory response of PCs? The average sensory-evoked IN-PC cross-correlograms for these two groups suggest that INs do not only differ in their recruitment, but also in their impact on PCs (Fig 7.6d right):

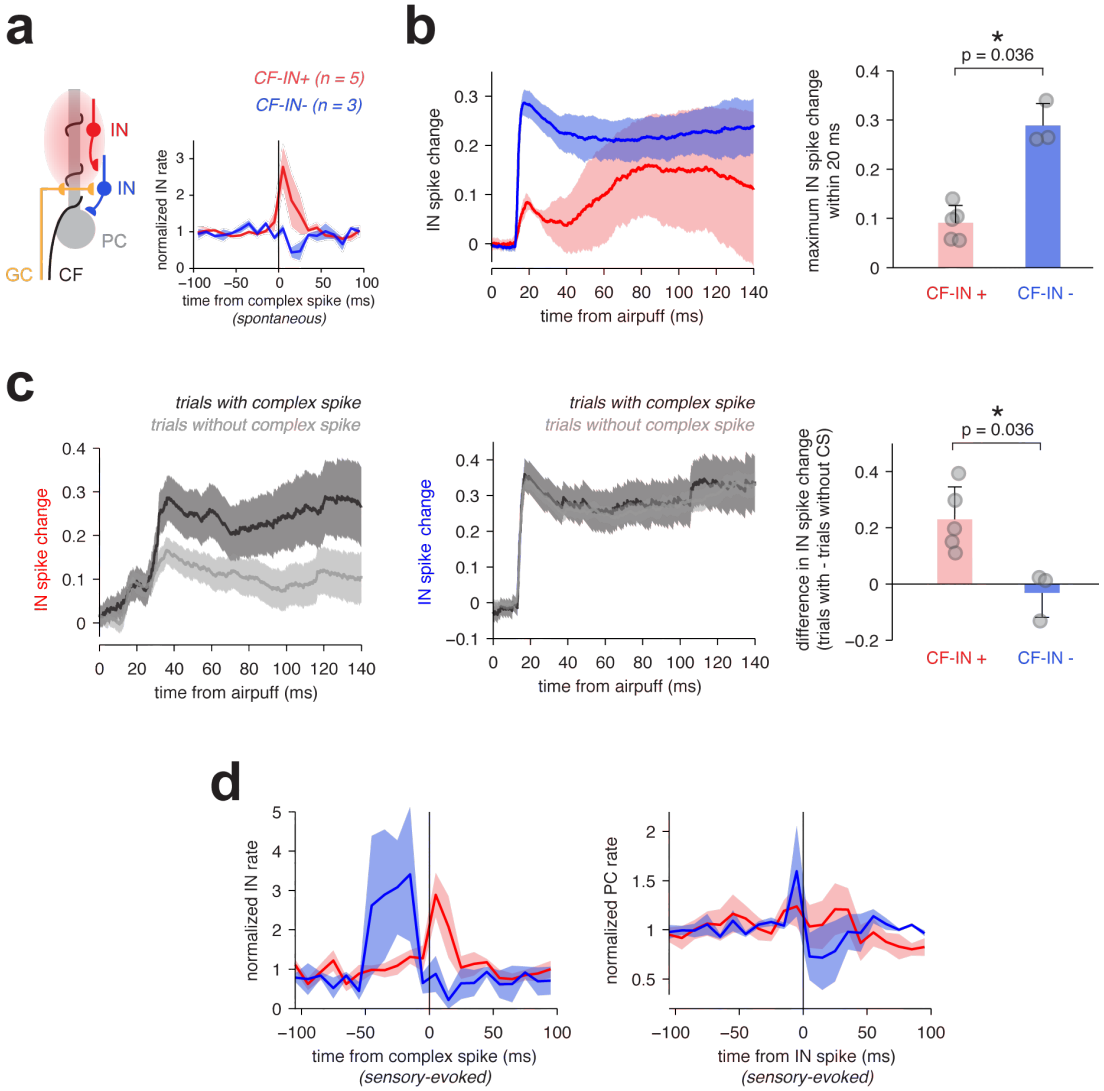

Fig 7.6 The recruitment of INs during sensory processing is pathway-specific

(a) Left: Diagram of the relevant microcircuit. Right: INs were categorized according to their firing rate modulation by spontaneous CF input. INs with excitation (CF-IN+) are shown in red (n = 5), INs with inhibition (CF-IN-) in blue (n = 3). (b) Left: Mean IN spike changes in response to airpuff stimulation for the same IN groups as shown in (a). Right: Comparison of maximum of mean IN spike change within 20 ms after airpuff onset for the CF-IN_ and CF-IN- groups (mean + SD). (c) Left: Example of airpuff-evoked mean spike changes in a single IN (CF-IN+ type), for trials with simultaneously recorded sensory-evoked PC complex spikes (black), and trials without (grey). Note that the secondary IN response was bigger in trials

*with PC complex spikes. Middle: Another example of same analysis as shown left, but for a CF-IN- type IN. Note that IN responses in trials with and without PC complex spikes overlap. Right: Comparison of mean differences of IN spike changes 0-140 ms from airpuff between trials with and trials without PC complex spikes for same groups as in (a) and (b). Note that the difference was positive for CF-IN+ pairs, but not for CF-IN- pairs (mean ± SD). (d) Left: Mean sensory-evoked complex spike–IN spike cross-correlograms. Right: Mean sensory-evoked IN spike–PC simple spike cross-correlograms (bin size = 10 ms), same groups as in (a-c). Shadings denote ± SEM. * $p < 0.05$.*

INs with spontaneous CF-IN inhibition exhibited fast co-activation with PCs followed by PC inhibition, similar to described spontaneous IN-PC cross-correlations in that group (see chapter 6 of this thesis). Spikes of INs with spontaneous CF-IN excitation, in contrast, on average did not seem to result in PC spiking inhibition during sensory processing.

These results highlight that opposing routes of IN recruitment by granule cell and climbing fibre input are not only apparent during spontaneous network activity, but also shape sensory representations in INs and PCs.

7.3 Discussion

In this chapter, I presented data on simultaneous molecular layer interneuron and Purkinje cell recordings during sensory processing. I uncovered several novel operational principles of the microcircuit consisting of sensory-driven excitatory inputs, INs and PCs. I demonstrated that not only PCs, but also INs displayed both rapid and delayed excitatory responses to tactile stimulation. Fast excitatory responses in INs occurred near-simultaneously with fast PC responses, and were largest in INs deeply positioned in the molecular layer. IN-PC cross-correlograms during sensory stimulation displayed signatures of feed-forward inhibition, consisting of co-activation followed by inhibition, both in functionally connected and unconnected IN-PC pairs. Finally, the presence and amplitude of delayed excitatory IN responses correlated with the presence of spontaneous climbing fibre-interneuron excitation in a given IN-PC pair, suggesting that delayed IN responses were generated by climbing fibre-mediated glutamate spillover onto INs. No delayed IN responses were observed in INs with spontaneous CF-IN inhibition.

7.3.1 Rapid granule cell responses in INs and PCs

To understand sensory representations in cerebellar cortex, several studies have used brief tactile stimulation to measure sensory responses in individual neurons, mainly in Purkinje cells. Purkinje cells can display very rapid excitatory responses to tactile stimulation with latencies on the order of 7-14 ms, following activation of the underlying granular layer within milliseconds (Bower and Woolston, 1983). These extremely rapid responses reflect sensory input via the direct pathway from the trigeminal nucleus to the cerebellar cortex via the pons. Longer latency granular layer responses with latencies of several tens of milliseconds have been shown to correlate with responses in somatosensory cortex, demonstrating the contribution of cerebral cortex to the generation of longer latency responses (Morissette and Bower, 1996). Purkinje cells in the dataset presented here exhibited rapid sensory responses with a mean latency of about 13 ms, thus generated by activation of the direct trigemino-cerebellar pathway.

While the literature on Purkinje cell tactile responses is vast (Bosman et al., 2010; Bower and Woolston, 1983; Chu et al., 2011b; Loewenstein et al., 2005), information on tactile responses of molecular layer interneurons remains relatively limited. Existing studies report rapid recruitment by sensory-driven granule cell inputs (Chu et al., 2012; Duguid et al., 2012; Jörntell and Ekerot, 2003). In line with these previous publications, my data showed rapid recruitment of INs by airpuff stimulation with an average spike response latency of about 14 ms, again in line with activation of the direct trigemino-cerebellar projection.

My data further demonstrate that rapid IN sensory responsiveness scaled with vertical position of the IN: INs with lower vertical positions in the molecular layer showed greater fast spike changes, i.e. they responded on a larger fraction of trials. One previous study investigated sensory responses of INs depending on molecular layer position, reporting a linear relationship between vertical IN position and the amplitude of fast sensory-evoked excitatory synaptic currents in INs (Chu et al., 2012). By revealing a linear relationship between IN vertical position and IN sensory-evoked spiking, my data extend this previous work to IN spike output. While the molecular layer interneuron population has traditionally been categorized into stellate cells higher up in the molecular layer and basket cells close to the Purkinje

cell layer (Palay and Chan-Palay, 1974), my data give further support to the notion that INs do not form two distinct classes, but rather represent a single neuronal class with characteristics that continuously vary along the vertical extent of the molecular layer (Sultan and Bower, 1998), both in terms of the effect on PC spike output (see chapter 3 of this thesis) as well as in terms of recruitment by sensory-evoked granule cell input.

What is the anatomical basis of vertically lower INs receiving stronger granule cell excitation? Previous studies have shown that the vertical extent of an IN's dendritic area varies with its position in the molecular layer: INs with low vertical positions have dendrites with larger vertical spread than superficial INs (Rieubland et al., 2014; Sultan and Bower, 1998). If sensory information were randomly distributed in the parallel fibre population across the vertical extent of the molecular layer, INs with lower vertical positions would thus have a larger dendritic area to sample from, resulting in bigger excitatory currents and spike probabilities in lower INs. However, a study directly investigating parallel fibre population activity by measuring axonal calcium levels revealed clustering of sensory-driven parallel fibre activity (Wilms and Häusser, 2015), suggesting that tactile IN responses might result from spatially clustered parallel fibre signalling. Dendritic integration in INs appears sublinear without engagement of active conductances (Abrahamsson et al., 2012). One possible scenario is thus that sensory-driven clusters of co-active parallel fibres are predominant lower in the molecular layer, recruiting spikes in INs with somata in proximity to clustered synaptic input.

Alternatively, ascending granule cell axons might play a crucial role in driving sensory IN responses. Ascending granule cell axons have been implicated to be the main driver of sensory-evoked excitatory responses in PCs based on ultrastructure between granule cells and PCs (Gundappa-Sulur et al., 1999) and excitatory PC responses being found directly above granular layer responses (Bower and Woolston, 1983). As granule cell and climbing fibre receptive fields have been shown to overlap (Brown and Bower, 2001), and climbing fibre inputs are reported to spatially overlap with IN responses (Ekerot and Jorntell, 2001; Jörntell and Ekerot, 2003), it is thus conceivable that strong excitatory IN responses might also be driven by ascending granule cell axons, which would be more numerous in lower INs than in superficial INs. Moreover, ascending granule cell axon synapses onto PCs have

been suggested to be resistant to plasticity induction protocols (Sims and Hartell, 2005), so it is conceivable that strong granule cell responses in INs, if driven by ascending granule cell axons, might be similarly resistant and relatively larger. This hypothesis of ascending axons mainly driving fast excitatory responses has recently been questioned: several clusters of IN and PC responses were found not only directly overlying an active patch of granule cells, but also at large transverse distances spanning hundreds of micrometers (Valera et al., 2016). Future ultrastructural investigations, as well as studies with systematic comparisons across different cerebellar regions might reconcile these notions and provide insight into the nature of granule cell-driven IN sensory responses.

7.3.2 Feed-forward inhibition during sensory processing

Temporally precise responses in INs and PCs to sensory stimulation in the same cerebellar regions have been suggested to stem from feed-forward inhibition. So far, IN-PC correlations indicative of monosynaptic inhibition have been investigated under spontaneous activity conditions using extracellular recording techniques (Bengtsson et al., 2013; Blot et al., 2016), and sensory-evoked activity has been studied in INs and PCs sequentially. The occurrence of sensory-evoked IN activity has often been linked to inhibitory PC responses, both in response to tactile as well as to optokinetic stimulation (Badura et al., 2013; Chu et al., 2012; Ekerot and Jorntell, 2001; ten Brinke et al., 2015), but no study has directly linked synaptic IN-PC inhibition on the pair level to inhibitory PC sensory responses.

In accordance with the notion that sensory-evoked IN activity causes PC inhibition, sensory-evoked IN-PC spike cross-correlograms presented in this chapter show PC inhibition following IN activation. Moreover, they show increases in PC spike rate in advance of sensory-evoked IN activity, reflecting slightly earlier PC than IN recruitment. These temporal relationships are in line with feed-forward inhibition (Mittmann et al., 2005; Pouille and Scanziani, 2001), where granule cell activity recruits both PCs and local INs, who then in turn provide inhibition to PCs, limiting the excitatory granule cell input in time and resulting in temporally precise PC activity.

The functional inhibition between an IN and a PC, as evident from spontaneous spike cross-correlograms, did not seem to inform the sensory-evoked IN-PC spike interactions: Sensory-evoked IN-PC cross-correlograms were similar for both functionally connected and unconnected IN-PC pairs. It thus appears that sensory stimulation induced correlations between many INs and PCs and introduced synchrony between neurons that otherwise fire independently of one another. Spontaneous activity in many IN neurons may be uncorrelated due to their intrinsic spiking properties not requiring excitatory inputs, and may be further enhanced by GABAergic connectivity among INs (Häusser and Clark, 1997; Rieubland et al., 2014). Due to low activity levels in granule cells under spontaneous conditions (Chadderton et al., 2004; Wilms and Häusser, 2015), precisely correlated activity among INs would then be restricted to INs with strong electrical coupling via gap junctions, and perhaps a few INs sharing a large amount of granule cell inputs (van Welie et al., 2016, also see chapter 5 of this thesis). The fact that in my dataset, sensory-evoked IN-PC inhibition appeared larger and longer lasting than spontaneous IN-PC inhibition further supports the notion that sensory stimulation increased synchrony among INs converging onto the same PC. In electrically coupled Golgi cells, sensory-evoked correlations have been shown to be higher than spontaneous correlations (van Welie et al., 2016), suggesting that the same may hold for molecular layer interneurons.

Finally, the fact that functionally connected IN-PC pairs also showed sensory-evoked feed-forward inhibition is in contrast to other reports suggesting that connected IN-PC pairs may not be activated by the same sensory-driven granule cell inputs (Ekerot and Jorntell, 2001; Jörntell et al., 2010). This discrepancy might result from differences in cerebellar regions recorded from, as the cited studies describe recordings from the paravermal area, whereas my dataset stems from Crus II.

7.3.3 IN recruitment and sensory-evoked climbing fibre input

Several studies have demonstrated that INs can be activated by climbing fibres via glutamate spillover (Coddington et al., 2013; Mathews et al., 2012; Szapiro and Barbour, 2007), yet tactile responses in INs so far have only been attributed to granule input, although it is established that tactile stimulation activates climbing

fibre input (Brown and Bower, 2001; Najafi et al., 2014; Ozden et al., 2009). In chapter 4 of this thesis, I previously described that spontaneous climbing fibre input segregates INs *in vivo*, resulting in rate increases in some and rate decreases in other INs, with rate decreases likely stemming from vertically organised inhibition among INs. By recording Purkinje cell complex spikes and IN activity simultaneously during tactile stimulation, I here demonstrated that during sensory processing, this segregation of IN activity was conserved: INs with spontaneous CF-IN rate inhibition only showed rapid granule-cell mediated responses, whereas INs with spontaneous CF-IN excitation displayed additional delayed sensory responses with a similar timecourse as sensory-evoked climbing fibre input. This link between delayed sensory responses in INs and sensory-evoked climbing fibre input was further strengthened by the finding that IN secondary responses were larger in trials with sensory-evoked PC complex spikes. Previously published data demonstrate that climbing fibre synchrony within sagittally oriented microbands is enhanced by sensory stimulation (Ozden et al., 2009; Schultz et al., 2009), and suggest that an IN receives input from at least two climbing fibres (Szapiro and Barbour, 2007). It is thus plausible that the secondary IN response was smaller, but still apparent in trials without a locally recorded PC complex spike because in those trials, the IN was excited by other climbing fibres that happened to respond to sensory stimulation on those trials. This scenario is likely as in PCs with complex spike responsiveness to sensory stimulation, complex spikes are only evoked in a subset of trials (Bosman et al., 2010), leaving room for inter-trial variability in the identity of recruited climbing fibres.

In contrast to fast granule cell-mediated IN responses, delayed IN responses did not significantly correlate with the IN's position in the molecular layer. This result is also in line with secondary responses stemming from sensory-evoked climbing fibre input, as spontaneous CF-IN excitation appeared homogeneous across the vertical extent of the molecular layer (see chapter 4 of this thesis).

7.3.4 Functional implications

What are the functional implications of segregated IN recruitment by different sensory-evoked excitatory inputs? In accordance with results from the analysis of

spontaneous IN-PC interactions (see chapter 6 of this thesis), the function of molecular layer interneurons as a population appears manifold, depending on the excitatory input activating INs.

The rapid and reliable recruitment of INs deep in the molecular layer by sensory-evoked granule cell input suggests that these interneurons specifically are important for feed-forward inhibition of Purkinje cells underneath, resulting in very crisply timed, short PC excitatory responses consisting of single simple spikes, followed by PC inhibition. This role is supported by the fact that INs lower in the molecular layer have a stronger effect on PC spike output than superficial INs (see chapter 3 of this thesis, Vincent and Marty, 1996). Nearby PCs have been suggested to converge onto single deep cerebellar nuclear (DCN) cells (Sugihara et al., 2009). As adjacent Purkinje cells respond to tactile stimulation with synchronous precisely timed spikes (Bosman et al., 2010), DCN neurons thus are bound to receive inhibitory inputs with enhanced synchrony relative to background activity. While asynchronous inhibitory inputs decrease DCN neuron firing rates overall, synchronous inhibitory inputs into DCN neurons result in phase-locking of DCN neurons (Person and Raman, 2012). The PC inhibition following initial excitation would then lead to general disinhibition of DCN neurons, allowing them to excite their extracerebellar targets over tens of milliseconds. Indeed, DCN neurons have been reported to respond to tactile stimulation with precisely timed short-latency spikes, often followed by longer lasting excitation (Rowland and Jaeger, 2005). By enforcing temporal fidelity of PC sensory responses via feed-forward inhibition, INs could therefore play a crucial role in time-locking DCN activity to the onset of a sensory event, allowing for a combination of spike time and rate codes to read out cerebellar activity during sensorimotor integration (Heck et al., 2013).

INs with delayed tactile responses co-occurring with sensory-evoked climbing fibre inputs on the other hand likely have a different functional role. Climbing fibre input is crucial for plasticity induction at various sites of the cerebellar circuit (Gao et al., 2012), and plasticity protocols using electrical inferior olive stimulation have been shown to shape interneuron and Purkinje cell parallel fibre receptive fields: When parallel fibre input was paired with inferior olive stimulation, IN receptive fields were enlarged, indicating potentiation of previously silent parallel fibre input (Jörntell and Ekerot, 2011, 2003, 2002). In line with these results, parallel fibre stimulation paired

with somatic depolarisation of INs favoured LTP of parallel fibre inputs (Rancillac and Crépel, 2004).

Interestingly, my data show an opposite relationship between granule cell- and putative climbing fibre-mediated IN responses: granule cell-mediated responses were smaller in INs with spontaneous climbing fibre-IN excitation and delayed sensory responses, whereas they were larger in INs with spontaneous climbing fibre-IN inhibition. It appears that spontaneous climbing fibre-IN interactions restrict the space of possible sensory IN responses to tactile stimulation, reminiscent of the relationship between spontaneous and sensory-evoked network activity on fast timescales in neocortex (Luczak et al., 2009). This may result from anatomical considerations, as INs with CF-IN inhibition have lower vertical positions and thereby larger dendritic areas. Alternatively, it may reflect history-dependent modifications of sensory-driven parallel fibre inputs into INs under the control of climbing fibre input. Future studies on the plasticity of excitatory inputs into INs during naturalistic sensory processing will be useful to distinguish these two possible explanations.

8 General Discussion

Marr and Poggio posited that in order to understand the operation of a neural circuit, different levels of understanding need to be addressed. The computational level represents the task that the system is carrying out, the algorithmic level describes the method that the system uses to achieve a task, and the implementational level constitutes the hardware carrying out the algorithm (Marr and Poggio, 1976). Knowledge about the hardware is necessary to assess the biological plausibility of any candidate algorithms, and thereby is crucial for an ultimate holistic understanding of brain function. One important hardware element across neural circuits are inhibitory interneurons. In the cerebellar cortex, molecular layer interneurons are the predominant interneuron type, yet their functional embedding in the cerebellar microcircuit remains poorly understood.

With this thesis, I contributed to our understanding of the hardware of the molecular layer in the cerebellar cortex. Utilizing the power of paired electrophysiological recordings *in vivo*, my work provides a bridge between *in vitro* circuit descriptions relying on artificial stimulation paradigms on one side, and circuit properties emerging *in vivo* during behaviour and learning on the other side. I revealed the following principles about excitatory and inhibitory functional connectivity in the cerebellar molecular layer:

1) Single molecular layer interneurons (INs) were found to have strong inhibitory effects on PC spike output, with similar effect sizes of spontaneous and electrically induced IN spikes. The inhibitory effect was confined parasagittally and depended on the IN's vertical distance from the PC layer (Fig 8.1a).
2) INs were recruited by spontaneous climbing fibre (CF) input *in vivo*, responding with spike rate increases (due to glutamate spillover) and/or delayed decreases (due to disynaptic inhibition). IN rate decreases were particularly apparent in INs with short vertical distances from the PC layer, while IN rate increases occurred throughout the vertical extent of the molecular layer (Fig 8.1c).
3) Pairs of INs could reveal different spiking interactions, exhibiting precise synchrony and slower inhibitory interactions. Inhibition among INs was organised vertically from top to bottom in the molecular layer.

4) Spontaneous granule cell (GC) and CF input recruited the inhibitory network fundamentally differently: GC input activated both INs with inhibitory effects on PC spiking and the PCs targeted by these INs, resulting in feed-forward inhibition (Fig 8.1b). Climbing fibre input, in contrast, did not activate these INs, but resulted in inhibition of INs inhibiting PC spiking, forming a motif of feed-forward disinhibition (Fig 8.1d).
5) Pathway-specificity of IN recruitment was also evident during sensory processing. Sensory-evoked GC input rapidly activated INs positioned low in the molecular layer and PCs near-simultaneously, evoking feed-forward inhibition. Sensory-evoked CF input, on the other hand, correlated with delayed excitatory responses in INs.

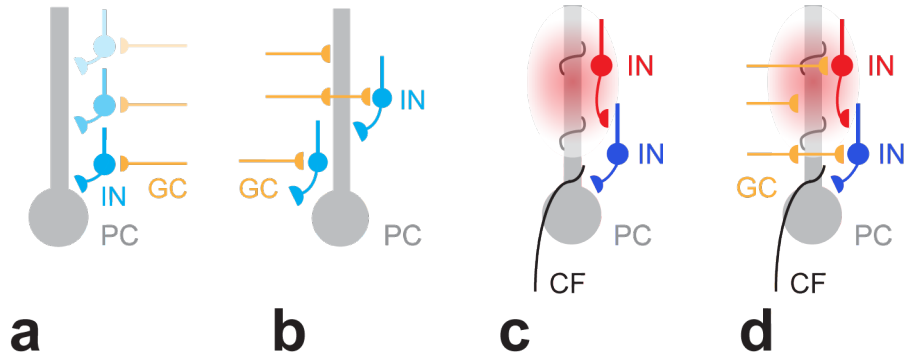

Fig 8.1. Principles of microcircuit connectivity in the cerebellar molecular layer.
Diagrams of functional connectivity principles. (a) The amplitude of IN-PC spiking inhibition decreases with increasing vertical distance of the IN from the PC layer (indicated by decreasing IN colour saturation). The recruitment of INs by sensory-driven granule cell (GC) input also decreases with increasing vertical IN-PC distance (indicated by decreasing granule cell axon colour saturation). (b) Common GC input into an IN-PC pair is accompanied by IN-PC inhibition, resulting in feed-forward inhibition. (c) Climbing fiber (CF) input results in IN excitation (red) and in delayed IN inhibition (blue), especially in INs with lower vertical positions, likely due to vertically organised inhibition among INs. These inhibited INs preferentially inhibit the PC receiving the CF input, resulting in feed-forward disinhibition. (d) INs that are inhibited by CF input (blue) mediate GC feed-forward inhibition of PCs.

8.1 Precise temporal relationships

The cerebellum has long been implicated in the fine coordination of movements, requiring patterns of muscle activation with millisecond precision (Heck et al., 2013). Also in less motor-centric views on cerebellar function, e.g. in the framework of the cerebellum as a sensory data acquisition optimization device (Bower, 1997), the exact temporal relationship between e.g. active whisker movement and sensory information is bound to be crucial. Thus, cerebellar processing has been suggested to rely on temporal coding, i.e. on the exact timing of individual spikes as opposed to spike rate modulations.

Several results presented in my thesis illustrate the high temporal precision of cerebellar processing, e.g. the finding that many INs and PCs received sensory-driven excitatory granule cell input almost simultaneously, often responding with a single short-latency spike within a millisecond. The temporally precise and rapid response in INs may be due to their sensitivity to quanta of inputs (Carter and Regehr, 2002), while the precision of PC spikes likely relies on the feed-forward connectivity involving INs with strong influence on PC spike output, as demonstrated in this thesis. The fact that single INs could inhibit PC spiking potently within milliseconds represents another network optimization for speed. The high levels of spontaneous activity in INs and PCs, coming at a high metabolic cost, seem to be an important feature of cerebellar processing, enabling incoming inputs to advance or delay spikes.

But how can individual spikes convey relevant information in a network with high spontaneous activity? ‘Signal’ versus ‘noise’ is likely encoded in the synchrony of neuronal populations. My data show that during sensory processing, both functionally connected and unconnected IN-PC pairs exhibited spiking profiles indicative of feed-forward inhibition, implying that the sensory stimulus introduced precise correlations between many INs that spontaneously did not fire synchronously. This arrangement allows sensory-driven IN spiking to generate greater PC inhibition than a more independently firing presynaptic IN population. PC synchrony with millisecond precision is known to entrain deep cerebellar nuclei neurons (Person and Raman, 2012), thereby mediating precisely timed output to extracerebellar targets. This framework matches the suggestion that under spontaneous conditions, INs contribute to the irregularity of PC spiking to avoid

spurious correlations between PCs from rhythmicity in their intrinsic activity (Häusser and Clark, 1997).

8.2 Vertical routes of functional connectivity

My data furthermore enriched our understanding of spatial interactions in the cerebellar cortex by revealing several vertical routes of functional connectivity *in vivo*. A top-to-bottom directionality of chemical inhibition among INs, first described by Rieubland et al (2014), appears to be a core feature of cerebellar circuit organisation, as it manifested in the spontaneous spiking interactions of IN pairs *in vivo* presented here. My data suggest that this top-to-bottom organisation is furthermore responsible for a vertical segregation of IN responses to CF input, where INs specifically lower in the molecular layer are inhibited by overlying INs that are excited by CF input via glutamate spillover.

This vertical organisation of inhibition mediated by INs may be a result of a simple developmental rule in the molecular layer: during postnatal development, molecular layer interneurons are formed with increasing delays the higher they are in the molecular layer, i.e. 'basket cells' appear around postnatal day 7, whereas 'stellate' cells' are formed on days 8 – 11, going from the bottom to the top of the molecular layer (Altman, 1972a). At the time point of its migration into the cerebellar cortex, and spatially confined by adjacent sagittally oriented PC dendrites, a given IN thus only has INs below as possible inhibitory targets to form synapses with. At the same time, PC dendritic trees are growing in vertical and parasagittal extent during the first postnatal weeks (Van Welie et al., 2011), offering superficial postsynaptic target areas only to late IN migrators, i.e. stellate cells.

My data not only revealed top-to-bottom directionality of inhibition, but also gradients of the IN's inhibitory effect and recruitment by excitation along the vertical axis of the molecular layer: The lower the IN was positioned in the molecular layer, the greater was its inhibitory effect on PC spiking and its response to sensory-driven granule cell input. How does this organisation of graded excitatory input to INs relate to the development of the cerebellar cortex? Granule cells are generated postnatally in a displaced proliferation zone and migrate to their final position in the granular layer within two weeks after birth. Again, the granule cell-associated parallel fibres

gradually stack up over time so that the vertical position of a parallel fibre indicate its age, whereas the granule cell somata acquire positions in the granular layer irrespective of their age (Espinosa and Luo, 2008; Komuro and Rakic, 1998), contrary to an earlier report (Altman, 1972b). Synaptic connections between INs with low vertical positions, i.e. basket-like INs, and PCs, as well as granule cell-basket cell synapses, form sooner than synapses associated with stellate cells (Altman, 1972a). More basket-like INs thus do not only migrate earlier than stellate cells, but may also receive synaptic input from older granule cells. The effect of a given IN on PC spike output and the IN's recruitment by tactile sensory-evoked granule cell input therefore appear to be a function of the age of a given IN and of its input, decreasing in amplitude with increasing age.

Rapid recruitment of lower INs mediating somatic PC inhibition may thereby constitute the developmentally oldest inhibitory microcircuit in the mammalian cerebellar molecular layer, highlighting the critical role of basket-like INs in inhibiting PC spike output upon granule cell activation. The involvement of basket-like INs in local granule cell feed-forward inhibition evident in my dataset furthermore demonstrates the importance of INs in limiting PC excitation.

8.3 Climbing fibre glutamate volume transmission in the cerebellar cortex

My data demonstrate that physiological climbing fibre input *in vivo* was associated with significant bidirectional spike rate changes in molecular layer interneurons (INs). CF glutamate spillover therefore affected the activity of the cerebellar cortical circuit via an extrasynaptic signalling pathway in ways that are not predictable from the synaptic wiring diagram, a.k.a. the connectome of the circuit alone.

The volume transmission from CFs to INs contrasts other forms of glutamate spillover described in the cerebellar cortex, e.g. at the mossy fibre-granule cell synapse (Powell et al., 2015): it does not enhance the communication between synaptically connected circuit elements, but rather provides the only means of transmission between CFs and INs, as no direct synaptic contacts have been identified (Kollo et al., 2006). In response to CF input, IN rates changed relatively slowly, within tens of milliseconds, showing that despite the lack of synaptic

contacts, CF input could robustly affect IN activity. This spillover transmission is supported by multivesicular release at CF-PC synapses and the close apposition of CF axons and IN somata and dendrites.

What is the role of this pure volume transmission in a circuit supposedly optimized for speed and precise spike timing mediated by fast synaptic signalling? Given that INs excited by CF glutamate spillover were found to rarely affect PC spike output in my dataset, the notion that excitatory CF-IN transmission precisely enforces PC pauses after CF input via somatic inhibition appears challenged. Yet, recordings in behaving mice performing conditioned eyeblinks can show positive correlations between the occurrence of PC complex spikes, IN spikes, PC pauses and the learned motor response, albeit recording from PCs and INs independently (ten Brinke et al., 2015). Although individually, INs excited by CF input rarely affect PC spike output as demonstrated in this thesis, it is conceivable that when these INs are activated simultaneously by CF input representing a motor command, their concerted activity may mediate inhibition of PC spiking.

Furthermore, CF-IN transmission may instruct IN plasticity, a notion supported by *in vitro* and *in vivo* data (Jörntell and Ekerot, 2002; Rancillac and Crépel, 2004). The dependence of plasticity induction on the exact timing of input pathway activation has been studied in mammalian Purkinje cells and Purkinje-like cells in the mormyrid electric fish (Bell et al., 1997; Wang et al., 2000). The emerging consensus seems that long-term depression (LTD) of parallel fibre (pf) input occurs if pf activation is paired with CF activation. The experimentally introduced delay between pf and CF input leading to LTD can range from 0 to 150 ms, suggesting that synaptic plasticity may be robust to temporal offsets of tens of milliseconds (Piochon et al., 2012). While data on spike-timing dependent plasticity at the level of INs is missing to this date, it seems plausible that CF glutamate spillover, causing IN spike rate increases within ten milliseconds, can serve as a signal for associative plasticity despite the lack of synaptic contacts ensuring millisecond precise transmission. CF input may furthermore provide a graded teaching signal depending on the number of axonal bursts and the level of synchrony of CF afferents, possibly leading to graded amounts of plasticity at the pf-IN synapse (Mathy et al., 2009; Yang and Lisberger, 2014).

Future studies will be necessary to assess how CF induced IN excitation and delayed inhibition, as described in this thesis, affect plasticity of INs, both intrinsically and synaptically. This information will be crucial to evaluate adaptive filter models of cerebellar function postulating the modifiability of pf-IN synapses by CF input (Dean et al., 2010). Finally, CF glutamate spillover may also reach other circuit elements of the cerebellar cortex such as Golgi cells, as already supposed by Palay & Chan-Palay from anatomical considerations (Palay and Chan-Palay, 1974), and thereby affect signalling and possibly plasticity at the input stage of the cerebellar cortex.

8.4 Effects of anaesthesia

While performing my recordings in anaesthetised animals brings the experiment much closer to a physiological state than comparable slice recordings, anaesthesia by definition alters central nervous system function compared to the awake state. The exact mechanisms by which different anaesthetics exert their function remain largely mysterious, but for many substances, the major receptor classes targeted are known. Ketamine, one commonly employed anaesthetic, exerts its function primarily via the blockade of NMDA receptors (Garcia et al., 2010). As an important aspect of my thesis work was the *in vivo* assessment of climbing fibre glutamate spillover onto INs, which is mediated by AMPA and NMDA receptors (Coddington et al., 2013; Szapiro and Barbour, 2007), I decided against the use of ketamine-xylazine as an anaesthetic. Isoflurane, the anaesthetic used here, does not primarily dampen excitation, but increases inhibition via allosteric modulation of $GABA_A$ transmission (Garcia et al., 2010).

How might this choice have affected the results described in this thesis? One concern is that the allosteric activation of $GABA_A$ receptors may lead to an overestimation of the amplitude of synaptic IN-PC inhibition. However, in a related study using ketamine-xylazine anaesthesia for simultaneous recordings of IN and PC spontaneous activity *in vivo*, Blot et al (2016) also observed large PC inhibition after IN spikes. These authors furthermore state that a single IN-PC recording in the awake rat exhibited similar cross-correlations as the ones obtained under anaesthesia. This suggests that in my dataset, isoflurane did not transform very weak, barely detectable IN-PC inhibition into large PC spiking decreases, and thus

did not qualitatively affect the basic results. Furthermore, airpuff responses of PCs were reported to be similar under ketamine-xylazine anaesthesia and in the awake state, although PC baseline rates were lower in the former case (Bosman et al., 2010). In contrast, sensory-evoked responses in visual cortex were found to be dominated by inhibition in the awake state compared to under isoflurane anaesthesia (Haider et al., 2013), highlighting that a simplistic view of isoflurane increasing inhibition does not hold. Various neuromodulatory inputs that are suppressed in anaesthetized animals have profound influences on neocortical activity patterns, e.g. during locomotion (Fu et al., 2014; Niell and Stryker, 2010). Given the richness of neuromodulatory projections into cerebellar cortex (Libster and Yarom, 2013), IN-PC interactions probably exhibit interesting dependencies on behavioural state.

The anaesthetised preparation presents obvious caveats compared to the awake state, but it also offers some advantages, especially in characterising functional interactions between IN-PC pairs: already with a simple sensory stimulus like an airpuff employed here, IN-PC pairs that were not connected exhibited signatures of feed-forward inhibition, indicating that large numbers of INs and PCs were synchronised by the stimulus, preventing the identification of truly connected pairs. The degree to which sensory input synchronises INs and PCs is valuable information in itself, but in an awake animal constantly processing sensory information and generating motor commands, varying activity patterns of the excitatory input population to IN-PC pairs would complicate the assessment of single IN-PC interactions. Under isoflurane anaesthesia, however, granule cell firing rates are low (Wilms and Häusser, 2015) and likely less synchronised across the granule cell population, suggesting that spontaneous IN-PC firing under anaesthesia can reveal true granule cell IN-PC feed-forward inhibition on the microcircuit level. Therefore, the characterization of IN-PC inhibition and its recruitment by excitatory afferents under anaesthesia presented in this thesis will likely be a useful reference for future studies investigating IN-PC interactions in awake behaving animals, where correlational structure of excitatory inputs is much more variable and the definition of ‘spontaneous data’ more ambiguous.

8.5 Differential somato-dendritic inhibition of PCs

I identified specific relationships between CF input, IN responses to CFs, and inhibition of PC spiking mediated by these INs: while interneurons that were activated by CF input rarely inhibited spike output of the Purkinje cell receiving the CF, interneurons inhibited by CF input had strong effects on PC spiking. Taken together with the different vertical positions of these IN groups in the molecular layer, and the fact that INs with more superficial somatic positions tend to inhibit PC dendritic compartments, it appears that upon CF input, the PC receives opposing levels of inhibition along its somato-dendritic axis: Dendritic inhibition provided by INs higher up in the molecular layer is increased, whereupon somatic inhibition by basket-like INs is reduced.

What may be the consequence of this differential inhibition on PC signalling? Purkinje cells have active dendrites, i.e. they can exhibit regenerative events localized to dendrites independent of somatic spiking. In Purkinje cells, dendritic spikes are mediated by voltage-gated calcium channels and by NMDA receptors in the adult, and are fundamental for synaptic plasticity given the crucial role of dendritic calcium levels in plasticity induction (Coesmans et al., 2004; Llinás and Sugimori, 1980; Piochon et al., 2010). Dendritic spikes in response to CF input appear decoupled from the waveform of the somatic complex spike output (Davie et al., 2008). Thus, dendritic and somatic signalling can occur in relative isolation from one another in Purkinje cells, supported by the PC's morphology and lack of dendritic voltage-gated sodium channels (Stuart and Häusser, 1994).

It appears that through opposite modulation of interneurons targeting somatic and dendritic PC compartments, CF input may extend the somato-dendritic uncoupling of PCs in time via the inhibitory network. CF input would create dendritic inhibition followed by somatic disinhibition tens of milliseconds after it synaptically excited the PC directly. Dendritic inhibition has been shown to strongly attenuate dendritic calcium levels without directly affecting PC spike output (Callaway et al., 1995). As dendritic inhibition via glutamate spillover-activated INs would lag a CF-induced dendritic spike in time, CF-activated dendritic inhibition may not directly affect the generation dendritic spiking, but rather curtail it and reduce the efficacy of following parallel fibre inputs into the dendrite via shunting inhibition. This would ensure that only the parallel fibre input that preceded or occurred simultaneously with CF input,

depending on the exact plasticity timing rule, would undergo LTD. Via such a mechanism, CF-activated dendritic inhibition could ensure the specificity of learning that seems crucial given the large number of parallel fibre inputs into a single PC. The role of delayed somatic disinhibition, on the other hand, might be to enable PC simple spike facilitation after complex spiking, and / or to provide a preferred time window for the reset of Purkinje cell simple spiking after CF input (De Zeeuw et al., 2011).

8.6 Outlook

In 1971, Albus suggested that molecular layer interneurons were too numerous to function as simple gain control devices (Albus, 1971). My work suggests that indeed, the function of molecular layer interneurons is manifold, coordinating precise timing and increasing the learning capacity of the cerebellar cortex. To build on the results presented in this thesis and further elucidate the role of molecular layer inhibition in cerebellar function, the following issues seem especially interesting to address:

What are the exact spike-timing dependent plasticity rules in interneurons, i.e. how does climbing fibre input affect the synaptic strength of preceding granule-cell input? How does plasticity differ in interneurons that are excited and in those that are inhibited by climbing fibre input? Do interneurons, depending on their vertical position in the molecular layer, contribute differently to cerebellar learning?

What is the transcriptomic variability in the molecular layer interneuron population? Can transcriptomics be used to functionally sub-categorize this population, and may the resulting categories correspond to interneurons mediating granule cell-feed forward inhibition versus interneurons activated by climbing fibre input?

What is the impact of single interneuron spikes on PC spike output in the awake animal? How does it depend on behavioural and neuromodulatory state, and how is it modified during cerebellar learning?

9 References

Abrahamsson, T., Cathala, L., Matsui, K., Shigemoto, R., Digregorio, D.A., 2012. Thin dendrites of cerebellar interneurons confer sublinear synaptic integration and a gradient of short-term plasticity. Neuron 73, 1159–72.

Adesnik, H., Bruns, W., Taniguchi, H., Huang, Z.J., Scanziani, M., 2012. A neural circuit for spatial summation in visual cortex. Nature 490, 226–231.

Albus, J.S., 1971. A theory of cerebellar function. Math. Biosci. 10, 25–61.

Alcami, P., Marty, A., 2013. Estimating functional connectivity in an electrically coupled interneuron network. Proc. Natl. Acad. Sci. U. S. A. 2013, 1–10.

Allen, N.J., Attwell, D., 2002. Modulation of ASIC channels in rat cerebellar Purkinje neurons by ischaemia-related signals. J. Physiol. 543, 521–529.

Altman, J., 1972a. Postnatal development of the cerebellar cortex in the rat. I. The external germinal layer and the transitional molecular layer. J. Comp. Neurol. 145, 353–97.

Altman, J., 1972b. Postnatal development of the cerebellar cortex in the rat. III. Maturation of the components of the granular layer. J. Comp. Neurol. 145, 465–513.

Andersen, P., Eccles, J.C., Løyning, Y., 1963. Pathway of postsynaptic inhibition in the hippocampus 608–619.

Andersen, P., Eccles, J.C., Voorhoeve, P.E., 1964. Postsynaptic inhibition of cerebellar Purkinje cells. J. Neurophysiol. 27, 1138–1153.

Armstrong, D.M., Rawson, J.A., 1979. Activity patterns of cerebellar cortical neurones and climbing fibre afferents in the awake cat. J. Physiol. 289, 425–48.

Asztely, F., Erdemli, G., Kullmann, D.M., 1997. Extrasynaptic glutamate spillover in the hippocampus: Dependence on temperature and the role of active glutamate uptake. Neuron 18, 281–293.

Auger, C., Attwell, D., 2000. Fast removal of synaptic glutamate by postsynaptic transporters. Neuron 28, 547–558.

Badura, A., Schonewille, M., Voges, K., Galliano, E., Renier, N., Gao, Z., Witter, L., Hoebeek, F.E., Chédotal, A., De Zeeuw, C.I., 2013. Climbing fiber input shapes reciprocity of Purkinje cell firing. Neuron 78, 700–13.

Barbour, B., Isope, P., 2000. Combining loose cell-attached stimulation and recording. J. Neurosci. Methods 103, 199–208.

Barth, A.L., Burkhalter, A., Callaway, E.M., Connors, B.W., Cauli, B., DeFelipe, J., Feldmeyer, D., Freund, T., Kawaguchi, Y., Kisvarday, Z., Kubota, Y., McBain, C., Oberlaender, M., Rossier, J., Rudy, B., Staiger, J.F., Somogyi, P., Tamas, G., Yuste, R., 2016. Comment on “Principles of connectivity among morphologically defined cell types in adult neocortex.” Science (80-.). 353, 1108–1108.

Barthó, P., Hirase, H., Monconduit, L., Zugaro, M., Harris, K.D., Buzsáki, G., 2004. Characterization of neocortical principal cells and interneurons by network interactions and extracellular features. J. Neurophysiol. 92, 600–8.

Bell, C.C., Han, V.Z., Sugawara, Y., Grant, K., 1997. Synaptic plasticity in a cerebellum-like structure depends on temporal order. Nature 387, 278–281.

Ben-Ari, Y., 2002. Excitatory actions of gaba during development: the nature of the nurture. Nat Rev Neurosci 3, 728–739.

Bengtsson, F., Geborek, P., Jörntell, H., 2013. Cross-correlations between pairs of neurons in cerebellar cortex in vivo. Neural Netw. 47, 88–94.

Bernander, O., Douglas, R.J., Martin, K. a, Koch, C., 1991. Synaptic background activity influences spatiotemporal integration in single pyramidal cells. Proc. Natl. Acad. Sci. U. S. A. 88, 11569–73.

Blazquez, P.M., Yakusheva, T.A., 2015. GABA-A Inhibition Shapes the Spatial and Temporal Response Properties of Purkinje Cells in the Macaque Cerebellum. Cell Rep. 11, 1043–53.

Blot, A., Barbour, B., 2014. Ultra-rapid axon-axon ephaptic inhibition of cerebellar Purkinje cells by the pinceau. Nat. Neurosci. 17, 289–295.

Blot, A., de Solages, C., Ostojic, S., Szapiro, G., Hakim, V., Léna, C., 2016. Time-invariant feed-forward inhibition of Purkinje cells in the cerebellar cortex in vivo. J. Physiol. 10, 2729–2749.

Borst, J.G.G., 2010. The low synaptic release probability in vivo. Trends Neurosci. 33, 259–66.

Bosman, L.W.J., Houweling, A.R., Owens, C.B., Tanke, N., Shevchouk, O.T., Rahmati, N., Teunissen, W.H.T., Ju, C., Gong, W., Koekkoek, S.K.E., De Zeeuw, C.I., 2011. Anatomical pathways involved in generating and sensing rhythmic whisker movements. Front. Integr. Neurosci. 5, 53.

Bosman, L.W.J., Koekkoek, S.K.E., Shapiro, J., Rijken, B.F.M., Zandstra, F., van der Ende, B., Owens, C.B., Potters, J.-W., de Gruijl, J.R., Ruigrok, T.J.H., De Zeeuw, C.I., 2010. Encoding of whisker input by cerebellar Purkinje cells. J.

Physiol. 588, 3757–83.

Bower, J.M., 1997. Is the cerebellum sensory for motor's sake, or motor for sensory's sake: the view from the whiskers of a rat? Prog. Brain Res. 114, 463–96.

Bower, J.M., 2010. Model-founded explorations of the roles of molecular layer inhibition in regulating Purkinje cell responses in cerebellar cortex: more trouble for the beam hypothesis. Front. Cell. Neurosci. 4, 27.

Bower, J.M., Woolston, D.C., 1983. Congruence of spatial organization of tactile projections to granule cell and Purkinje cell layers of cerebellar hemispheres of the albino rat: vertical organization of cerebellar cortex. J. Neurophysiol. 49, 745–766.

Boyden, E.S., Katoh, A., Raymond, J.L., 2004. Cerebellum-dependent learning: the role of multiple plasticity mechanisms. Annu. Rev. Neurosci. 27, 581–609.

Brenowitz, S.D., Regehr, W.G., 2005. Associative short-term synaptic plasticity mediated by endocannabinoids. Neuron 45, 419–431.

Brivanlou, I.H., Warland, D.K., Meister, M., 1998. Mechanisms of concerted firing among retinal ganglion cells. Neuron 20, 527–39.

Brochu, G., Maler, L., Hawkes, R., 1990. Zebrin II: a polypeptide antigen expressed selectively by Purkinje cells reveals compartments in rat and fish cerebellum. J. Comp. Neurol. 291, 538–52.

Brown, I.E., Bower, J.M., 2001. Congruence of mossy fiber and climbing fiber tactile projections in the lateral hemispheres of the rat cerebellum. J. Comp. Neurol. 429, 59–70.

Brown, K.M., Sugihara, I., Shinoda, Y., Ascoli, G. a., 2012. Digital morphometry of rat cerebellar climbing fibers reveals distinct branch and bouton types. J. Neurosci. 32, 14670–84.

Buetfering, C., Allen, K., Monyer, H., 2014. Parvalbumin interneurons provide grid cell-driven recurrent inhibition in the medial entorhinal cortex. Nat. Neurosci. 17, 710–8.

Callaway, J.C., Lasser Ross, N., Ross, W.N., 1995. IPSPs strongly inhibit climbing fiber-activated [Ca2+] increases in the dendrites of cerebellar Purkinje neurons. J. Neurosci. 15, 2777–2787.

Carter, A.G., Regehr, W.G., 2002. Quantal events shape cerebellar interneuron firing. Nat. Neurosci. 5, 1309–18.

Cesana, E., Pietrajtis, K., Bidoret, C., Isope, P., D'Angelo, E., Dieudonné, S., Forti,

L., 2013. Granule cell ascending axon excitatory synapses onto Golgi cells implement a potent feedback circuit in the cerebellar granular layer. J. Neurosci. 33, 12430–46.

Chadderton, P., Margrie, T.W., Häusser, M., 2004. Integration of quanta in cerebellar granule cells during sensory processing. Nature 428, 856–60.

Chaumont, J., Guyon, N., Valera, A.M., Dugué, G.P., Popa, D., Marcaggi, P., Gautheron, V., Reibel-Foisset, S., Dieudonné, S., Stephan, A., Barrot, M., Cassel, J.-C., Dupont, J.-L., Doussau, F., Poulain, B., Selimi, F., Léna, C., Isope, P., 2013. Clusters of cerebellar Purkinje cells control their afferent climbing fiber discharge. Proc. Natl. Acad. Sci. U. S. A. 110, 16223–8.

Chu, C.-P., Bing, Y.-H., Liu, H., Qiu, D.-L., 2012. Roles of molecular layer interneurons in sensory information processing in mouse cerebellar cortex Crus II in vivo. PLoS One 7, e37031.

Chu, C.-P., Bing, Y.-H., Liu, Q.-R., Qiu, D.-L., 2011a. Synaptic responses evoked by tactile stimuli in Purkinje cells in mouse cerebellar cortex Crus II in vivo. PLoS One 6, e22752.

Chu, C.-P., Bing, Y.-H., Qiu, D.-L., 2011b. Sensory stimulus evokes inhibition rather than excitation in cerebellar Purkinje cells in vivo in mice. Neurosci. Lett. 487, 182–6.

Chuong, A.S., Miri, M.L., Busskamp, V., Matthews, G.A.C., Acker, L.C., Sørensen, A.T., Young, A., Klapoetke, N.C., Henninger, M.A., Kodandaramaiah, S.B., Ogawa, M., Ramanlal, S.B., Bandler, R.C., Allen, B.D., Forest, C.R., Chow, B.Y., Han, X., Lin, Y., Tye, K.M., Roska, B., Cardin, J.A., Boyden, E.S., 2014. Noninvasive optical inhibition with a red-shifted microbial rhodopsin. Nat. Neurosci. 17, 1123–9.

Clark, B.A., Cull-Candy, S.G., 2002. Activity-dependent recruitment of extrasynaptic NMDA receptor activation at an AMPA receptor-only synapse. J. Neurosci. 22, 4428–4436.

Clark, B.D., Goldberg, E.M., Rudy, B., 2009. Electrogenic tuning of the axon initial segment. Neuroscientist 15, 651–68.

Clopath, C., Badura, A., De Zeeuw, C.I., Brunel, N., 2014. A cerebellar learning model of vestibulo-ocular reflex adaptation in wild-type and mutant mice. J. Neurosci. 34, 7203–15.

Coddington, L.T., Rudolph, S., Vande Lune, P., Overstreet-Wadiche, L., Wadiche, J.I., 2013. Spillover-mediated feedforward inhibition functionally segregates

interneuron activity. Neuron 78, 1050–62.

Coesmans, M., Weber, J.T., De Zeeuw, C.I., Hansel, C., 2004. Bidirectional parallel fiber plasticity in the cerebellum under climbing fiber control. Neuron 44, 691–700.

Cohen, D., Yarom, Y., 1998. Patches of synchronized activity in the cerebellar cortex evoked by mossy-fiber stimulation: questioning the role of parallel fibers. Proc. Natl. Acad. Sci. U. S. A. 95, 15032–15036.

Cossell, L., Iacaruso, M.F., Muir, D.R., Houlton, R., Sader, E.N., Ko, H., Hofer, S.B., Mrsic-Flogel, T.D., 2015. Functional organization of excitatory synaptic strength in primary visual cortex. Nature 518, 399–403.

Davie, J.T., Clark, B. a, Häusser, M., 2008. The origin of the complex spike in cerebellar Purkinje cells. J. Neurosci. 28, 7599–609.

Dean, P., Porrill, J., Ekerot, C.-F., Jörntell, H., 2010. The cerebellar microcircuit as an adaptive filter: experimental and computational evidence. Nat. Rev. Neurosci. 11, 30–43.

De Zeeuw, C.I., Hoebeek, F.E., Bosman, L.W.J., Schonewille, M., Witter, L., Koekkoek, S.K., 2011. Spatiotemporal firing patterns in the cerebellum. Nat. Rev. Neurosci. 12, 327–44.

De Zeeuw, C.I., Hoogenraad, C.C., Koekkoek, S.K.E., Ruigrok, T.J.H., Galjart, N., Simpson, J.I., 1998. Microcircuitry and function of the inferior olive. Trends Neurosci. 21, 391–400.

Denk, W., Strickler, J.H., Webb, W.W., 1990. Two-photon laser scanning fluorescence microscopy. Science (80-.). 248, 73–76.

Destexhe, A., Paré, D., 1999. Impact of network activity on the integrative properties of neocortical pyramidal neurons in vivo. J. Neurophysiol. 81, 1531–47.

Diba, K., Amarasingham, A., Mizuseki, K., Buzsáki, G., 2014. Millisecond timescale synchrony among hippocampal neurons. J. Neurosci. 34, 14984–94.

Dieudonné, S., Dumoulin, A., 2000. Serotonin-driven long-range inhibitory connections in the cerebellar cortex. J. Neurosci. 20, 1837–48.

DiGregorio, D. a., Nusser, Z., Silver, R.A., 2002. Spillover of glutamate onto synaptic AMPA receptors enhances fast transmission at a cerebellar synapse. Neuron 35, 521–533.

Dizon, M.J., Khodakhah, K., 2011. The role of interneurons in shaping Purkinje cell responses in the cerebellar cortex. J. Neurosci. 31, 10463–73.

Dombeck, D.A., Harvey, C.D., Tian, L., Looger, L.L., Tank, D.W., 2010. Functional

imaging of hippocampal place cells at cellular resolution during virtual navigation. Nat. Neurosci. 13, 1433–40.

Doron, G., von Heimendahl, M., Schlattmann, P., Houweling, A.R., Brecht, M., 2014. Spiking irregularity and frequency modulate the behavioral report of single-neuron stimulation. Neuron 81, 653–63.

Dugué, G.P., Brunel, N., Hakim, V., Schwartz, E., Chat, M., Lévesque, M., Courtemanche, R., Léna, C., Dieudonné, S., 2009. Electrical coupling mediates tunable low-frequency oscillations and resonance in the cerebellar Golgi cell network. Neuron 61, 126–39.

Duguid, I., Branco, T., Chadderton, P., Arlt, C., Powell, K., Häusser, M., 2015. Control of cerebellar granule cell output by sensory-evoked Golgi cell inhibition. Proc. Natl. Acad. Sci. 112, 201510249.

Duguid, I., Branco, T., London, M., Chadderton, P., Häusser, M., 2012. Tonic inhibition enhances fidelity of sensory information transmission in the cerebellar cortex. J. Neurosci. 32, 11132–43.

Dzubay, J. a, Jahr, C.E., 1999. The concentration of synaptically released glutamate outside of the climbing fiber-Purkinje cell synaptic cleft. J. Neurosci. 19, 5265–5274.

Eccles, J.C., 1943. The ionic mechanism of postsynaptic inhibition. Nobel lecture. In: The Nobel Prize in Physiology or Medicine 1943. pp. 1140–1147.

Eccles, J.C., Ito, M., Szentágothai, J., 1967. The cerebellum as a neuronal machine. Springer Science & Business Media, New York.

Eccles, J.C., Llinás, R., Sasaki, K., 1966. The excitatory synaptic action of climbing fibres on the Purkinje cells of the cerebellum. J. Physiol. 182, 268–96.

Eccles, J.C., Llinás, R., Sasaki, K., 1966. The inhibitory interneurones within the cerebellar cortex. Exp. Brain Res. 1, 1–16.

Ekerot, C., Jorntell, H., 2001. Parallel fibre receptive fields of Purkinje cells and interneurons are climbing fibre-specific. Eur. J. Neurosci. 13, 1303–1310.

Espinosa, J.S., Luo, L., 2008. Timing neurogenesis and differentiation: insights from quantitative clonal analyses of cerebellar granule cells. J. Neurosci. 28, 2301–12.

Faisal, a A., Selen, L.P.J., Wolpert, D.M., 2008. Noise in the nervous system. Nat. Rev. Neurosci. 9, 292–303.

Farrant, M., Nusser, Z., 2005. Variations on an inhibitory theme: phasic and tonic activation of GABA(A) receptors. Nat. Rev. Neurosci. 6, 215–29.

Flourens, P., 1824. Rechérches expérimentales sur les propriétés et les fonctions du système nerveux dans les animaux vertébrés. Crevot, Paris.

Franconville, R., Revet, G., Astorga, G., Schwaller, B., Llano, I., 2011. Somatic calcium level reports integrated spiking activity of cerebellar interneurons in vitro and in vivo. J. Neurophysiol. 106, 1793–1805.

Fu, Y., Tucciarone, J.M., Espinosa, J.S., Sheng, N., Darcy, D.P., Nicoll, R. a, Huang, Z.J., Stryker, M.P., 2014. A cortical circuit for gain control by behavioral state. Cell 156, 1139–52.

Fujita, M., 1982. Adaptive filter model of the cerebellum. Biol. Cybern. 45, 195–206.

Gabernet, L., Jadhav, S.P., Feldman, D.E., Carandini, M., Scanziani, M., 2005. Somatosensory integration controlled by dynamic thalamocortical feed-forward inhibition. Neuron 48, 315–327.

Gao, Z., van Beugen, B.J., De Zeeuw, C.I., 2012. Distributed synergistic plasticity and cerebellar learning. Nat. Rev. Neurosci. 13, 619–35.

Garcia, P.S., Kolesky, S.E., Jenkins, A., 2010. General anesthetic actions on GABA(A) receptors. Curr. Neuropharmacol. 8, 2–9.

Gefter, A., 2015. The man who tried to redeem the world with logic: Walter Pitts rose from the streets to MIT, but couldn't escape himself. Nautilus (Philadelphia).

Gentet, L.J., Kremer, Y., Taniguchi, H., Huang, Z.J., Staiger, J.F., Petersen, C.C., 2012. Unique functional properties of somatostatin-expressing GABAergic neurons in mouse barrel cortex. Nat Neurosci 15, 607–612.

Gidon, A., Segev, I., 2012. Principles governing the operation of synaptic inhibition in dendrites. Neuron 75, 330–41.

Golding, N.L., Spruston, N., 1998. Dendritic sodium spikes are variable triggers of axonal action potentials in hippocampal CA1 pyramidal neurons. Neuron 21, 1189–1200.

Govorunova, E.G., Sineshchekov, O.A., Janz, R., Liu, X., Spudich, J.L., 2015. NEUROSCIENCE. Natural light-gated anion channels: A family of microbial rhodopsins for advanced optogenetics. Science 349, 647–50.

Gradinaru, V., Zhang, F., Ramakrishnan, C., Mattis, J., Prakash, R., Diester, I., Goshen, I., Thompson, K.R., Deisseroth, K., 2010. Molecular and cellular approaches for diversifying and extending optogenetics. Cell 141, 154–65.

Gundappa-Sulur, G., De Schutter, E., Bower, J.M., 1999. Ascending granule cell axon: an important component of cerebellar cortical circuitry. J. Comp. Neurol. 408, 580–96.

Haider, B., Duque, A., Hasenstaub, A.R., McCormick, D. a, 2006. Neocortical network activity in vivo is generated through a dynamic balance of excitation and inhibition. J. Neurosci. 26, 4535–45.

Haider, B., Häusser, M., Carandini, M., 2013. Inhibition dominates sensory responses in the awake cortex. Nature 493, 97–100.

Han, X., Chow, B.Y., Zhou, H., Klapoetke, N.C., Chuong, A., Rajimehr, R., Yang, A., Baratta, M. V, Winkle, J., Desimone, R., Boyden, E.S., 2011. A high-light sensitivity optical neural silencer: development and application to optogenetic control of non-human primate cortex. Front. Syst. Neurosci. 5, 18.

Häusser, M., Clark, B.A., 1997. Tonic synaptic inhibition modulates neuronal output pattern and spatiotemporal synaptic integration. Neuron 19, 665–78.

Hayashi, S., McMahon, A.P., 2002. Efficient recombination in diverse tissues by a tamoxifen-inducible form of Cre: a tool for temporally regulated gene activation/inactivation in the mouse. Dev. Biol. 244, 305–18.

Heck, D.H., De Zeeuw, C.I., Jaeger, D., Khodakhah, K., Person, A.L., 2013. The neuronal code(s) of the cerebellum. J. Neurosci. 33, 17603–9.

Heiney, S. a., Kim, J., Augustine, G.J., Medina, J.F., 2014. Precise control of movement kinematics by optogenetic inhibition of Purkinje cell activity. J. Neurosci. 34, 2321–30.

Helmstaedter, M., Briggman, K.L., Turaga, S.C., Jain, V., Seung, H.S., Denk, W., 2013. Connectomic reconstruction of the inner plexiform layer in the mouse retina. Nature 500, 168–74.

Herculano-Houzel, S., 2010. Coordinated scaling of cortical and cerebellar numbers of neurons. Front. Neuroanat. 4, 12.

Holthoff, K., Kovalchuk, Y., Konnerth, A., 2006. Dendritic spikes and activity-dependent synaptic plasticity. Cell Tissue Res. 326, 369–377.

Hu, H., Gan, J., Jonas, P., 2014. Interneurons. Fast-spiking, parvalbumin^{+} GABAergic interneurons: from cellular design to microcircuit function. Science 345, 1255263 1-13.

Hubel, D.H., Wiesel, T.N., 1959. Receptive fields of single neurones in the cat's striate cortex. J. Physiol. 148, 574–591.

Hubel, D.H., Wiesel, T.N., 1962. Receptive fields, binocular interaction and functional architecture in the cat's visual cortex. J. Physiol. 160, 106–154.

Isaacson, J.S., Scanziani, M., 2011. How inhibition shapes cortical activity. Neuron 72, 231–43.

Isope, P., Barbour, B., 2002. Properties of unitary granule cell-->Purkinje cell synapses in adult rat cerebellar slices. J. Neurosci. 22, 9668–78.

Ito, M., Kano, M., 1982. Long-lasting depression of parallel fiber-Purkinje cell transmission induced by conjunctive stimulation of parallel fibers and climbing fibers in the cerebellar cortex. Neurosci. Lett. 33, 253–258.

Jaeger, D., De Schutter, E., Bower, J.M., 1997. The role of synaptic and voltage-gated currents in the control of Purkinje cell spiking: a modeling study. J. Neurosci. 17, 91–106.

Jain, V., Seung, H.S., Turaga, S.C., 2010. Machines that learn to segment images: A crucial technology for connectomics. Curr. Opin. Neurobiol. 20, 653–666.

Jenkinson, E.W., Glickstein, M., 2000. Whiskers, barrels, and cortical efferent pathways in gap crossing by rats. J. Neurophysiol. 84, 1781–1789.

Jiang, X., Shen, S., Cadwell, C.R., Berens, P., Sinz, F., Ecker, A.S., Patel, S., Tolias, A.S., 2015. Principles of connectivity among morphologically defined cell types in adult neocortex. Science 350, aac9462.

Jirenhed, D.-A., Bengtsson, F., Jörntell, H., 2013. Parallel fiber and climbing fiber responses in rat cerebellar cortical neurons in vivo. Front. Syst. Neurosci. 7, 16.

Johansson, F., Carlsson, H.A.E., Rasmussen, A., Yeo, C.H., Hesslow, G., 2015. Activation of a temporal memory in Purkinje cells by the mGluR7 receptor. Cell Rep. 13, 1741–6.

Johansson, F., Jirenhed, D.D. -a., Rasmussen, A., Zucca, R., Hesslow, G., 2014. Memory trace and timing mechanism localized to cerebellar Purkinje cells. Proc. Natl. Acad. Sci. U. S. A. 111, 14930–4.

Jörntell, H., Bengtsson, F., Schonewille, M., De Zeeuw, C.I., 2010. Cerebellar molecular layer interneurons - computational properties and roles in learning. Trends Neurosci. 33, 524–32.

Jörntell, H., Ekerot, C.-F., 2003. Receptive field plasticity profoundly alters the cutaneous parallel fiber synaptic input to cerebellar interneurons in vivo. J. Neurosci. 23, 9620–31.

Jörntell, H., Ekerot, C.-F., 2011. Receptive field remodeling induced by skin stimulation in cerebellar neurons in vivo. Front. Neural Circuits 5, 1–10.

Jörntell, H., Ekerot, C.F., 2002. Reciprocal bidirectional plasticity of parallel fiber receptive fields in cerebellar Purkinje cells and their afferent interneurons. Neuron 34, 797–806.

Jouhanneau, J.-S., Kremkow, J., Dorrn, A.L., Poulet, J.F.A., 2015. In vivo

monosynaptic excitatory transmission between layer 2 cortical pyramidal neurons. Cell Rep. 13, 2098–106.

Judkewitz, B., Rizzi, M., Kitamura, K., Häusser, M., 2009. Targeted single-cell electroporation of mammalian neurons in vivo. Nat. Protoc. 4, 862–9.

Kandel, E.R., Schwartz, J.H., Jessell, T.M., 2000. Principles of neural science, 4th ed. McGraw-Hill, New York.

Kaneda, M., Farrant, M., Cull-Candy, S.G., 1995. Whole-cell and single-channel currents activated by GABA and glycine in granule cells of the rat cerebellum. J. Physiol. 485 (Pt 2), 419–35.

Kanichay, R.T., Silver, R.A., 2008. Synaptic and cellular properties of the feedforward inhibitory circuit within the input layer of the cerebellar cortex. J. Neurosci. 28, 8955–67.

Karnani, M.M., Jackson, J., Ayzenshtat, I., Tucciarone, J., Manoocheri, K., Snider, W.G., Yuste, R., 2016. Cooperative subnetworks of molecularly similar interneurons in mouse neocortex. Neuron 90, 86–100.

Kim, H.G., Beierlein, M., Connors, B.W., 1995. Inhibitory control of excitabile dendrites in neocortex. J. Neurophysiol. 74, 1810–1814.

Kim, J., Lee, S., Tsuda, S., Zhang, X., Asrican, B., Gloss, B., Feng, G., Augustine, G.J., 2014. Optogenetic mapping of cerebellar inhibitory circuitry reveals spatially biased coordination of interneurons via electrical synapses. Cell Rep. 7, 1601–13.

Kimpo, R.R., Rinaldi, J.M., Kim, C.K., Payne, H.L., Raymond, J.L., 2014. Gating of neural error signals during motor learning 1–23.

Kirov, S.A., Sorra, K.E., Harris, K.M., 1999. Slices have more synapses than perfusion-fixed hippocampus from both young and mature rats. J. Neurosci. 19, 2876–86.

Kitamura, K., Häusser, M., 2011. Dendritic calcium signaling triggered by spontaneous and sensory-evoked climbing fiber input to cerebellar Purkinje cells in vivo. J. Neurosci. 31, 10847–58.

Kitamura, K., Judkewitz, B., Kano, M., Denk, W., Häusser, M., 2008. Targeted patch-clamp recordings and single-cell electroporation of unlabeled neurons in vivo. Nat. Methods 5, 61–7.

Ko, H., Hofer, S.B., Pichler, B., Buchanan, K. a, Sjöström, P.J., Mrsic-Flogel, T.D., 2011. Functional specificity of local synaptic connections in neocortical networks. Nature 473, 87–91.

Kollo, M., Holderith, N.B., Nusser, Z., 2006. Novel subcellular distribution pattern of A-type K+ channels on neuronal surface. J. Neurosci. 26, 2684–2691.

Komuro, H., Rakic, P., 1998. Distinct modes of neuronal migration in different domains of developing cerebellar cortex. J. Neurosci. 18, 1478–1490.

Kondo, S., Marty, A., 1998. Synaptic currents at individual connections among stellate cells in rat cerebellar slices. J. Physiol. 509, 221–232.

Kreiman, G., Koch, C., Fried, I., 2000. Category-specific visual responses of single neurons in the human medial temporal lobe. Nat Neurosci 3, 946–953.

Kreitzer, A.C., Carter, A.G., Regehr, W.G., 2002. Inhibition of interneuron firing extends the spread of endocannabinoid signaling in the cerebellum. Neuron 34, 787–796.

Larkum, M.E., Zhu, J.J., Sakmann, B., 1999. A new cellular mechanism for coupling inputs arriving at different cortical layers. Nature 398, 338–341.

Lee, S., Kruglikov, I., Huang, Z.J., Fishell, G., Rudy, B., 2013. A disinhibitory circuit mediates motor integration in the somatosensory cortex. Nat. Neurosci. 16, 1662–70.

Letzkus, J.J., Wolff, S.B.E., Lüthi, A., 2015. Disinhibition, a circuit mechanism for associative learning and memory. Neuron 88, 264–76.

Letzkus, J.J., Wolff, S.B.E., Meyer, E.M.M., Tovote, P., Courtin, J., Herry, C., Lüthi, A., 2011. A disinhibitory microcircuit for associative fear learning in the auditory cortex. Nature 480, 331–335.

Lev-Ram, V., Wong, S.T., Storm, D.R., Tsien, R.Y., 2002. A new form of cerebellar long-term potentiation is postsynaptic and depends on nitric oxide but not cAMP. Proc. Natl. Acad. Sci. 99, 8389–8393.

Libster, A.M., Yarom, Y., 2013. In and out of the loop: external and internal modulation of the olivo-cerebellar loop. Front. Neural Circuits 7, 73.

Liu, G., 2004. Local structural balance and functional interaction of excitatory and inhibitory synapses in hippocampal dendrites. Nat. Neurosci. 7, 373–379.

Liu, S.Q., Cull-Candy, S.G., 2000. Synaptic activity at calcium-permeable AMPA receptors induces a switch in receptor subtype. Nature 405, 454–8.

Llinás, R., Sugimori, M., 1980. Electrophysiological properties of in vitro Purkinje cell dendrites in mammalian cerebellar slices. J. Physiol. 305, 197–213.

Llinás, R.R., 2013. The olivo-cerebellar system: a key to understanding the functional significance of intrinsic oscillatory brain properties. Front. Neural Circuits 7, 96.

Loewenstein, Y., Mahon, S., Chadderton, P., Kitamura, K., Sompolinsky, H., Yarom, Y., Häusser, M., 2005. Bistability of cerebellar Purkinje cells modulated by sensory stimulation. Nat. Neurosci. 8, 202–11.

London, M., Häusser, M., 2005. Dendritic computation. Annu. Rev. Neurosci. 28, 503–32.

Lu, H., Hartmann, M.J., Bower, J.M., 2005. Correlations between purkinje cell single-unit activity and simultaneously recorded field potentials in the immediately underlying granule cell layer. J. Neurophysiol. 94, 1849–1860.

Luczak, A., Barthó, P., Harris, K.D., 2009. Spontaneous events outline the realm of possible sensory responses in neocortical populations. Neuron 62, 413–25.

Mann-Metzer, P., Yarom, Y., 1999. Electrotonic coupling interacts with intrinsic properties to generate synchronized activity in cerebellar networks of inhibitory interneurons. J. Neurosci. 19, 3298–306.

Margrie, T.W., Meyer, A.H., Caputi, A., Monyer, H., Hasan, M.T., Schaefer, A.T., Denk, W., Brecht, M., 2003. Targeted whole-cell recordings in the mammalian brain in vivo. Neuron 39, 911–918.

Markram, H., Toledo-Rodriguez, M., Wang, Y., Gupta, A., Silberberg, G., Wu, C., 2004. Interneurons of the neocortical inhibitory system. Nat. Rev. Neurosci. 5, 793–807.

Marr, D., 1969. A theory of cerebellar cortex. J. Physiol. 202, 437–470.

Marr, D., Poggio, T., 1976. From understanding computation to understanding neural circuitry.

Marshall, S.P., Lang, E.J., 2009. Local changes in the excitability of the cerebellar cortex produce spatially restricted changes in complex spike synchrony. J. Neurosci. 29, 14352–14362.

Mathews, P.J., Lee, K.H., Peng, Z., Houser, C.R., Otis, T.S., 2012. Effects of climbing fiber driven inhibition on Purkinje neuron spiking. J. Neurosci. 32, 17988–97.

Mathy, A., Ho, S.S.N., Davie, J.T., Duguid, I.C., Clark, B. a, Häusser, M., 2009. Encoding of oscillations by axonal bursts in inferior olive neurons. Neuron 62, 388–99.

McCulloch, W.S., Pitts, W., 1943. A logical calculus of the ideas immanent in nervous activity. Bull. Math. Biophys. 5, 115–133.

Medina, J.F., Lisberger, S.G., 2008. Links from complex spikes to local plasticity and motor learning in the cerebellum of awake-behaving monkeys. Nat. Neurosci.

11, 1185–92.

Meyer, A.H., Katona, I., Blatow, M., Rozov, A., Monyer, H., 2002. In vivo labeling of parvalbumin-positive interneurons and analysis of electrical coupling in identified neurons. J. Neurosci. 22, 7055–64.

Midtgaard, J., 1992a. Stellate cell inhibition of Purkinje cells in the turtle cerebellum in vitro. J. Physiol. 457, 355–67.

Midtgaard, J., 1992b. Membrane properties and synaptic responses of Golgi cells and stellate cells in the turtle cerebellum in vitro. J. Physiol. 457, 329–54.

Miles, R., Tóth, K., Gulyás, A.I., Hájos, N., Freund, T.F., 1996. Differences between somatic and dendritic inhibition in the hippocampus. Neuron 16, 815–823.

Mittmann, W., Häusser, M., 2007. Linking synaptic plasticity and spike output at excitatory and inhibitory synapses onto cerebellar Purkinje cells. J. Neurosci. 27, 5559–70.

Mittmann, W., Koch, U., Häusser, M., 2005. Feed-forward inhibition shapes the spike output of cerebellar Purkinje cells. J. Physiol. 563, 369–78.

Morissette, J., Bower, J.M., 1996. Contribution of somatosensory cortex to responses in the rat cerebellar granule cell layer following peripheral tactile stimulation. Exp. brain Res. 109, 240–50.

Mostofi, A., Holtzman, T., Grout, A.S., Yeo, C.H., Edgley, S.A., 2010. Electrophysiological localization of eyeblink-related microzones in rabbit cerebellar cortex. J. Neurosci. 30, 8920–34.

Mugnaini, E., Sekerková, G., Martina, M., 2011. The unipolar brush cell: A remarkable neuron finally receiving deserved attention. Brain Res. Rev. 66, 220–245.

Najafi, F., Giovannucci, A., Wang, S.S.-H., Medina, J.F., 2014. Sensory-driven enhancement of calcium signals in individual Purkinje cell dendrites of awake mice. Cell Rep. 6, 792–8.

Napper, R.M., Harvey, R.J., 1988. Number of parallel fiber synapses on an individual Purkinje cell in the cerebellum of the rat. J. Comp. Neurol. 274, 168–177.

Niell, C.M., Stryker, M.P., 2010. Modulation of visual responses by behavioral state in mouse visual cortex. Neuron 65, 472–9.

Northoff, G., 2012. Psychoanalysis and the brain - why did Freud abandon neuroscience? Front. Psychol. 3, 1–11.

Ohki, K., Chung, S., Ch'ng, Y.H., Kara, P., Reid, R.C., 2005. Functional imaging with

cellular resolution reveals precise micro-architecture in visual cortex. Nature 433, 597–603.

Ohmae, S., Medina, J.F., 2015. Climbing fibers encode a temporal-difference prediction error during cerebellar learning in mice. Nat. Neurosci. 18.

Okun, M., Lampl, I., 2008. Instantaneous correlation of excitation and inhibition during ongoing and sensory-evoked activities. Nat. Neurosci. 11, 535–7.

Oláh, S., Füle, M., Komlósi, G., Varga, C., Báldi, R., Barzó, P., Tamás, G., 2009. Regulation of cortical microcircuits by unitary GABA-mediated volume transmission. Nature 461, 1278–1281.

Olsen, S.R., Bortone, D.S., Adesnik, H., Scanziani, M., 2012. Gain control by layer six in cortical circuits of vision. Nature 483, 47–52.

Ozden, I., Sullivan, M.R., Lee, H.M., Wang, S.S.-H., 2009. Reliable coding emerges from coactivation of climbing fibers in microbands of cerebellar Purkinje neurons. J. Neurosci. 29, 10463–73.

Packer, A.M., Peterka, D.S., Hirtz, J.J., Prakash, R., Deisseroth, K., Yuste, R., 2012. Two-photon optogenetics of dendritic spines and neural circuits. Nat. Methods 9, 1202–1205.

Packer, A.M., Yuste, R., 2011. Dense, unspecific connectivity of neocortical parvalbumin-positive interneurons: a canonical microcircuit for inhibition? J. Neurosci. 31, 13260–71.

Pala, A., Petersen, C.C.H., 2015. In vivo measurement of cell-type-specific synaptic connectivity and synaptic transmission in layer 2/3 mouse barrel cortex. Neuron 85, 68–75.

Palay, S., 1956. Synapses in the central nervous system. J. Biophys. Biochem. Cytol. 2, 239–256.

Palay, S.L., Chan-Palay, V., 1974. Cerebellar Cortex: Cytology and Organization. Springer, Berlin.

Person, A.L., Raman, I.M., 2012. Purkinje neuron synchrony elicits time-locked spiking in the cerebellar nuclei. Nature 481, 502–5.

Pfeffer, C.K., Xue, M., He, M., Huang, Z.J., Scanziani, M., 2013. Inhibition of inhibition in visual cortex: the logic of connections between molecularly distinct interneurons. Nat. Neurosci. 16, 1068–76.

Pichitpornchai, C., Rawson, J. a, Rees, S., 1994. Morphology of parallel fibres in the cerebellar cortex of the rat: an experimental light and electron microscopic study with biocytin. J. Comp. Neurol. 342, 206–20.

Piochon, C., Kruskal, P., Maclean, J., Hansel, C., 2012. Non-Hebbian spike-timing-dependent plasticity in cerebellar circuits. Front. Neural Circuits 6, 124.

Piochon, C., Levenes, C., Ohtsuki, G., Hansel, C., 2010. Purkinje cell NMDA receptors assume a key role in synaptic gain control in the mature cerebellum. J. Neurosci. 30, 15330–5.

Pologruto, T.A., Sabatini, B.L., Svoboda, K., 2003. ScanImage: flexible software for operating laser scanning microscopes. Biomed. Eng. Online 2, 13.

Porrill, J., Dean, P., Anderson, S.R., 2013. Adaptive filters and internal models: Multilevel description of cerebellar function. Neural Networks 47, 134–149.

Porter, K.R., Claude, A., Fullam, E.F., 1945. A study of tissue culture cells by electron microscopy: methods and preliminary observations. J. Exp. Med. 81, 233–246.

Pouille, F., Marin-Burgin, A., Adesnik, H., Atallah, B. V, Scanziani, M., 2009. Input normalization by global feedforward inhibition expands cortical dynamic range. Nat. Neurosci. 12, 1577–85.

Pouille, F., Scanziani, M., 2001. Enforcement of temporal fidelity in pyramidal cells by somatic feed-forward inhibition. Science 293, 1159–1163.

Pouille, F., Scanziani, M., 2004. Routing of spike series by dynamic circuits in the hippocampus. Nature 429, 717–23.

Poulet, J.F. a, Petersen, C.C.H., 2008. Internal brain state regulates membrane potential synchrony in barrel cortex of behaving mice. Nature 454, 881–5.

Pouzat, C., Hestrin, S., 1997. Developmental regulation of basket/stellate cell-->Purkinje cell synapses in the cerebellum. J. Neurosci. 17, 9104–9112.

Powell, K., Mathy, A., Duguid, I., Häusser, M., 2015. Synaptic representation of locomotion in single cerebellar granule cells. Elife.

Proville, R.D., Spolidoro, M., Guyon, N., Dugué, G.P., Selimi, F., Isope, P., Popa, D., Léna, C., 2014. Cerebellum involvement in cortical sensorimotor circuits for the control of voluntary movements. Nat. Neurosci. 17, 1233–9.

Quian Quiroga, R., Reddy, L., Kreiman, G., Koch, C., Fried, I., 2005. Invariant visual representation by single neurons in the human brain. Nature 435, 1102–1107.

Rajan, K., Harvey, C.D., Tank, D.W., 2016. Recurrent Network Models of Sequence Generation and Memory. Neuron 90, 128–142.

Rall, W., 1967. Distinguishing theoretical synaptic potentials computed for different soma-dendritic distributions of synaptic input. J. Neurophysiol. 30, 1138–68.

Ramadoss, J., Lunde, E.R., Ouyang, N., Chen, W.-J.A., Cudd, T.A., 2008. Acid-

sensitive channel inhibition prevents fetal alcohol spectrum disorders cerebellar Purkinje cell loss. Am. J. Physiol. - Regul. Integr. Comp. Physiol. 295, 596–603.

Ramón y Cajal, S., 1888. Estructura de los centros nerviosos de las aves. Rev. Trim. Histol. Norm. Pat. 1, 1–10.

Rancillac, A., Crépel, F., 2004. Synapses between parallel fibres and stellate cells express long-term changes in synaptic efficacy in rat cerebellum. J. Physiol. 554, 707–20.

Rapp, M., Yarom, Y., Segev, I., 1992. The impact of parallel fiber background activity on the cable properties of cerebellar Purkinje cells. Neural Comput. 533, 518–533.

Rieubland, S., Roth, A., Häusser, M., 2014. Structured connectivity in cerebellar inhibitory networks. Neuron 81, 913–29.

Rosenblatt, F., 1958. The perceptron: a probabilistic model for information storage and organization in the brain. Psychol. Rev. 65, 386–408.

Roth, A., Häusser, M., 2001. Compartmental models of rat cerebellar Purkinje cells based on simultaneous somatic and dendritic patch-clamp recordings. J. Physiol. 535, 445–72.

Rowland, N.C., Jaeger, D., 2005. Coding of tactile response properties in the rat deep cerebellar nuclei. J. Neurophysiol. 94, 1236–51.

Royer, S. eacute bastien, Zemelman, B. V, Losonczy, A., Kim, J., Chance, F., Magee, J.C., Ki, G. ouml rgy B. aacute, 2012. Control of timing, rate and bursts of hippocampal place cells by dendritic and somatic inhibition. Nat. Neurosci. 15, 1–10.

Ruffin, V.A., Salameh, A.I., Boron, W.F., Parker, M.D., 2014. Intracellular pH regulation by acid-base transporters in mammalian neurons. Front. Physiol. 5 FEB, 1–11.

Safo, P., Cravatt, B., Regehr, W., 2006. Retrograde endocannabinoid signaling in the cerebellar cortex. The Cerebellum 5, 134–145.

Santamaria, F., Tripp, P.G., Bower, J.M., 2007. Feedforward inhibition controls the spread of granule cell-induced Purkinje cell activity in the cerebellar cortex. J. Neurophysiol. 97, 248–63.

Scanziani, M., 2000. GABA spillover activates postsynaptic GABA(B) receptors to control rhythmic hippocampal activity. Neuron 25, 673–81.

Schilling, K., Oberdick, J., Rossi, F., Baader, S.L., 2008. Besides Purkinje cells and granule neurons: an appraisal of the cell biology of the interneurons of the

cerebellar cortex. Histochem. Cell Biol. 130, 601–15.

Schmidt-Hieber, C., Häusser, M., 2013. Cellular mechanisms of spatial navigation in the medial entorhinal cortex. Nat. Neurosci. 16, 325–31.

Schultz, S.R., Kitamura, K., Post-Uiterweer, A., Krupic, J., Häusser, M., 2009. Spatial pattern coding of sensory information by climbing fiber-evoked calcium signals in networks of neighboring cerebellar Purkinje cells. J. Neurosci. 29, 8005–15.

Shadlen, M.N., Newsome, W.T., 1998. The variable discharge of cortical neurons: implications for connectivity, computation, and information coding. J. Neurosci. 18, 3870–3896.

Shambes, G.M., Gibson, J.M., Welker, W., 1978. Fractured somatotopy in granule cell tactile areas of rat cerebellar hemispheres revealed by micromapping. Brain. Behav. Evol. 15, 94–140.

Sheffield, M.E.J., Dombeck, D. a., 2015. Calcium transient prevalence across the dendritic arbour predicts place field properties. Nature 517, 200–4.

Sherrington, C., 1932. Inhibition as a Coordinative Factor. Nobel Lecture. In: The Nobel Prize in Physiology or Medicine 1932.

Sims, R.E., Hartell, N.A., 2005. Differences in transmission properties and susceptibility to long-term depression reveal functional specialization of ascending axon and parallel fiber synapses to Purkinje cells. J. Neurosci. 25, 3246–57.

Smith, S.L., Smith, I.T., Branco, T., Häusser, M., 2013. Dendritic spikes enhance stimulus selectivity in cortical neurons in vivo. Nature 503, 115–20.

Sotelo, C., 2003. Viewing the brain through the master hand of Ramón y Cajal. Nat. Rev. Neurosci. 4, 71–7.

Stosiek, C., Garaschuk, O., Holthoff, K., Konnerth, A., 2003. In vivo two-photon calcium imaging of neuronal networks. Proc. Natl. Acad. Sci. U. S. A. 100, 7319–24.

Stuart, G., Häusser, M., 1994. Initiation and spread of sodium action potentials in cerebellar Purkinje cells. Neuron 13, 703–712.

Sugihara, I., Fujita, H., Na, J., Quy, P.N., Li, B.Y., Ikeda, D., 2009. Projection of reconstructed single Purkinje cell axons in relation to the cortical and nuclear aldolase C compartments of the rat cerebellum. J. Comp. Neurol. 512, 282–304.

Sultan, F., Bower, J.M., 1998. Quantitative Golgi study of the rat cerebellar

molecular layer interneurons using principal component analysis. J Comp Neurol 393, 353–373.

Szapiro, G., Barbour, B., 2007. Multiple climbing fibers signal to molecular layer interneurons exclusively via glutamate spillover. Nat. Neurosci. 10, 735–42.

ten Brinke, M.M., Boele, H.-J., Spanke, J.K., Potters, J.-W., Kornysheva, K., Wulff, P., IJpelaar, A.C.H.G., Koekkoek, S.K.E., De Zeeuw, C.I., 2015. Evolving models of Pavlovian conditioning: cerebellar cortical dynamics in awake behaving mice. Cell Rep. 13, 1977–88.

Tremblay, R., Lee, S., Rudy, B., 2016. GABAergic interneurons in the neocortex: from cellular properties to circuits. Neuron 91, 260–92.

Tsutsumi, S., Yamazaki, M., Miyazaki, T., Watanabe, M., Sakimura, K., Kano, M., Kitamura, K., 2015. Structure-function relationships between aldolase C/zebrin II expression and complex spike synchrony in the cerebellum. J. Neurosci. 35, 843–52.

Valera, A.M., Binda, F., Pawlowski, S.A., Dupont, J.-L., Casella, J.-F., Rothstein, J.D., Poulain, B., Isope, P., 2016. Stereotyped spatial patterns of functional synaptic connectivity in the cerebellar cortex. Elife 5, 1–22.

Van Der Giessen, R.S., Maxeiner, S., French, P.J., Willecke, K., De Zeeuw, C.I., 2006. Spatiotemporal distribution of Connexin45 in the olivocerebellar system. J. Comp. Neurol. 495, 173–184.

van Welie, I., Roth, A., Ho, S.S.N., Komai, S., Häusser, M., 2016. Conditional spike transmission mediated by electrical coupling ensures millisecond precision-correlated activity among interneurons in vivo. Neuron 90, 810–23.

Van Welie, I., Smith, I.T., Watt, A.J., 2011. The metamorphosis of the developing cerebellar microcircuit. Curr. Opin. Neurobiol. 21, 245–253.

Vervaeke, K., Lorincz, A., Gleeson, P., Farinella, M., Nusser, Z., Silver, R.A., 2010. Rapid desynchronization of an electrically coupled interneuron network with sparse excitatory synaptic input. Neuron 67, 435–51.

Vincent, P., Marty, A., 1996. Fluctuations of inhibitory postsynaptic currents in Purkinje cells from rat cerebellar slices. J. Physiol. 494, 183–199.

Wang, S.S., Denk, W., Häusser, M., 2000. Coincidence detection in single dendritic spines mediated by calcium release. Nat. Neurosci. 3, 1266–1273.

Wang, X.J., Buzsáki, G., 1996. Gamma oscillation by synaptic inhibition in a hippocampal interneuronal network model. J. Neurosci. 16, 6402–13.

Waters, J., Helmchen, F., 2006. Background synaptic activity is sparse in neocortex.

J. Neurosci. 26, 8267–77.

White, J.G., Southgate, E., Thomson, J.N., Brenner, S., 1986. The structure of the nervous system of the nematode Caenorhabditis elegans. Philos. Trans. R. Soc. Lond. B. Biol. Sci. 314, 1–340.

Wilms, C.D., Häusser, M., 2015. Reading out a spatiotemporal population code by imaging neighbouring parallel fibre axons in vivo. Nat. Commun. 6, 6464.

Witter, L., Rudolph, S., Pressler, R.T., Lahlaf, S.I., Regehr, W.G., 2016. Purkinje cell collaterals enable output signals from the cerebellar cortex to feed back to Purkinje cells and interneurons. Neuron 91, 312–9.

Wolpert, D.M., Miall, R.C., Kawato, M., 1998. Internal models in the cerebellum. Trends Cogn. Sci. 2, 338–347.

Woolston, D.C., Kassel, J., Gibson, J.M., 1981. Trigeminocerebellar mossy fiber branching to granule cell layer patches in the rat cerebellum. Brain Res. 209, 255–269.

Wulff, P., Schonewille, M., Renzi, M., Viltono, L., Sassoè-Pognetto, M., Badura, A., Gao, Z., Hoebeek, F.E., van Dorp, S., Wisden, W., Farrant, M., De Zeeuw, C.I., 2009. Synaptic inhibition of Purkinje cells mediates consolidation of vestibulo-cerebellar motor learning. Nat. Neurosci. 12, 1042–1049.

Yang, Y., Lisberger, S.G., 2014. Purkinje-cell plasticity and cerebellar motor learning are graded by complex-spike duration. Nature 510, 529–32.

Yeo, C.H., Hesslow, G., 1998. Cerebellum and conditioned reflexes. Trends Cogn. Sci. 2, 322–30.

Yoshimura, Y., Dantzker, J.L.M., Callaway, E.M., 2005. Excitatory cortical neurons from fine-scale functional networks. Nature 5, 2005–2005.

Yuste, R., 2015. From the neuron doctrine to neural networks. Nat. Rev. Neurosci. 16, 487–497.

Zeisel, A., Muñoz-Manchado, A.B., Codeluppi, S., Lönnerberg, P., La Manno, G., Juréus, A., Marques, S., Munguba, H., He, L., Betsholtz, C., Rolny, C., Castelo-Branco, G., Hjerling-Leffler, J., Linnarsson, S., 2015. Brain structure. Cell types in the mouse cortex and hippocampus revealed by single-cell RNA-seq. Science 347, 1138–42.

Zhou, H., Lin, Z., Voges, K., Ju, C., Gao, Z., Bosman, L.W., Ruigrok, T.J., Hoebeek, F.E., De Zeeuw, C.I., Schonewille, M., 2014. Cerebellar modules operate at different frequencies. Elife e02536.